The Development of Seahorse Vision: Morphological and Behavioural Aspects

Hie Rin Lee

March 2013

A thesis submitted in fulfilment of the requirements for the degree of Doctor of Philosophy of The Australian National University

Declaration

This declaration certifies that the following work entitled ‘The Development of Seahorse Vision: Morphological and Behavioural Aspects’ is the author’s own original work, complies with The Australian National University Research Award Rules 4.4(2), and has not previously been accepted for award of a degree or diploma to any other university or institution of higher learning.

Signed: _____

Date: _____

Acknowledgements

It would not be possible to complete this doctoral thesis without the help and support of those lovely people around me. Without them, my whole experiences as a PhD candidate would not have been the same.

Foremost, I would like to acknowledge Rachelle Hawkins of Seahorse Australia for her assistance with these experiments, Dr. Eldon Ball at the Research School of Biology for generously letting me use Alexa Flour 594 goat anti-rat secondary antibody for preliminary data gathering, and Terry Neeman at the statistical consulting unit (ANU) for advice on statistical analysis of my data.

I am grateful to my collegues who made the lab as my second home. Special thanks go to Riccardo Natoli who sometimes had to explain things from the scratch with patience. Thank you for all your valuable advices and support. Big thanks also go to Rizsa Albarracin, Zabrina Abdool, Kartik Saxena, Angeliza Querubin, Matt Rutar, Maria Kolic, Faran Sabeti, Corinne Carle and Peter Kozulin for being such a wonderful team. My experiences would not have been the same without them.

I give the most sincere thanks to my supervisors. First, to Dr. Keely Bumsted O'Brien for her years of support and guidance since first she introduced me to research all those years ago. Her passion in science inspired me to pursue research further. Not only as a woman scientist, as a mother and a wife, all those caring advices and support remain precious to me. Second, to Dr. Krisztina Valter for the help and support, especially with the techniques of intraocular BrdU injections and valuable discussions on future investigations. Krisztina also poured me with enthusiasm and passion for new discovery. I really appreciate it. Third, to Prof. Jan Provis for fostering me so that I could be a part of the lab family. Not only with her excellence in research, but also her positive attitudes, humour and love of fashion made her one of my role models in science field. Fourth, to Prof. Ted Maddess for adopting me and giving me all the support to complete this thesis. I am really greatful that you have provided me with

different perspectives to my PhD projects which broadened my horizon to more clinical thinking.

I would like to thank to my friends and families from Canberra Korean Presbyterian Church who faithfully prayed for me and were willing to give support in every form. Your consistent and faithful love was always more than I deserved.

Finally, and most importantly of all, I would like to thank my beloved family. In particular, thanks Mum and Dad for your unfailing love, support and patience, and to Hie Jung, my little sister for believing in me. I also believe in you. Special thanks to my parents-in-laws for your unending support and for accepting me as who I am. I would also like to thank to my precious Joshua and Emma. You have been alway the first in my mind. Last, but not the least, big thanks go to Jeremy, my dearest husband, a great partner, a mentor, and a hero!

‘God spoke: "Earth, generate life! Every sort and kind: cattle and reptiles and wild animals - all kinds." And there it was: wild animals of every kind, Cattle of all kinds, every sort of reptile and bug. God saw that it was good.’

- **Genesis 1:24-25 (‘Message’)**

Abstract

Seahorses are visually guided feeders that rely on a well-developed visual system to successfully predate on small shrimp and plankton. Despite their dependence on vision for feeding and survival, very little is known about seahorse vision and visual development. Many species of seahorse have a specialisation in their retina associated with acute vision, a convexiclivate, rod-free fovea located at the centre of gaze. In the first part of this thesis, the foveae of temperate *Hippocampus abdominalis* and tropical *H. taeniopterus* seahorses are characterised. Both species possess a rod-free convexiclivate fovea and the pattern of photoreceptor and ganglion cell distribution is similar. Despite these similarities, *H. taeniopterus* has higher cell densities on the foveal slope and better theoretical and behaviourally measured visual resolution compared to *H. abdominalis*. These data indicate that seahorses have a well-developed acute visual system, and this tropical seahorse species has higher visual resolution compared to this species of temperate seahorse. In the second part of the thesis, developmental changes in foveal morphology are analysed using three increasingly larger sized groups of *H. taeniopterus* seahorses. Morphologically, the depression of the foveal pit deepens as the fish grows. The area of rod-free zone also increases with fish size. The photoreceptor and ganglion cell densities increase at the foveal slope, although there is a decrease in cone and ganglion cell density at the foveal centre this is observed as the fish grows. Both the theoretical and the behavioural visual resolution improve with increasing fish size, with larger fish being able to detect the same sized prey at a greater distance. The behaviourally measured increased visual function correlates with changes in morphology with fish size. The last aspect of the thesis uses five *H. taeniopterus* seahorse groups of increasing size to analyse the morphological and behavioural development of the fovea and rod-free zone, with an emphasis on the contribution of cell death and proliferation. The behavioural visual resolution improves with size. Morphologically, the area of rod-free zone increases in size during development. BrdU labelling, a measure of cell proliferation, shows the absence of cell division in the ONL; however, there are dividing neuroretinal cells in the INL within the rod-free zone. The TUNEL assay confirms the lack of programmed large-scale photoreceptor cell death in and around the rod-free zone during development. Taken together, our data are not able to rule out the possibility of cone photoreceptor cell generation from INL stem cells within the rod-free zone, although cell death is not likely to be a major mechanism of

foveal development. Future studies are designed to determine the underlying mechanism in the establishment of the adult rod-free zone.

Publications and Abstracts

This work is encompassing one peer-reviewed paper. Journal formatting – including abstracts and references – is preserved with respect to the papers in chapter 2, 3 and 4; a complete references is diplayed in Appendix 1. The findings in this thesis were also featured in the abstracts listed below.

Peer reviewed papers

1. **Lee, H. R.** and Bumsted O'Brien, K. M. (2011) Morphological and behavioral limit of visual resolution in temperate (*Hippocampus abdominalis*) and tropical (*Hippocampus taeniopterus*) seahorses. Visual Neuroscience, 28(4):351-360.

Conference Abstracts

1. **Lee, H. R.** and Bumsted O'Brien, K. M. (2006) How Different are Seahorse (*Hippocampus abdominalis* and *Hippocampus kuda*) Central Retinae: Foveate vs Nonfoveate Specialisations? Proceedings of the Australasian Ophthalmic and Visual Sciences Meeting. Canberra Australia.
2. **Lee, H. R.** and Bumsted O'Brien, K. M. (2007) Foveate vs Non Foveate Specialisations: a comparison of *Hippocampus abdominalis* and *Hippocampus kuda*. Proceedings of Vision Down Under Meeting. Cairns Australia.
3. **Lee, H. R.** and Bumsted O'Brien, K. M. (2009) Measurement of Adult Visual Acuity and the Morphological Development of the Seahorse (*Hippocampus abdominalis*) Fovea. Proceedings of the Australian Neuroscience Society. Canberra Australia.
4. **Lee, H. R.** and Bumsted O'Brien, K. M. (2010) Theoretical and Behavioural Limit of Visual Resolution in Temperate and Tropical Seahorses. ARVO abstract.
5. **Lee, H. R.** and Bumsted O'Brien, K. M. (2011) Development Of The Fovea And Visual Resolution In The Tropical Seahorse (*Hippocampus taeniopterus)*. Proceedings of the Australian Neuroscience Society. Auckland New Zealand

6. Keely M. Bumsted O'Brien, **Hie Rin Lee**. (2011) Development Of The Fovea And Visual Resolution In The Tropical Seahorse (*Hippocampus taeniopterus)*. ARVO abstract.

7. **Lee, H. R.** and Bumsted O'Brien, K. M. (2012) Development Of The Fovea And Visual Resolution In The Tropical Seahorse (*Hippocampus taeniopterus)*. Proceedings of Vision Down Under. Queensland Australia

8. **Lee, H. R.** and Bumsted O'Brien, K. M. (2012) Development Of The Fovea And Visual Resolution In The Tropical Seahorse (*Hippocampus taeniopterus)*. Proceedings of the Australian Neuroscience Society. Gold Coast Australia

9. **Lee, H. R.** and Bumsted O'Brien, K. M. (2012) Development Of The Fovea And Visual Resolution In The Tropical Seahorse (*Hippocampus taeniopterus)*. Proceedings of the *International Society for Eye Research*. Berlin Germany

Table of Contents

List of Figures

Chapter ONE

Chapter TWO

Chapter THREE

Chapter FOUR

List of Tables

Chapter 2

Chapter 3

Chapter 4

List of Abbreviations

℃	degrees Celsius
α	minimum separable angle measured in minutes of arc/ angle subtending 1 mm on the retina
A. curacao	*Amblyglyphidodon curacao*
ANOVA	Analysis of variance
B. benedicti	*Bathylagus benedicti*
B. conspicillum	*Balistoides conspicillum*
BrdU	Bromodeoxyuridine (5-bromo-2'-deoxyuridine)
c	inter-cone spacing
C. auratus	*Carassius auratus*
C. paxtoni	*Corythoichthyes paxtoni*
CGZ	circumferential germinal zone
cpd	cycles per degree
d	cone density
D	dorsal
D. rerio	*Danio rerio*
deg	degree
DNA	deoxyribonucleic acid
dpf	days post-fertilisation
f	focal length of the lens
Fd	fetal days
Fwk	fetal week
GABA	γ-amino-butyric acid
GC	ganglion cell
GCL	ganglion cell layer
h	prey size
h	hour
H. abdominalis (Ha)	*Hippocampus abdominalis*
H. barbouri	*Hippocampus barbouri*
H. burtoni	*Haplochromis burtoni*
H. subelongatus	*Hippocampus subelongatus*
H. taeniopterus (Ht)	*Hippocampus taeniopterus*
H. kuda	*Hippocampus kuda*
H_2O_2	Hydrogen peroxide
HCl	hydrochloric acid
INL	inner nuclear layer
IPL	inner plexiform layer
LWS	long-wavelength sensitive
min	minute
MR	mature retina
MWS	medium-wavelength sensitive
L. fasciatus	*Limnichthyes fasciatus*
NaCl	Sodium Chloride
NFL	nerve fibre layer
N	Nasal

NH_3	Ammonia
OD	optic disc
OKR	optokinetic response
OMR	optomotor responses
ONL	outer nuclear layer
OPL	outer plexiform layer
PBS	phosphate-buffered saline
PFA	paraformaldehyde
PI	propidium iodide
PND	posterior nodal distance
PR	photoreceptor cell
r	radius of the lens
RD	reactive distance
REML	Restricted Maximum Likelihood
RFZ	rod-free zone
RPE	retinal pigment epithelium
S.D.	standard deviation
S. pleurostictus	*Sphaeroides pleurostictus*
S-phase	synthesis phase of the cell cycle
SSC	saline sodium citrate
SWS	short-wavelength sensitive
T	Temporal
TPBS	0.1% Triton X-100 in 1x PBS
TUNEL	Terminal deoxynucleotidyl transferase (TdT)-mediated dUTP-biotin nick end labelling
V	Ventral

Chapter One

INTRODUCTION

General Introduction

Syngnathidae, the family to which seahorses belong, are subclassified as the genus *Hippocampus*. As its name 'jaw-fused' indicates, this family is characterised by a fused jaw, which forms a conical snout (Kuiter, 2000). Other Syngnathidae family members include seadragons, pipefishes (*Corythoichthyes*) and pipehorses (Kuiter, 2000). Most species inhabit shallow waters near land masses where they live amongst the vegetation (Kuiter, 2000). The local environment in these shallow waters ranges from marine to estuarine habitats, including coral reefs, mangroves, and temperate sea grass beds (Kuiter, 2000) with each species generally localised to a particular region.

Unlike many other fish, seahorses are oriented in an upright position with a horse-like head set at right angles to the body. Along the seahorse body, scales have been replaced by rectangular bony plates forming rings that encase the body in a semi-rigid skeleton (ProjectSeahorse, 1996-2013). Even more unusual is the pouch located on the male's ventral side that is used for reproduction (Blumer, 1979, ProjectSeahorse, 1996-2013). The females deposit eggs into the pouch. Males fertilise and protect the eggs until hatching. Small baby seahorses are "born" by being ejected from the pouch.

Seahorses are generally diurnal with the majority of their feeding behaviour occurring during daylight hours under photopic conditions (Kuiter, 2000). As an ambush predator, seahorse feeding behaviour is visuall guided (Bergert and Wainwright, 1997, Mosk et al., 2007). To catch the zooplanktion upon which they feed, seahorses wrap their prehensile tails around stationary objects like seaweed and coral, and lie in wait (James and Heck Jr, 1994, Foster and Vincent, 2004, Choo and Liew, 2006). Once a prey item is visually detected, seahorses orient their eyes towards the prey, and then reach forward to use a distinctive rapid suction mechanism to capture the prey (Bergert and Wainwright, 1997). This strategy must depend on an acute visual system with the ability to detect small moving prey; however, their visual resolution has not been well investigated.

In this chapter, I will review literature encompassing the current knowledge of teleost vision in relation to the habitat and discuss the morphological and functional aspects of vision during development.

1.1. AQUATIC VISION: HABITATS AND LIGHT ENVIRONMENTS

Light in the aquatic environment differs in the available spectrum compared to the terrestrial environment (Jerlov, 1976). This is due to the light scattering in the water and the spectral absorption of water and is also dependant on other components present in water including chlorophyll, the breakdown products of plants, and yellow substances known variously as Gelbstoff, gilvins or Dissolved Organic Matter (Partridge, 1990). Different waters contain varying proportion of these components and this influences light transmission and spectral irradiance at different depths (Partridge, 1990). Previous authors have categorised waters according to their diverse spectral radiance distributions, such as "blue water" at coral reefs, "green water" in coastal habitats, or "red-shifted" tannin-stained lakes and rivers (Mosk et al., 2007). The "blue water" at coral reefs has the least amount of those components. As a result, the water appears blue because tropical waters absorb the long wavelengths of light and transmit the short wavelengths (or blue) of light. The maximum transmission reaches close to 460nm and only the blue part of the spectrum remains at depth (Partridge, 1990). On the other hand, coastal waters have increased level of chlorophylls, Gelbstoff and particulate matter from phytoplankton and run-off from the land; therefore, the water-colour becomes "green" or yellow. The "red-shifted" tannin-stained lakes and rivers show even more effects of those components.

The two seahorse species investigated in this thesis inhabit different environments. *H. abdominalis*, also known as the New Zealand pot-belly seahorse, is found in habitats in temperate New Zealand and south-east Australian waters around various locations which include sheltered harbours with silty waters, algae rich reefs and 50 m deep off-shore sponge beds (ProjectSeahorse, 1996-2013, Kuiter, 2000). Temperate coastal habitats are considered to be 'green waters' that transmit a narrow spectrum with a maximum wavelength transmission between 510-550 nm (Partridge, 1990). On the other hand, *H. taeniopterus* is usually found in tropical regions, typically shallow water, near reefs and along the margins of seagrass beds or marine algae, which is rarely deeper than 15 m (ProjectSeahorse, 1996-2013, Kuiter, 2000). Shallow tropical coral reef waters where *H. taeniopterus* are found transmit a broad spectrum of

light including relatively large amounts of ultraviolet (less than 390 nm) and the far-red (600-700 nm) wavelengths (Mosk et al., 2007).

The light spectrum available for vision also varies depending on water depth (Walls, 1942, Jerlov, 1976). As the water depth increases, both ends of visible light spectrum are absorbed with the longer-wavelengths having a tendency to be absorbed earlier as one moves deeper into the water column. Only three quarters of red light entering the water remains at a depth of 1 metre. Approximately, 90% of the infra-red (heat) rays are eliminated at a depth of 5 meters (Walls, 1942). Almost all of the ultra-violet light rays on the other side of spectrum are also cut off within a few millimetres of depth, although traces of ultraviolet light have been recorded at greater depths compared with any other wavelengths (Walls, 1942). Both ends of the spectrum are absorbed leaving a band of spectrum from 510 nm to 540nm wavelengths, which continue to penetrate equally well (Walls, 1942).

Visual pigments within the cone photoreceptors of fish are spectrally tuned to the most abundant wavelengths within a given habitat (Loew and Lythgoe, 1978, Lythgoe et al., 1994, Mosk et al., 2007). Deeper water fishes possess visual pigments sensitive to a narrower range in the absorption spectrum in comparison to shallow water species (Lythgoe, 1984, Bowmaker et al., 1994). The deeper water species are maximally sensitive to 475-480 nm of light, whereas the maximum sensitivity of the shallow water species is around 430-580 nm (Mosk et al., 2007). Seahorses are generally considered to be shallow water species, although varying depths have been recorded for their habitats (Kuiter, 2000). According to Mosk et al. (2007), the eyes of both temperate species (the pipefish, *Stigmatopora argus* and the seahorse, *H. subelongatus*) and a tropical species (the seahorse, *H. barbouri*) contain visual pigments with a maximum absorption at approximately 500 nm. While the temperate species are adapted to 460 nm based on their single cones, the tropical species possess an additional class of single cone tuned to 430 nm (Mosk et al., 2007). The spectral range of double cones are “fine-tuned” to provide increased sensitivity along a specific visual axis (Mosk et al., 2007).

A number of fish living in shallow tropical coral reef waters and some larval fish in the planktivorous phase of their lifecycle possess an ultraviolet sensitive visual pigment in the retina (Hawryshyn et al., 1989, McFarland and Loew, 1994, Siebeck and Marshall, 2001, Losey et al.,

2003, Mosk et al., 2007). Plankton in shallow water absorbs ultraviolet light, thus appearing dark against back-scattered ultraviolet light (Loew et al., 1993, Novales-Flamarique and Hawryshyn, 1994, Losey et al., 1999). Syngnathids lack ultraviolet sensitive cones in their retina as most short wavelengths of light are absorbed in the lens. This combined with the fact that their habitats including coral or algae reflect short wavelengths and often have ultraviolet-absorbing protective pigments means that wavelengths other than those in the ultraviolet region of the spectrum are more useful for detecting their prey (Mosk et al., 2007).

1.2. THE ADULT FISH EYE

1.2.1. Gross Structure (in Relation to Their Habitats)

Fish eyes share common structures with primate and other 'camera style' vertebrate eyes. The eyeball is shaped like a hemisphere with the axial length shorter compared with either the horizontal or vertical diameter (Walls, 1942, Fernald, 1988). The eye is covered with opaque scleral tissue, with a transparent anterior portion called the cornea (Figure 1). The cornea can be divided into two regions; an anterior zone which is known as the dermal cornea or secondary spectacle, and a posterior zone which is known as the scleral cornea (Collin and Collin, 1995). Inside the globe, starting from anterior to posterior, teleosts possess a fixed iris, spherical lens, retina and choroid (Figure 1).

The cornea in teleost fish (Figure 1) is known to play various roles including providing an optically smooth surface and a transparent window, filtering scattered light (Moreland and Lythgoe, 1968), camouflaging the pupil (Lythgoe, 1975), and providing a protective cover for the eye (Walls, 1942). The corneas of aquatic vertebrates share similarities with those of most aerial and terrestrial vertebrates although there may be differences in the number and composition of corneal layers (Fernald, 1988, Collin and Collin, 1995, Pettigrew and Collin, 1995, Zhao et al., 2006). In general, the cornea is composed of five different layers; 1) a multi-layered epithelium with an underlying basement membrane, 2) Bowman's layer, 3) a thick stroma and 4) an endothelium with a thick basement membrane known as 5) Desçemet's membrane which separates the endothelium from the stroma. The outermost corneal epithelium or dermal cornea is continuous with the conjunctiva and the skin in the periphery. By forming a barrier, the cornea plays a crucial role in limiting corneal hydration and maintaining transparency. In the absence of eyelids and the constant contact of the eye with the aqueous environment, it has been suggested that the corneal epithelium is much stronger compared with that of terrestrial vertebrates. In the zebrafish (*Danio rerio*) cornea, the epithelium, not the endothelium, provides the major protective barrier (Zhao et al., 2006). Bowman's layer is regarded as a part of the corneal barrier to sodium and water movement although it is absent in many teleosts (Collin and Collin, 1995). The sclera cornea is composed of numerous collagen

Figure removed due to copyright restrictions.

Figure 1: Schematic Diagram of a Teleost Eye
A simplified diagram depicting the vertical cross-section of a teleost eye. Modified from figure 169 (p. 577) of Walls (1942)

lamellae, a Desçemet's membrane and an endothelium (Collin and Collin, 1995). The scleral cornea extends and is continuous with the sclera. Desçemet's membrane may strengthen the cornea and the anterior segment mechanically, and to maintain stromal integrity. The pipefishes *Corythoichthyes paxtoni* (Collin and Collin, 1995) and *Syngnathus syphle* possess a very thick Desçemet's membrane (2 μm and 4 μm, respectively). The endothelium, a single layer of hexagonal and pentagonal cells up to 3 μm in thickness (Collin and Collin, 1996), in combination with the multi-layered epithelium, maintains adequate levels of corneal hydration by actively pumping bicarbonate ions and water out of the corneal stroma (Hodson et al., 1977). Its presence is also vital for maintaining corneal transparency.

The fish cornea has a refractive index that is nearly identical to that of water (Fernald, 1988). This means that the refractive power of the cornea is negligible in most aquatic eyes (Fernald, 1988). Walls (1942) has suggested that there is no need for the cornea to be smooth and has reported that the cornea is often irregular and concentrically ridged (Walls, 1942). Most teleosts have an immovable and fixed iris without constriction or dilation. Shallow, benthic species with eyes that receive input from the dorsal visual field commonly possess corneal iridescence, which reduces intraocular flare produced by bright down-welling light (Lythgoe, 1979). It also acts as a birefringent filter and may function to camouflage the pupil.

The lens protrudes through the pupil (Fernald, 1988) (Figure 1). Most fish eyes contain a spherically shaped lens with a refractive index gradient. The refractive index values of the teleost lens decrease continuously and symmetrically from the centre towards the periphery (Fernald, 1988, Shand et al., 1999). These changes in refractive index provide high quality vision up to the edges of the lens as it corrects for spherical aberration. Unlike mammals, the teleost fish moves its spherical lens position backwards and forwards without changing the lens shape in order to accommodate. Due to the negligible refractive power provided by the cornea, the crystalline lens contributes to the majority of the total refractive power of the eye (Powers and Easter Jr, 1983, Fernald, 1988, Pettigrew and Collin, 1995). Along with the accommodative state of the eye and the inter-cone spacing within the retina, the resolving power of the lens contributes to the absolute limit of visual detection in teleosts (Pankhurst et al., 1993). Previous studies have demonstrated that the resolving power of the teleost lens does not limit visual

acuity because the lens has approximately ten times greater resolving power than that which can be resolved by the cone mosaic (Northmore and Dvorak, 1979, Fernald and Wright, 1985). Teleost lenses provide high transmission of long wavelengths with a short wavelength cut-off, displaying Class I ocular media transmission spectra among four classes distinguished by Siebeck & Marshall (2001) (Siebeck and Marshall, 2001, Mosk et al., 2007). However, tropical species of seahorse have a greater transmission of shorter wavelengths (Mosk et al., 2007). There is an exception to this basic set up of the lens in the fish eye. The sandlance *Limnichthyes fasciatus* does not possess a spherical lens but has a flattened lens, which contributes approximately 60% of the total optical power of the eye (Collin and Collin, 1988a, Pettigrew and Collin, 1995). The rest is dependent on the cornea, which consists of a high concentration of refractive material forming a lenticle, the cells of which have an electron-dense appearance like that of the crystalline lens (Pettigrew and Collin, 1995). This cornea has an accommodative role from changing corneal curvature using the *cornealis* muscle (Pettigrew et al., 1999).

At the back of the fish eye, a transparent neural retinal layer is present (Figure 1). One peculiarity of most teleost retinas is the presence of a falciform process (Figure 1). This process is a pigmented protrusion of the choroid, which extends to an elongated optic nerve head within the dorso-temporal or ventro-temporal quadrant of the retina (Collin and Pettigrew, 1989). The retina will be discussed with more depth in the next section. The retina is underpinned by the choroid layer which is nourished with blood vessels that supply nutrients to the avascular retina (Figure 1) (Fernald, 1988).

1.2.2. Retina

In many teleost retinas, a light-reflecting layer called the *tapetum lucidum* is present. There are two different morphological types of *tapeta lucida* reported for fish eyes depending on the location of the reflecting material. If the tapetal material is located within the cytoplasm of the retinal pigment epithelial cells (Ollivier et al., 2004), it is defined as a retinal tapetum. If the tapetal material is located within the choroid, as is often the case in elasmobranchs, the term used is the choroidal guanine tapetum (Ollivier et al., 2004). The *tapetum lucidum* enhances the

Figure removed due to copyright restrictions.

Figure 2: Retinal Cross-section
A retinal cross-section with three nuclear layers (ONL, INL and GCL) and two synaptic layers (OPL and IPL) modified from the original image in Garoutte (1981). ONL = outer nuclear layer, INL = inner nuclear layer, GCL = ganglion cell layer, OPL = outer plexiform layer, IPL = inner plexiform layer.

light availability to the photoreceptors and improves vision at low light levels. Generally, nocturnal animals and many deep-sea fish possess this structure.

The retina is a light sensitive layer lining the back of the eye, which consists of two separate layers, the RPE and the neural retina (Figure 2). The RPE provides structural and physiological support for the retina. Through the tight junctions, the RPE forms a blood-retinal barrier between the subretinal space and choriocapillaris (Ban and Rizzolo, 2000, Strauss, 2005). From the basal aspect of the cell, the RPE mediates the transfer of nutrients from the choroid to the photoreceptors and removes waste products including ions and water produced during the metabolic turnover in photoreceptors, and lactic acid produced by photoreceptor outer segments from the subretinal space to choriocapillaris (Steinberg, 1985, Hamann, 2002, Strauss, 2005). The pigmented cells of the RPE absorb scattered photons of light and enhance the quality of retinal images (Strauss, 2005). A main role of the RPE is to phagocytose photoreceptor outer segments and participate in the visual cycle via reisomerisation of all-*trans*-retinal back into 11-*cis*-retinal and transport back to photoreceptors for further availability (Steinberg, 1985, Nguyen-Legros and Hicks, 2000, Arshavsky, 2002, Strauss, 2005). The RPE is essential for the function and maintenance of the neural retina.

The neural retina plays a more direct and specific role in visual processing. The optically transparent neural retina consists of three nuclear layers separated by two synaptic layers (Figure 2). The visual process is initiated in the photoreceptor cells within this neural retina. The photons of light are converted into electrochemical signals in the outer retina. The G-protein coupled receptors in the photoreceptor outer segments are called opsins, which is the molecule that initially transforms the light evergy into an electrochemical signal. Opsins contain the chromophore 11-*cis*-retinal. When photons of light are introduced and excite the retinal, it undergoes a configuration change, also known as an isomerisation from 11-*cis* to all-*trans*. This change in conformation triggers the process of phototransduction and results in hyperpolarisation in the photoreceptor (Burns and Baylor, 2001, Arshavsky et al., 2002). This inital synaptic signal is followed by a sequence of events mediated by cells and synapses in the different layers that function to carry the visual signal to the brain.

The neural retina is composed of three nuclear layers: the outer nuclear layer (ONL), the inner nuclear layer (INL) and the ganglion cell layer (GCL) (Figure 2). The ONL contains the nuclei of rod and cone photoreceptors. Photoreceptor cell bodies that lie in the ONL synapse in the outer plexiform layer (OPL) with bipolar cells in vertical pathway of the retina where glutamate, a neurotransmitter is passed from photoreceptors to bipolar cells to ganglion cells transmitting signals - and with horizontal and amacrine cells in horizontal signal pathway, where reciprocal feed-back messages are sent to photoreceptors to regulate cell responses. The nuclei of those bipolar and horizontal cells are located in the INL. Also in the INL are the nuclei of amacrine cells, which mediate lateral processing of the visual signal, and Müller glial cells, which generally provide structural supports and metabolic processing. Cell bodies of ganglion cells, the projection neurons in the retina, are found in the INL (displaced ganglion cells) and the GCL. Ganglion cells synapse with bipolar and amacrine cells in inner plexiform layer (IPL). The GCL also includes the nuclei of displaced amacrine cells. Ganglion cell axons run in the nerve fiber layer (NFL) and exit the eye at the optic disc in which congregated signals are conveyed to the brain for processing.

ONL

The ONL of nearly all teleosts contains the nuclei of rods and cone photoreceptors although the ratios vary. Unlike mammals, the nuclei of rods and cones in teleosts are divided into two sublaminae within the ONL with rod nuclei laying vitreal to the cone nuclei (Fernald, 1988). There are some exceptions, for instance, in the pipefish (*C. paxtoni*) retina, the rod nuclei are located scleral to the cone nuclei (Collin and Collin, 1999). This arrangement in the pipefish (*C. paxtoni*) retina enables the large numbers of cone nuclei, bipolar and ganglion cells to spread over a wider retinal region without further increasing retinal thickness (Collin and Collin, 1999). Rods are specialised for dim light vision and contain an opsin that is maximally sensitive ~500 nm of light (Mosk et al., 2007). Cones are designed for daylight vision, high visual acuity and colour vision (Pignatelli et al., 2010). Teleosts contain multiple cone types, which are subdivided depending on the properties of the maximum absorption wavelength of the opsin expressed. In general, most teleosts have three opsins and two basic cone types, Short-

wavelength sensitive (SWS) single cones, and the double cones maximally sensitive to medium (MWS), and long wavelengths (LWS) (Walls, 1942, Mosk et al., 2007). The photoreceptor cell contains transversely arranged discs stacked on one another within its outer segment (Arshavsky et al., 2002). The stacks of discs in the outer segment form particular shapes from which the names, rod and cone were derived. Within the membrane of the discs, the photosensitive pigment, either rhodopsin in rods, or cone opsin in cones are present, which initiates phototransduction by absorbing photons of light. In humans, discs are produced at the junction between inner and outer segments and shed at the end of outer segments everyday in a 24-hour cycle (Strauss, 2005).

Among different types of cone photoreceptors (Lyall, 1957a), the most common cone photoreceptor type in diurnal fish, as well as reptiles and birds, is the double cone (Mosk et al., 2007, Pignatelli et al., 2010). Double cones are found in most vertebrate groups excluding agnathans, chondrichtyans, and placental mammals. The structure of a double cone is based on two single cones fused together, with each individual member having different spectral sensitivity (Harosi and MacNichol, 1974, Marchiafava, 1985). The cone photoreceptors have regular spatial arrangements including the most common pattern, a square mosaic where four double cones surround a central single cone as in the retina of the pipefish *C. paxtoni*, the sandlance *L. fasciatus* and African cichlid *Haplochromis burtoni* (Lyall, 1957a, Fernald, 1981, Collin and Collin, 1988a, 1999). Although the exact function of the double cones are as yet unknown, it has been suggested that this arrangement of double cones and/or the double cones themselves contribute to high acuity sampling and/or provides advantage in the prey detection as they are involved in achromatic tasks, such as luminance and/or contrast detection (Lythgoe, 1979, Marchiafava, 1985, Lythgoe and Partridge, 1989, Cummings and Partridge, 2001, Marshall and Vorobyev, 2003, Marshall et al., 2006), motion detection (in goldfish (*Carassius auratus*) (Schaerer and Neumeyer, 1996), zebrafish (*D. rerio)* (Krauss and Neumeyer, 2003) , the two spotted goby **(***Gobiusculus flavescens)* (Utne-Palm and Bowmaker, 2006) for review (Collin and Collin, 1999, Collin and Shand, 2003)) and polarisation vision (Lythgoe, 1979, Cameron and Pugh, 1991, Cameron and Easter, 1993, Hawryshyn et al., 2003, Marshall et al., 2006, Mosk et al., 2007, Kamermans and Hawryshyn, 2011). Double cones may likely to be

involved in colour vision although this has been debated (Lythgoe, 1979, Wikler et al., 1996, Campenhausen and Kirschfeld, 1998, Kroger et al., 2003, Marshall and Vorobyev, 2003, Marshall et al., 2003, Marshall et al., 2006, Utne-Palm and Bowmaker, 2006, Mosk et al., 2007, Siebeck et al., 2008, Pignatelli et al., 2010). Behavioural colour mixture experiments in goldfish demonstrate that the double cones are not involved in colour discrimination (*C. auratus*) (Neumeyer, 1986, 1992). Walls (1942) has also suggested that the double cones are associated with exposure to bright light as he observed that the relative number of double cones in teleosts decreased with an increase in habitat depth (Walls, 1942).

INL

The INL is composed of bipolar, amacrine, horizontal cell and displaced ganglion cell nuclei. Cajal (1909) initially described two kinds of bipolar cells based on morphology, a rod bipolar cell and a cone bipolar cell (Kaneko, 1970). The rod bipolar cells in fish synapse with both rods and cones, whereas the cone bipolar cells have exclusively contact cones (Stell, 1967, Kaneko, 1970). Functionally, there are two fundamentally different types of retinal bipolar cells classified according to the response properties to monochromatic light; ON-centre and OFF-centre (Kaneko and Hashimoto, 1969, Werblin and Dowling, 1969, Kaneko, 1973). Both types have antagonistic centre-surround organisation. This means that a small spot of light in the central receptive field leads to depolarisation in ON-centre bipolar cells and hyperpolarisation in OFF-centre bipolar cells. Both types of bipolar cells play crucial roles in the vertical transmission of information through the retina. ON- and OFF-centre bipolar cells have separate pathways to higher brain centres for independent image processing (Nelson and Connaughton, 2013). Each of them has both transient and sustained signal types postsynaptic to bipolar cells (Nelson and Connaughton, 2013).

Horizontal cells in the fish retina were initially described as brick-like structures occupying much of the inner nuclear layer (Niemeye and Gouras, 1973, Ammermuller et al., 1998). Cajal (1909) described three types of horizontal cells; the external horizontal cells in the most scleral part of the inner nuclear layer, the intermediate horizontal cells in the middle, and the internal horizontal cells in the most vitreal (Cajal, 1909, Kaneko, 1970). They form an

important link between inner and outer retina by controlling distal retinal signal processing (Perlman et al., 2012). The functions of horizontal cells include 1) generating spatially opponent receptive fields for second and third order neurons in the retina, 2) modulating the photoreceptor signal with different lighting conditions and 3) adjusting synaptic gain (Perlman et al., 2012). Horizontal cells synapse onto photoreceptors directly and influence the kinetics and spatial organisation of the photoreceptor response. As a consequence, the physiology of all downstream retinal neurons, distal colour opponency, centre-surround opponency, and gain regulation at the photoreceptor synapse is modulated. Horizontal cells are also under the influence of a centrifugal neuromodulatory control, and are able to reorganise their synaptic connections, glutamate sensitivity, and receptive field under the influence of dopamine, retinoic acid and nitric oxide (Perlman et al., 2012).

Amacrine cells of the teleost retina were studied in depth by Wagner and Wagner (1988). Amacrine cells are the main local circuit neurons in the IPL of the vertebrate retina. Light-evoked responses in amacrine cells are divided into two types, sustained and transient where the former is either depolarising 'on' or hyperpolarising 'off' (Werblin, 1970, Kaneko, 1973, Murakami and Shimoda, 1977). Amacrine cells synapse with every retinal neuron class except photoreceptors (interplexiform cells (Dowling and Ehinger, 1975), horizontal cells (Marshak and Dowling, 1987), centrifugal fibres (Marchiafava, 1976), and ganglion cells (Werblin and Dowling, 1969, Witkovsky and Dowling, 1969, West and Dowling, 1972). Amacrie cells establish radially and horizontally orientated local circuits and contribute to the modification of transmission from bipolar terminals to ganglion cell dendrites. In addition, amacrine cells shape the geometrical and dynamic properties of ganglion-cell receptive fields (Wagner and Wagner, 1988). In the teleost retina, amacrine cells have shown to exhibit chromatic components in their light-evoked responses (Kaneko, 1973, Mitarai et al., 1978).

Also present in the INL are the nuclei of Müller glial cells, the radial glia. Müller cells (Cajal, 1982, Peterson et al., 2001) are important for the glutamate/gluatmaine cycle and also critical for maintaining differentiated retinal structure and function (Bringmann et al., 2006). There have been extensive studies published on the possible functions of Müller cells in teleost retina. During normal development, Müller cells are associated with producing late-stage retinal

progenitors of the rod photoreceptor lineage (Julian et al., 1998, Otteson et al., 2001, Bernardos et al., 2007, Morris et al., 2008, Stenkamp, 2011) and the migration of rod progenitors from the INL into the ONL using the radial fibres of Müller glia (Raymond and Rivlin, 1987, Julian et al., 1998, Otteson et al., 2001, Raymond et al., 2006). In uninjured zebrafish (*D. rerio)* retina, Müller glia were suggested to function as multipotent retinal stem cells (Bernardos et al., 2007). Müller cells are also associated with retinal injury in teleost fish (Wu et al., 2001, Yurco and Cameron, 2005, Bernardos et al., 2007, Morris et al., 2008). They proliferate following the injury and produce the INL stem cells. These stem cells in the INL become the sources for new neurons in the regenerating retina and the type of cell population generated depends on the extent of damage (Wu et al., 2001, Yurco and Cameron, 2005). Their multipotency was also revealed from Pax6 expression, which marks retinal progenitor cells (Hitchcock et al., 1996, Otteson et al., 2001). Hence, the Müller cells have been suggested to be retinal stem cells in regenerating teleost retinas as well.

GCL

The GCL in teleost retina is composed of ganglion and displaced amacrine cell nuclei. Ganglion cells are known to convey the neural information from the photoreceptors via the INL to the brain. In the foveal region of teleost retina, ganglion to photoreceptor cell ratio is smaller compared that in the retinal periphery. Retinal ganglion cells can be classified into five main types based on their projections and functions including midget cells (parvocellular cells), parasol cells (magnocellular cells), bistratified cells (koniocellular cells) and photosensitive ganglion cells. There are various types of ganglion cells classified according to their morphology including dendritic field sizes, soma size and stratification (Mangrum et al., 2002, Pushchin et al., 2007).

Like ganglion cells, there are various types of amacrine cells present in teleost retina (Wagner and Wagner, 1988). In general, amacrine cells are found in the inner INL. However, there are some amacrine cells located within the GCL and they are called displaced amacrine cells (Perry and Walker, 1980, Wassle et al., 1987). Due to their closer location within the GCL, they are likely to influence the output activity of ganglion cells more strongly with their

inhibitory transmitters such as γ-amino-butyric acid (GABA) and glycine (Yazulla et al., 1986). Mack et al. (2004) have shown that the proportion of these displaced amacrine cells is reduced towards the centre of the teleost retina during development. They have suggested that these amacrine cells are migrating through the IPL to the INL (Mack et al., 2004).

1.3. MORPHOLOGICAL ASPECTS OF VISION

1.3.1. Retinal Topography

Retinal topography describes how the retinal neurons are distributed across the spatial surface of the retina. In many cases, the topography reflects the symmetry of an animal's perceived world and determines the spatial information of visual field projected onto the visual cortex. Topographical patterns have been considered as a unique 'fingerprint' of each teleost species (Collin, 1999) and therefore, each topographical pattern shows characteristics associated with the habitat. Visual behaviour such as ocular movements and adaptations to increase the visual field along certain axes may also contribute to the topographic patterning of cells (Collin, 1999). Most teleosts are known to possess some sort of retinal specialisation, which often take one of three different forms; visual streaks, *areae centrales* and *foveae* (Collin, 1999). Within the retinas of those teleost fish that possess retinal specialisations, photoreceptor and ganglion cells are distributed in an asymmetric pattern with distinct characteristics reflecting the perceived world.

According to the 'terrain theory' of Hughes (1977), the topography of ganglion cells in the teleost retina depends on the symmetry or openness of the visual world (Hughes, 1977, Collin and Pettigrew, 1988c). Species inhabiting open-water environments without visual interruptions on the horizon have been suggested to possess a temporal *area centralis* which may be extended to, or exist in conjunction with a horizontal band-shaped area of increased cell density, known as a 'horizontal streak' (Hughes, 1977, Collin and Pettigrew, 1988c, 1989, Collin and Shand, 2003). Examples of the topography of retinal ganglion cells have been shown in previous literature (Collin and Pettigrew, 1988c, 1989). Reef fishes such as the sharp-nosed weever fish *Parapercis cylindrica*, the clown triggerfish *Balistoides conspicillum*, the blue tuskfish *Choerodon albigena*, the painted flutemouth *Aulostoma chinensis*, the red-throated emperor *Lethrinus chrysostomas*, the collared sea bream *Gymnocranius bitorqua*tus, and the banded toado *Sphaeroides pleurostictus* possess a temporal *area centralis* and a strong horizontal streak (Collin and Pettigrew, 1988c, b). There are two different forms of the horizontal streak. The cyprinodontid *Fundulus heteroclitus* (Butcher, 1938) and two species of

mudskippers *Boleophthalmus* and *Periophthalmus* (Collin and Shand, 2003)) possess a band-shaped increase in retinal thickness across the retinal meridian while the balistids *Navodon modestus* (Ito and Murakami, 1984), *Balistoides conspicillum* (Collin and Pettigrew, 1988c) and the yellow-finned trevally *Caranx ignobilis* (Collin and Shand, 2003)) have increased cell densities (Collin, 1999).

Various functions of these horizontal streaks have been postulated. While the temporal area is thought to subserve binocular vision in feeding situations, it has been postulated that the horizontal streak is useful in scanning a broad sand-water or a water-air horizon without the distinctive eye movements (Collin and Pettigrew, 1988c) suggesting an important role in predatory surveillance of potential predators when swimming over areas of open water (Collin and Pettigrew, 1988c). Any small movements or changes either from prey or predators are likely to be exaggerated. This implies that the horizontal streak provides a lower threshold for movement detection (clown triggerfish *B. conspicillum*; (Collin and Pettigrew, 1988c)). The acute zone within the streak can be used in fish behaviour. For instance, the balistid *Navodon modestus* has a zone of peak ganglion cell density of over 16 000 cells per mm^2 located on the nasal margin of the visual streak. This zone was suggested to be used for fish to manoeuvre backwards (Ito and Murakami, 1984). It was also suggested that a streak provides an important cue for the stabilisation of a species in the water column.

Species inhabiting ‘enclosed’ environments with an interrupted view of their sand-water horizon are found to possess a concentric arrangement of iso-density lines of ganglion cells surrounding one or more *areae centrales* across their retina (Collin and Pettigrew, 1989). In general, acute vision in teleosts is achieved by an *area centralis* located in the temporal retina. Some species including the staghorn damselfish *Amblyglyphidodon curacao* possess multiple acute zones (Collin and Pettigrew, 1989). Each *area centralis* was suggested to have a unique function; for instance, the temporal and ventro-temporal *area centrales* are specialised for feeding as they receive visual information from the frontal space where as and the dorso-nasal specialisation is for predator surveillance by providing information from a caudal eccentric space (Collin and Pettigrew, 1988b, Collin, 1999). The concentric iso-density contours are also suggested to be associated with increased ocular motility as found in the coral cod

Cephalopholis miniatus, the blue angel fish *Pomacanthus semicirculatus* and the staghorn damselfish *A. curacao* (Collin and Pettigrew, 1988b). Other examples of 'enclosed' species include the Australian frogfish *Halophryne diemensis* and the sabre-toothed blenny *Dasson variabilis* (Collin and Pettigrew, 1988b). "Enclosed" species do not take advantages of the horizontal streak, which provides a panoramic visual field with high acuity. Rather, they have increased eye mobility to capture prey and observe potential predators (Collin, 1999). In actinopterygians, the presence and location of a retinal specialisation is associated with ocular mobility (Collin, 1999). It has been suggested that the presence of a fovea is related to independent eye movements (Walls, 1942, Fritsches and Marshall, 2002). In the retinas of 'enclosed' species, a weak horizontal streak is found in the ones that periodically venture out into open water (Collin and Pettigrew, 1988c). This weak horizontal streak may enable the fish to conduct surveillance of predators.

Both the horizontal streak and the *area centralis* may contain a pit-like structure, a fovea. A fovea may be shallow (concaviclivate) or deep (convexiclivate) in shape (Walls, 1942). This will be discussed in more detail in the next section.

1.3.2. Retinal Specialisations

A large number of fish including the syngnathids possess a retinal specialisation, which is responsible for high spatial visual resolution and hence, acute vision. Typically this specialisation is located at the centre of gaze which would be in the temporal retina in teleosts with laterally positioned eyes in respect to the head in order to subtend some part of the frontal binocular field (Collin, 1999). This specialisation is termed as an *area centralis*, or a *fovea centralis* when an indentation is present. This area is mostly characterised by the increased cell densities. In this section, I will concentrate on the *fovea centralis* as the syngnathid is known to possess this specialisation. The fovea can be categorised into two different groups morphologically; concaviclivate and convexiclivate (Slonaker, 1897, Walls, 1942). Concaviclivate foveal pits are shallow with a wide base and found in human (Hendrickson and Yuodelis, 1984, Hendrickson, 1992, Provis et al., 1998), pigeon (Galifret, 1968, Querubin et al.,

2009) and some teleosts including the banded toado *S. pleurostictus* (Collin and Shand, 2003) and the deep-sea teleosts *Bathylagus benedicti* (Collin and Shand, 2003). Convexiclivate foveal pits, on the other hand, are deep with steep sloping edges. They form a sharp pointed base and are commonly found in certain species of raptor including hawks, lizards (chameleon), and some fish including the seahorse *Hippocampus sp*. and the pipefish *C. paxtoni* (Slonaker, 1897, Walls, 1942, Galifret, 1968, Fite and Lister, 1981, Collin, 1997, Collin and Collin, 1999, Tucker, 2000, Boire et al., 2001, Mosk et al., 2007, Querubin et al., 2009). In general, the fovea is characterised as having distinctive morphological characteristics such as the presence of a retinal pit, absence of rod photoreceptors, increased cell densities in this region and low conversion ratios between the photoreceptors and the ganglion cells.

Collin and Collin (1999) subdivided teleosts fovea into four distinct types based on morphological, ecological and functional diversity. Type I fovea possesses a convexiclivate retinal pit without a lateral displacement of the inner retinal layers. It is found in the syngnathid such as the pipefish *C. paxtoni* (Collin and Collin, 1999), the bass *Paralabrax nebulifer* (Schwassmann, 1968) and the barred sand perch *Parapercis nebulosis* (Easter, 1992). Type II foveae are convexiclivate in shape, similar to a type I fovea; however, the inner retinal layers are displaced laterally and the underlying photoreceptor cells are exposed to the incident light. Examples of type II foveae include the sandlance *L. fasciatus* (Collin and Collin, 1988a) and notosudid *Scopelosaurus hoedti* (Munk, 1975, Collin and Shand, 2003). A type III fovea is also convexiclivate but contains a thick lining of radial fibre processes over the fovea. Examples are found in the deep-sea alepocephalids *Conocara macroptera* (Collin and Ali, 1994, Wagner et al., 1998) and *Alepocephalus bairdii* (Locket, 1992). The type IV fovea possesses a concaviclivate foveal pit with no lateral displacement of inner retinal layers and radial fibres. Type IV foveae are found in the banded toado *S. pleurostictus* (Collin and Shand, 2003) and the deep-sea teleost *B. benedicti* (Vilter, 1954, Collin and Shand, 2003).

The pipefish *C. paxtoni* is the closest relative of the seahorse. It possesses a type I fovea with a deep retinal pit characterised by the absence of rod photoreceptors, increased cell densities, a low summation ratio between the photoreceptors and the ganglion cells and high spatial resolving power (Collin and Collin, 1999). The exact function of this convexiclivate

fovea is unclear. There have been several suggestions including magnifying an image on the retina, detecting small angular movements, acting as a directional focus indicator and subserving high visual acuity. According to Walls (1942), the convexiclivate foveal pit magnifies the retinal image (Walls, 1942). He postulated that the steep walls of the foveal pit enhance the light refraction at the vitreous-retina border and this would magnify of images projected onto the photoreceptor array resulting in higher resolution. Pumphrey (1948) disputed this theory because the retinal image would be rather distorted as a result of the sharp changes in curvature at the centre of the foveal pit. He argued that this would reduce clarity. He suggested that the pointed centre of a convexiclivate fovea is effective in maintaining fixation and detecting small movements of objects in the visual field. The pointed centre of the pit allows an image of a point source to reach at the retina in different phases. Thin retinal layers let the image to arrive with a delay and to leave earlier in comparison to the surrounding thick slopes. This enhances movement detection ability (Pumphrey, 1948). Harkness and Bennet-Clark (1978) have also proposed that a convexiclivate fovea functions as a sensitive, directional focus indicator as refraction at the sharp foveal surface could provide sensitive unambiguous information on focus error (Harkness and Bennet-Clark, 1978). It has also been suggested that this convexiclivate fovea subserves high visual acuity. Raptors, such as hawks and eagles, possess two retinal specialisations for acute vision, a deep and a shallow fovea and it has been proposed that the deep fovea has higher acuity (Tucker, 2000).

1.4. FUNCTIONAL ASPECTS OF VISION

The functional aspects of teleost vision have been determined in various ways. Here, I will discuss two main categories: morphological calculations and experimental measures.

1.4.1. Biological measure of visual resolution

Visual acuity can be calculated from the histological/biological data and estimated from the resolving power of the lens and dioptric accommodation (Tamura (1957) in (Collin and Pettigrew, 1989)), but most commonly retinal cone photoreceptor cell density (Neave, 1984) and ganglion cell density with a lens diameter are taken into account (Collin and Pettigrew, 1989). It has been postulated that cone photoreceptors set the finite limit of vision and hence, the distance between two adjacent cone photoreceptors, the inter-cone spacing, is considered to be most important when determining visual acuity (Fernald, 1988). The inter-cone spacing generally decreases as fish grow. This results in the increased angular cell density as the eye enlarges (Fernald, 1988). It has been suggested that the photoreceptor cell density changes within the region of retinal specialisation is associated with the improvement of visual acuity during development in teleosts (Neave, 1984).

The theoretical limits of visual resolution can also be calculated using ganglion cell density values. Collin and Pettigrew (1989) used inter-ganglion cell distance in areas of highest ganglion cell density to calculate the spatial visual resolution of the animal (Collin and Pettigrew, 1989). The spatial distribution of the retinal ganglion cells was proposed to place an upper limit on the visual acuity as the retinal ganglion cell mosaic provides the only link between the eye and behavioural output (Collin and Pettigrew, 1989). Collin and Pattigrew along with other authors (Collin and Pettigrew, 1988c, b, 1989, Shand, 1997) suggested that the larger eye size with a corresponding larger lens diameter is correlated with better calculated visual acuity regardless of the ganglion cell density values (Collin and Pettigrew, 1989).

1.4.2. Behavioural measure of visual resolution

Using the behavioural responses of the animal, visual acuity and resolution can be measured behaviourally in experimental conditions. A variety of techniques are used which are customised to each animal species. The most popular method involves using either horizontal or vertical gratings (vertical gratings in goldfish (*C. auratus*) (Northmore and Dvorak, 1979) and optokinesis in teleost fish (Fritsches and Marshall, 2002)). Visual acuity in teleost fishes is commonly determined using the optokinetic response (OKR) (Rahmann et al., 1979, Neave, 1984, Beck et al., 2004, Hodel and Neuhauss, 2008, Haug et al., 2010, Mueller and Neuhauss, 2010, Tappeiner et al., 2012), optomotor responses (OMR) (Easter, 1972, Schaerer and Neumeyer, 1996, Krauss and Neumeyer, 2003, Orger et al., 2004), escape responses (Fleisch and Neuhauss, 2006), or two-alternative forced-choice procedure (Powers and Easter Jr, 1978, Bilotta and Powers, 1991, Schuster and Amtsfeld, 2002, Siebeck et al., 2008) including discrimination training experiments (Risner et al., 2006, Mueller and Neuhauss, 2012).

The OKR is a reflexive eye movement innate in all vertebrates (Haug et al., 2010, Mueller and Neuhauss, 2010). OKR stabilises visual gaze by matching eye rotation to the rotation of the visual surround (Fritsches and Marshall, 2002). A simple neuronal circuit allows OKR to be elicited independently of the optic tectum in teleosts or the cerebral cortex in mammals. Detection of OKRs can be automated and quantified which makes it a reliable tool to assess visual system properties including contrast sensitivity, visual acuity and temporal resolution. OKR has been also used for testing colour vision and motion detection ability (Beck et al., 2004, Haug et al., 2010, Mueller and Neuhauss, 2010, Zou et al., 2010). The OKR is composed of two different phases of eye movements: initially with tracking smooth pursuit eye movements in the direction of the moving stimulus, which is followed by resetting fast saccadic eye movements once the maximal deflection angle is reached. In general, vertical sinusoidal gratings of variable spatial frequencies are presented to the fish and their eye movements are recorded and analysed (Northmore and Dvorak, 1979, Fritsches and Marshall, 2002). The stimulus can be either a rotating drum fitted with black and white stripes or stripes projected onto a screen. The computer-based analysis enables a more complicated quantitative assay to

measure visual performances (Hodel and Neuhauss, 2008). The OKR has been frequently used to determine visual acuity (and to quantify other visual performances) in larval zebrafish (*D. rerio*) (Haug et al., 2010) and other fish of small sizes that would fit in a petridish (medaka (*Oryzias latipes*) (Mueller and Neuhauss, 2010)). It was only recently that a new technique was developed to measure the OKR of adult zebrafish (*D. rerio*) (Mueller and Neuhauss, 2010). The spatial visual resolution was found to be in the range from 0.04 to 0.35 cycles per degree at 70% contrast and at an angular velocity of 12 degrees per second (Mueller and Neuhauss, 2010).

The OMR is the whole-body responses of the fish to visual stimuli. Directionally moving grating of alternating black and white stripes elicits an OMR response in the larval zebrafish (*D. rerio*) (Maaswinkel and Li, 2003, Orger and Baier, 2005, Fleisch and Neuhauss, 2006). Fish swim in the direction of the moving stimuli, either following a leading or escaping a trailing stripe. OMR can be used as a measure of visual performance (e.g. (Maaswinkel and Li, 2003)- establishing the relationship between spatial and temporal frequencies in motion detection) as the absence of responsiveness to the moving grating implies that the fish cannot perceive the visual stimuli (Fleisch and Neuhauss, 2006). OMR has been used in visual testing for both larval and adult fish. In the larval stage, a group of fish can be tested simultaneously, whereas in the adult stage testing is done individually to avoid the schooling effect. The OMR is considered as colour-blind since it is based on the L-cone type (Schaerer and Neumeyer, 1996).

Similar to OMR, there is an escape response (Fleisch and Neuhauss, 2006). It is also an innate behaviour, which is generally elicited when a fish is threatened by a potential predator. Li and Dowling (1997) mimicked the potential threatening predator with a single black stripe on an otherwise white circular rotating drum for testing visual performance in the zebrafish (*D. rerio)* (Li and Dowling, 1997). The lack of response indicates that the fish cannot detect the target.

The two-alternative forced-choice procedure involves the psychophysical responses of a fish (Mueller and Neuhauss, 2010), which is conceptually identical to forced-choice preferential looking techniques used for infant vision testing (Teller, 1979). Upon the presence of a stimulus and a distracter, the fish is trained to select the stimulus. This technique has been used to determine different properties of visual system in teleosts including the spatial visual resolution and colour vision. When stimuli with variable spatial frequencies are presented, the limit of

visual resolution is determined when the fish is not able to discriminate the stimulus from the distracter (Bilotta and Powers, 1991, Siebeck et al., 2008). A two- alternative forced-choice training procedure is used for the detection of a small moving object (Gehres and Neumeyer, 2007).

Another technique that has been frequently used to measure visual resolution is the reactive distance (Wanzenbock and Schiemer, 1989, Miller et al., 1993). Reactive distance is the distance at which the fish responds behaviourally to prey (Wanzenbock and Schiemer, 1989). Visual acuity can be estimated from this reactive distance value if the prey size is known using simple trigonometric relations (Wanzenbock and Schiemer, 1989). O'Brien et al. (1990); however, disputed that the foraging strategy of the fish may bias the measurements of the reactive distances which therefore, underestimate visual acuity (O'Brien et al., 1990). They suggested that many fish use a pause-travel search strategy where they stop and scan their visual field for prey. The fish only search when they are stationary; therefore, the detected prey could be present at a random distance from the fish, which was limited by the maximum reactive distance (O'Brien et al., 1990, Miller et al., 1993). However, this method does not require physical restraining of fish and the experimental conditions mimic the natural prey-capturing environments. It also shows a linear size-dependent relation without significant species effects (Miller et al., 1993). This is one of the most common techniques used for determining the visual resolution in teleost fish. This technique is useful when the fish is larger in size, does not show consistent optomotor responses, or is harder to train for the two-alternative force-choice procedure.

The sandlance (*L. fasciatus*), the pipefish (*C. intestinalis*) and the seahorse (*Hippocampus spp.*) have similar oculomotor strategies of uncoupling of the eyes during optokinesis (Fritsches and Marshall, 2002). Fritsches and Marshall (2002) described various eye movements of fishes including conjugate (moving the eyes in the same direction), vergent (moving the eyes in opposite directions), and independent eye movements. The three species commonly have chameleon-like spontaneous, independent eye movements (Walls, 1942, Pettigrew et al., 1999, Pettigrew et al., 2000, Fritsches and Marshall, 2002) unlike in most other fish including the goldfish (*C. auratus*) (Easter, 1972) that have restricted yoked/conjugate

ocular motility. As ambush predators, they can detect prey using their eyes in stationary postures. They use monocular parallax cues created with eye rotation and this special design enables the fish to be stable while observing or detecting stimuli (Land, 1995, Land, 1999). Both the sandlance (*L. fasciatus*) and the pipefish (*C. intestinalis*) exhibit optokinetic responses of slow tracking and fast fixational saccades to a moving grating, which also strongly suggests the presence of a fovea, and hence high visual acuity (Fritsches and Marshall, 2002). In addition to the saccades (fast resetting eye shifts), smooth pursuit movements (that follow moving objects) and vergence (which adjusts the eyes for different viewing distances), the independent eye movement is associated with the presence of a retinal specialisation, an *area centralis* or a *fovea* which is responsible for a high visual resolution (Walls, 1942, Collin and Shand, 2003). The acuity also depends on the feeding strategies (Collin and Pettigrew, 1989). Collin and Pettigrew (1989) found that the species which ambush their prey have higher acuities compared to the species that graze on encrusting organisms or slow-moving prey on or near the substrate (Collin and Pettigrew, 1989).

1.5. VISUAL DEVELOPMENT IN FISH

1.5.1. Morphological Changes during Development

Unlike mammals, cold-blooded vertebrates including frogs, toads, newts and fishes possess continuously growing eyes throughout their lifetime (Müller, 1952, Scholes, 1976, Johns, 1977, Johns and Easter, 1977, Meyer, 1978). This enlargement of the eye in fish is strongly associated with the increase in their body length (Fernald, 1988). Johns and Easter (1977) quantitatively established that the retinal area increased from 20 to 120 mm^2 while the body length increased from 5 to 20 cm in the goldfish (*C. auratus*) (Johns and Easter, 1977). It has been proposed that this enlargement is attributed by the combination of two mechanisms; first, the addition of new neurons (Müller, 1952, Johns and Easter, 1977, Otteson and Hitchcock, 2003, Hitchcock and Raymond, 2004) and second, the stretching of the existing retinal tissues (Lyall, 1957a, Johns, 1977, Johns and Easter, 1977, Otteson and Hitchcock, 2003, Hitchcock and Raymond, 2004).

Wunder (Wunder, 1926, Hoke and Fernald, 1997) was the first to propose the addition of new neurons in the retina after development. From microscopic examination, he proposed that cell division must occur at the margin of the teleost eye, although he was unable to find mitotic figures to support his hypothesis. Based on the histological appearance and the presence of mitotic figures observed with advanced techniques, the germinal zone at the retinal margin at the ora serrata, the junction between the neural retina and the iris epithelium was further recognised in 1950's as a location with active cell division occurring (Müller, 1952, Lyall, 1957a). This region is known as the ciliary marginal zone or circumferential germinal zone (CGZ) (Lyall, 1957b, Otteson and Hitchcock, 2003, Hitchcock and Raymond, 2004, Raymond et al., 2006, Morris et al., 2008) and in teleost retina most new neuronal cells are continually generated here throughout the life of the fish (Raymond and Rivlin, 1987, Fernald, 1988, Otteson and Hitchcock, 2003)). In the early 1970's, new techniques using ^{3}H-thymidine were introduced that further enabled the identification of cells (Hollyfield, 1972, Gratzner et al., 1975, Scholes, 1976, Johns, 1977, Meyer, 1978, Sharma and Ungar, 1980, Gratzner, 1982, Hoke and Fernald, 1997). ^{3}H-thymidine is a radioactively labelled deoxyribonucleic acid (DNA) precursor

incorporated into DNA of the dividing cells during the DNA synthesis phase of the mitotic cycle. Dividing cells are detected using autoradiography or scintillation counting. This technique shows the time at which cells become postmitotic during development (Barrow Heaton, 1982). Hollyfield (1972) used ^{3}H-thymidine to label cells that had completed mitotic division between injection and sacrifice (Hoke and Fernald, 1997). Various survival periods following an injection of ^{3}H-thymidine have been used to study proliferating cells and their progeny (Raymond and Rivlin, 1987). From experiments looking at the histogenesis of *Fundulus heteroclitus* retina as well as older animals, Hollyfield reported the labelled cell nuclei near the margin of the retina (Hollyfield, 1972, Hoke and Fernald, 1997).

Bromodeoxyuridine (5-bromo-2'-deoxyuridine, BrdU) was developed as an alternative to ^{3}H-thymidine autoradiography in the mid 1970's (Gratzner et al., 1975, Johns, 1977, Meyer, 1978, Gratzner, 1982, Stenkamp et al., 1997). BrdU is a synthetic analogue of thymidine that substitutes for thymidine during the Synthesis (S) phase of the cell cycle when DNA replication occurs. Antibodies specific for BrdU label the cells that have replicated their DNA. This technique allows for a more rapid processing of slides in order to measure cell kinetics as compared to the lenghthy time necessary to expose ^{3}H-thymidine during the autoradiography process (Gratzner et al., 1975). BrdU has been used for labelling and fate-mapping the proliferating cells in the teleost retina including the zebrafish (*D. rerio)* and the goldfish (*C. auratus*) (Raymond et al., 2006). Both ^{3}H-thymidine autoradiographic and BrdU imminocytochemistrical techniques further demonstrated the presence of CGZ (Johns, 1977, Meyer, 1978, Fernald, 1988, Julian et al., 1998, Raymond et al., 2006).

Recently, it has been shown that all neuronal cell types excluding rod photoreceptor cells are added in the CGZ (Otteson and Hitchcock, 2003, Hitchcock and Raymond, 2004, Morris et al., 2008). As demonstrated in Figure 3, the germinal cells located in the CGZ are fusiform shaped. The addition of new neurons in the CGZ follows the characteristic spatial ordering observed during retinal development. Therefore, mature cells reside more central retina compared with newly generated cells, which lie closer to the CGZ (Meyer, 1978, Otteson and Hitchcock, 2003). These results demonstrate the growth pattern of retina during development (Müller, 1952, Johns and Easter, 1977, Kock, 1982, Easter, 1992). From the first cell counting

Figure removed due to copyright restrictions.

Figure 3 : Model of retinal neurogenesis and the generation of rod photoreceptors in the retinas of teleosts

Figure 1 from Otteson and Hitchcock (2003) illustrating retinal neurogenesis and rod photoreceptor lineage. The CGZ is present at the teleosts retinal margin (shown in red on the hemisphere) where all the retinal neurons are generated (clusters of cells in red at the retinal margin) except rod photoreceptors. Rod photoreceptors are generated from more centrally located INL stem cells (red round dots sparsely located at the inner margin of INL). These cells transform into more elongated INL progenitors (shown in white) which migrate from INL to ONL becoming rod precursors, then rod photoreceptors (illustrated in the panel on the right). CGZ = circumferential germinal zone, ONL = outer nuclear layer, INL = inner nuclear layer, GCL = ganglion cell layer, MR = mature retina.

studies in ^{3}H-thymidine labelled retinas of growing urodeles (Mö11er, 1950, Hoke and Fernald, 1997)) and four size classes of the guppy *Lebistes reticulates* (Müller, 1952, Otteson and Hitchcock, 2003), Müller found that the absolute number of all cell types such as ganglion cells, inner nuclear layer cells, rods and cones increased. He showed the ratio of other cell types to ganglion cells during the fish's development. He reported that while the fish size increased four-fold in length, the ratio of rods to ganglion cells increased by 250% as compared to that of inner nuclear layer cells - 12% - or even that of cones which remained constant (Otteson and Hitchcock, 2003). He also reported that despite the absolute number of cells increasing, the densities of ganglion and cone photoreceptors decreased in all species he studied (Hoke and Fernald, 1997). Johns and Easter (1977) agreed that the density of all other retinal neurons decreases, but they observed that the rod density remains constant with growth in the developing goldfish (*C. auratus*) retina (Johns and Easter, 1977, Hoke and Fernald, 1997, Mueller and Neuhauss, 2010). These observations led to the conclusion that the existing retinal tissue expands by the addition of new rods (Easter, 1992, Fadool, 2003, Otteson and Hitchcock, 2003, Morris et al., 2008).

Rod photoreceptors do not follow the general histogenesis pattern of other neuronal cells. Müller (1952) once suggested that the rod photoreceptors are generated only from the marginal zone and migrated into the centre of the retina following the observation of mitotic figures only in the marginal zone (Müller, 1952, Hoke and Fernald, 1997). In contrast to the other neurons that are generated in the CGZ, rod photoreceptors are added across the differentiated central retina (Johns, 1977, Fernald and Johns, 1980, Johns and Fernald, 1981, Fernald, 1988, Collin and Shand, 2003, Otteson and Hitchcock, 2003, Hitchcock and Raymond, 2004). The source of these newly added rod photoreceptors were observed in the ONL of fish retina using autoradiography and termed rod progenitors in the goldfish (*C. auratus*) and the cichlid (*H. burtoni*) retinas (Scholes, 1976, Meyer, 1978, Johns and Fernald, 1981, Johns, 1982, Morris et al., 2008).

Where did these rod progenitors originate? Various techniques including ^{3}H-thymidine followed by BrdU injections coupled with electron microscopy demonstrated that there were two proliferating cells that were located in different regions of the larval teleost retina.

Proliferating cells are found as clusters in the INL and single scattered cells in the ONL (Raymond and Rivlin, 1987). These Pax6-positive more slowly differentiating cells in the INL are spindle shape and arranged perpendicularly to the retinal laminae (Hitchcock et al., 1996, Otteson et al., 2001). These slowly-dividing INL cells have been suggested to be the true neuroretinal stem cells of the retina which possess regenerating properties (Raymond et al., 1988, Fadool, 2003, Otteson and Hitchcock, 2003, Morris et al., 2008).

The proliferating cells in the INL were closely associated with Müller fibres although there were cells found to be migrating from the INL across the OPL into the ONL (Raymond and Rivlin, 1987, Hitchcock and Raymond, 2004) to generate rods (Raymond and Rivlin, 1987, Julian et al., 1998, Otteson et al., 2001, Hitchcock and Raymond, 2004, Morris et al., 2008). Rod progenitors were more rounded in shape and occured singly or in pairs (Raymond and Rivlin, 1987). As their name implies, they differentiate exclusively only into rod photoreceptors (Hitchcock and Raymond, 2004, Morris et al., 2008).

During development, rod photoreceptors are the last cells to be differentiated during the secondary phase of neurogenesis (Johns, 1982, Raymond, 1985a); however, there is also a prolonged process by which rod photoreceptor generation is continued throughout the lifetime of the fish (Blaxter and Jones, 1967, Blaxter and Staines, 1970, Johns and Fernald, 1981, Johns, 1982). This delayed but prolonged addition of new rods occurs at a faster rate compared to the retinal expansion, which results in the increase in cell numbers as well as cell density (Müller, 1952, Johns and Easter, 1977, Johns, 1982).

The continual addition of new neurons at the margins of the retina during retinal enlargement creates an annular pattern of cell generation. Easter (1992) demonstrated the retinal growth pattern of 15 different teleost families (Easter, 1992) and categorised the teleost families into two different groups according to whether the retinas grew symmetrically or asymmetrically. Teleosts, which lack a retinal specialisation characterised by increased cell densities, had symmetrical retinal growth. The symmetry was indicated by the uniform space between any pair of annuli at all positions along their arcs. On the other hand, teleost retinas with a temporally positioned fovea grew asymmetrically. The space between adjacent annuli was not uniform, but narrowest temporodorsally where a retinal specialisation is located. The

space between adjacent annuli was widest in the opposite nasoventral region. This indicated the nasal half of the retina enlarged the most during growth in order to preserve the location of the fovea to the temporal retina (Easter, 1992). Two different mechanisms of this asymmetrical retinal growth were hypothesised. Cameron (1995) demonstrated that the green sunfish *Lepomis cyanellus* has asymmetrical retinal growth during development and postulated that this asymmetry resulted from differential addition of new retinal neurons (Cameron, 1995). More cells were added in ventronasal retina compared to dorsotemporal retina. Zygar et al. (1999) on the other hand, suggested that the nasotemporal asymmetrical retinal growth is due to a faster rate of expansion at the nasal pole of the eye as the absolute number of cells added is approximately equal at all margins of the African cichlid *H. burtoni* retina (Zygar et al., 1999).

Rod photoreceptors, like other cell types produced at the CGZ, are added asymmetrically into the central retina (Cameron, 1996). Fewer rod photoreceptors are added in the temporal quadrant compared to the other quadrant and this asymmetrical growth pattern was suggested to be regulated by a retinotopic mechanism that is independent of body-axis coordinates (Cameron, 1996). This differential addition and expansion of the retina implies the presence of underlying mechanisms to preserve a temporal retinal specialisation.

Another mechanism that was suggested to occur during teleost retinal development was apoptosis. In general, apoptosis, as a widespread, physiological phenomenon, occurs to regulate the size of the cell population during the embryonic development and adult life of multicellular organisms (Biehlmaier et al., 2001). Among teleost fish, cell death in the retina was investigated in the embryonic and adult zebrafish (*D. rerio)* and the African cichlid (*H. burtoni*) (Hoke and Fernald, 1998). In the zebrafish (*D. rerio)* retina, apoptotic processes were detected in GCL and INL first at around 3-4 days post-fertilisation (dpf) (Biehlmaier et al., 2001). In the ONL, photoreceptor apoptosis began at 5 dpf and peaked at 7 dpf (Biehlmaier et al., 2001). In the African cichlid *H. burtoni*, Hoke and Fernald (1998) observed that during embryonic development, peak apoptosis in the central retina occured in advance of rod photoreceptor neurogenesis and after that cell death is significantly reduced (Hoke and Fernald, 1998). In the adult retina, no such pattern existed at the proliferating CGZ (Hoke and Fernald, 1998). From this change in apoptotic patterning with growth, they suggested that apoptosis is likely not an

important factor in establishing cell type distribution. A slow rate of cell generation and differentiation at the adult retinal margin allowed more precise production of cells (Hoke and Fernald, 1998).

1.5.2. Functional Changes during Development

Behavioural studies of various teleosts demonstrated the improvement of visual resolution as the size of fish increased during development (Otten, 1980, Hairston et al., 1982, Neave, 1984, Fernald, 1990, Miller et al., 1993, Pankhurst et al., 1993, van der Meer, 1995, Wanzenböck et al., 1996). A rapid development of behavioural acuity occurred during the early free-swimming phases of teleost fishes (Rahmann et al., 1979, Schmitt and Kunz, 1989, Pankhurst et al., 1993). This functional change may result from the structural maturation in the retina itself, including neuronal circuitry and in the neuronal projections to the higher-order processing centres in the brain (Rahmann et al., 1979, Schmitt and Kunz, 1989, Shand et al., 1999).

Various hypotheses have been put forward concerning the improvement of visual resolution during growth in teleosts. First, better visual resolution requires a higher angular density of cones (Guma'a, 1982, Fernald, 1988, Pankhurst et al., 1993). Despite the decrease in the actual density of cone photoreceptors, the angular density increases during development. An enlarged eye and increased lens size generate a longer focal length, which allows for the image to fall on an enlarger retinal area. This means that a larger number of cones per visual angle were stimulated resulting in a magnified retinal image and hence, better visual resolution (Easter et al., 1977, Guma'a, 1982, Neave, 1984, Browman et al., 1990, Pankhurst et al., 1993). The increased diameter of cone photoreceptor outer segments during development (Blaxter and Jones, 1967, Guma'a, 1982, Pankhurst and Montgomery, 1990, Pankhurst et al., 1993) in addition to the decreased inter-cone spacing (Collin and Pettigrew, 1989) has also been postulated to contribute to the enhanced sensitivity and visual acuity with the increased chances of photon capture (Pankhurst et al., 1993). (Collin and Pettigrew, 1989). However, further

improvement in visual resolution is limited by the constraints set by size at which light spills onto adjacent photoreceptors (Lythgoe, 1980).

From the theoretical visual resolution calculated based on the ganglion cell density, Collin and Pettigrew (1989) reported that acuities vary directly with eye size and lens diameter; whilst ganglion cell densities play a lesser role in determining visual acuity (Hairston et al., 1982, Collin and Pettigrew, 1989). Their thypothesis suggests that teleost species with larger eye sizes have better visual resolution (Collin and Pettigrew, 1989). Several behavioural studies have confirmed a positive correlation between intraspecific eye size and visual prey detection (Hairston et al., 1982, Breck and Gitter, 1983, Li et al., 1985).

As predicted from morphological development, the behaviourally measured visual resolution in teleosts improves as the fish grows (Hairston et al., 1982, van der Meer, 1995, Wanzenböck et al., 1996, Haug et al., 2010). Changes in the refractive state during development are believed to be one of the contributions to this improvement (Pankhurst et al., 1993). Teleost fish are considered to be strongly myopic and become more emmetropic as they mature (Pankhurst et al., 1993, Pankhurst, 1994, Shand et al., 1999) although Easter & Nicola (1996) demonstrated that the larval zebrafish (*D. rerio)* is initially hyperopic and become emmetropic (Easter and Nicola, 1996). The temporal retinal specialisation of the elliptical eye has a longer lens-to-retina distance and this region is considered to be more myopic, whereas elsewhere would be hypermetropic (Collin, 1999). The mature fish become able to compensate for potential refraction errors (myopia) caused by Matthiessen's ratio – the distance from lens centre to retina (posterior nodal distance, PND) is 2.55 times the radius of the lens (Matthiessen, 1880) - via a more developed accommodative system (Sivak, 1974, Pankhurst, 1994) including the stabilisation of Matthiessen's ratio (Matthiessen, 1880, Walls, 1942, Collin and Pettigrew, 1989) and maturation of the retractor lentis muscle (Shand et al., 1999). Furthermore, other morphological and structural maturation in the retina and connection to the higher order processing centres in the brain results in the changes of refractive state (Pankhurst, 1994, Wanzenböck et al., 1996). Therefore, the adult fish have better behavioural visual resolution compared to the larval fish.

Summary and Aims

In summary, the retinae of teleosts from various environments display characteristics related to their habitat including the presence or absence of various types of retinal specialisations and the degree of uniform retinal cell type distribution. Spatial visual acuities have been estimated either from morphological parameters or from behavioural vision testing. The morphological parameters include the lens diameter and the photoreceptor or ganglion cell densities. Various techniques have been used for behavioural vision testing. Both theoretically and behaviourally estimated visual resolution improves as the fish grows. Photopic visual acuity improves with the larger solid angle viewed by the eye, the smaller cone photoreceptor spacing across the retina, and the smaller convergence of cones onto higher-order processing cells (Fernald, 1988).

In this thesis, I investigated the development of the seahorse retina and visual resolution. Two species of adult seahorses (a temperate *H. abdominalis* and a tropical *H. taeniopterus*) were compared. The morphological and functional characteristics of their retinal specialisation were investigated and the correlation between the morphological and functional aspects of vision was evaluated. Second, the morphological and behavioural development of *H. taeniopterus* fovea and visual resolution was investigated. Finally, the developmental changes occurring in the fovea as compared with the improvements in visual resolution were studied in five different age groups of *H. taeniopterus* with an emphasis on the rod-free zone. My data have contributed to a better understanding of the seahorse visual system and its development with a particular interest in the retinal specialisation, the fovea. Seahorses, therefore, has the potential to become another animal model system for developmental studies of the fovea. Furthermore, as the prey capturing activities in seahorses rely on vision, better understanding of their visual system may provide a better chance of survival.

References

Ammermuller J, Itzhaki A, Weiler R, Perlman I (1998) UV-sensitive input to horizontal cells in the turtle retina. Eur J Neurosci 10:1544-1552.

Arshavsky V (2002) Like night and day: rods and cones have different pigment regeneration pathways. Neuron 36:1-3.

Arshavsky VY, Lamb TD, Pugh EN, Jr. (2002) G proteins and phototransduction. Annu Rev Physiol 64:153-187.

Ban Y, Rizzolo LJ (2000) Differential regulation of tight junction permeability during development of the retinal pigment epithelium. Am J Physiol Cell Physiol 279:C744-750.

Barrow Heaton M (1982) A technique for improved resolution of [3H]thymidine autoradiography in the avian embryo: a preliminary report. Journal of Neuroscience Methods 5:61-72.

Beck JC, Gilland E, Tank DW, Baker R (2004) Quantifying the ontogeny of optokinetic and vestibuloocular behaviors in zebrafish, medaka, and goldfish. J Neurophysiol 92:3546-3561.

Bergert BA, Wainwright PC (1997) Morphology and kinematics of prey capture in the syngnathid fishes Hippocampus erectus and Syngnathus floridae. Marine Biology 127:563-570.

Bernardos RL, Barthel LK, Meyers JR, Raymond PA (2007) Late-Stage Neuronal Progenitors in the Retina Are Radial Müller Glia That Function as Retinal Stem Cells. The Journal of Neuroscience 27:7028-7040.

Biehlmaier O, Neuhauss S, Kohler K (2001) Onset and time course of apoptosis in the developing zebrafish retina. Cell Tissue Res 306:199-207.

Bilotta J, Powers MK (1991) Spatial contrast sensitivity of goldfish: Mean luminance, temporal frequency and a new psychophysical technique. Vision Research 31:577-585.

Blaxter JHS, Jones MP (1967) The Development of the Retina and Retinomotor Responses in the Herring. Journal of the Marine Biological Association of the United Kingdom 47:677-697.

Blaxter JHS, Staines M (1970) Pure-Cone Retinae and Retinomotor Responses in Larval Teleosts. Journal of the Marine Biological Association of the United Kingdom 50:449-464.

Blumer LS (1979) Male Parental Care in the Bony Fishes. The Quarterly Review of Biology 54:149-161.

Boire D, Dufour JS, Theoret H, Ptito M (2001) Quantitative analysis of the retinal ganglion cell layer in the ostrich, Struthio camelus. Brain Behav Evol 58:343-355.

Bowmaker JK, Govardovskii VI, Shukolyukov SA, Zueva LV, Hunt DM, Sideleva VG, Smirnova OG (1994) Visual pigments and the photic environment: the cottoid fish of Lake Baikal. Vision Res 34:591-605.

Breck JE, Gitter MJ (1983) Effect of fish size on the reactive distance of bluegill (Lepomis macrochirus) sunfish. Can J Fish Aquat Sci 40:162-167.

Bringmann A, Pannicke T, Grosche J, Francke M, Wiedemann P, Skatchkov SN, Osborne NN, Reichenbach A (2006) Muller cells in the healthy and diseased retina. Prog Retin Eye Res 25:397-424.

Browman HI, Gordon WC, Evans BI, O'Brien WJ (1990) Correlation between histological and behavioral measures of visual acuity in a zooplanktivorous fish, the white crappie (Pomoxis annularis). Brain Behav Evol 35:85-97.

Burns ME, Baylor DA (2001) Activation, deactivation, and adaptation in vertebrate photoreceptor cells. Annu Rev Neurosci 24:779-805.

Butcher EO (1938) The structure of the retina of fundulus heteroclitus and the regions of the retina associated with the different chromatophoric responses. Journal of Experimental Zoology 79:275-297.

Cajal SR (1909) Histologie du système nerveux de l'homme & des vertébrés. Paris: A. Maloine.

Cajal SR (1982) La retina de los teleosteos y algunas observaciones sobre la de los vertebrados superiores. Anales Sociedad Esppanola de Historia Natural Madrid 21:281-305.

Cameron DA (1995) Asymmetric retinal growth in the adult teleost green sunfish (Lepomis cyanellus). Vis Neurosci 12:95-102.
Cameron DA (1996) Asymmetric retinal growth: evidence for regulation by a retinotopic mechanism. Vis Neurosci 13:493-500.
Cameron DA, Easter SS (1993) The cone photoreceptor mosaic of the green sunfish, Lepomis cyanellus. Visual Neuroscience 10:375-384.
Cameron DA, Pugh EN (1991) Double cones as a basis for a new type of polarization vision in vertebrates. Nature 353:161-164.
Campenhausen MV, Kirschfeld K (1998) Spectral sensitivity of the accessory optic system of the pigeon. J Comp Physiol A 183:1-6.
Choo CK, Liew HC (2006) Morphological development and allometric growth patterns in the juvenile seahorse Hippocampus kuda Bleeker. Journal of Fish Biology 69:426-445.
Collin HB, Collin SP (1995) Ultrastructure and organisation of the cornea, lens and iris in the pipefish, Corythoichthyes paxtoni (Syngnathidae, Teleostei). Histol Histopathol 10:313-323.
Collin HB, Collin SP (1996) The fine structure of the cornea of the salamanderfish, Lepidogalaxias salamandroides (Lepidogalaxiidae, Teleostei). Cornea 15:414-426.
Collin SP (1997) Specialisations of the teleost visual system: adaptive diversity from shallow-water to deep-sea. Acta Physiol Scand Suppl 161:5-24.
Collin SP (1999) Behavioural ecology and retinal cell topography. In: Adaptive Mechanisms in The Ecology of Vision (Archer, S. N. et al., eds), pp 509-535 Dordrecht: Kluwer Academic Publishers.
Collin SP, Ali MA (1994) Multiple areas of acute vision in two freshwater teleosts, the creek chub, Semotilus atromaculatus (Mitchill) and the cutlips minnow, Exoglossum maxillingua (Lesuer). Can J Zool 72:721-730.
Collin SP, Collin HB (1988a) The morphology of the retina and lens of the sandlance, Limnichthyes fasciatus (Creeiidae). Exp Biol 47:209-218.
Collin SP, Collin HB (1999) The foveal photoreceptor mosaic in the pipefish, Corythoichthyes paxtoni (Syngnathidae, Teleostei). Histol Histopathol 14:369-382.
Collin SP, Pettigrew JD (1988b) Retinal Topography in Reef Teleosts, I. Some Species with Well-Developed Areae but Poorly-Developed Streaks. Brain Behav Evol 31:269-282.
Collin SP, Pettigrew JD (1988c) Retinal Topography in Reef Teleosts, II. Some Species with Prominent Horizontal Streaks and High-Density Areae. Brain Behav Evol 31:283-295.
Collin SP, Pettigrew JD (1989) Quantitative Comparison of the Limits on Visual Spatial Resolution Set by the Ganglion Cell Layer in Twelve Species of Reef Teleosts. Brain Behav Evol 34:184-192.
Collin SP, Shand J (2003) Retinal Sampling and the Visual Field in Fishes. In: Sensory Processing in Aquatic Environments (Collin, S. P. and Marshall, N. J., eds), pp 139-169 New York: Springer Verlag.
Cummings ME, Partridge JC (2001) Visual pigments and optical habitats of surfperch (Embiotocidae) in the California kelp forest. J Comp Physiol A Neuroethol Sens Neural Behav Physiol 187:875-889.
Dowling JE, Ehinger B (1975) Synaptic organization of the amine-containing interplexiform cells of the goldfish and Cebus monkey retinas. Science 188:270-273.
Easter SS, Jr. (1972) Pursuit eye movements in goldfish (Carassius auratus). Vision Res 12:673-688.
Easter SS, Jr. (1992) Retinal growth in foveated teleosts: nasotemporal asymmetry keeps the fovea in temporal retina. J Neurosci 12:2381-2392.
Easter SS, Jr., Johns PR, Baumann LR (1977) Growth of the adult goldfish eye--I: Optics. Vision Res 17:469-477.
Easter SS, Jr., Nicola GN (1996) The development of vision in the zebrafish (Danio rerio). Dev Biol 180:646-663.
Fadool JM (2003) Development of a rod photoreceptor mosaic revealed in transgenic zebrafish. Developmental Biology 258:277-290.
Fernald RD (1981) Chromatic organization of a cichlid fish retina. Vision Res 21:1749-1753.

Fernald RD (1988) Aquatic adaptations in fish eyes. In: Sensory Biology of Aquatic Animals (Atema, J. et al., eds), pp 435-466 Berlin: Springer.
Fernald RD (1990) Teleost vision: seeing while growing. J Exp Zool Suppl 5:167-180.
Fernald RD, Johns PR (1980) Retinal structure and growth in the cichlid fish, *Haplochromis burtoni*. Invest Ophthalmol Vis Sci supp.:69.
Fernald RD, Wright SE (1985) Growth of the visual system in the African cichlid fish, Haplochromis burtoni. Optics. Vision Res 25:155-161.
Fite KV, Lister BC (1981) Bifoveal vision in anolis lizards. Brain Behav Evol 19:144-154.
Fite KV, Rosenfield-Wessels S (1975) A Comparative Study of Deep Avian Foveas. Brain, Behavior and Evolution 12:97-115.
Fleisch VC, Neuhauss SC (2006) Visual behavior in zebrafish. Zebrafish 3:191-201.
Foster SJ, Vincent ACJ (2004) Life history and ecology of seahorses: implications for conservation and management. Journal of Fish Biology 65:1-61.
Fritsches KA, Marshall NJ (2002) Independent and conjugate eye movements during optokinesis in teleost fish. J Exp Biol 205:1241-1252.
Galifret Y (1968) Les diverses aires fonctionnelles de la retine du pigeon. Z Zellforsch Mikrosk Anat 86:535–545.
Gehres M, Neumeyer C (2007) Small field motion detection in goldfish is red-green color blind and mediated by the M-cone type. Vis Neurosci 24:399-407.
Gratzner HG (1982) Monoclonal antibody to 5-bromo- and 5-iododeoxyuridine: A new reagent for detection of DNA replication. Science 218:474-475.
Gratzner HG, Leif RC, Ingram DJ, Castro A (1975) The use of antibody specific for bromodeoxyuridine for the immunofluorescent determination of DNA replication in single cells and chromosomes. Experimental Cell Research 95:88-94.
Guma'a SA (1982) Retinal development and retinomotor responses in perch, Perca fluviatilis L. Journal of Fish Biology 20:611-618.
Hairston NG, Jr., Li KT, Easter SS, Jr. (1982) Fish vision and the detection of planktonic prey. Science 218:1240-1242.
Hamann S (2002) Molecular mechanisms of water transport in the eye. In: International Review of Cytology, vol. Volume 215 (Thomas Zeuthen, W. D. S., ed), pp 395-431: Academic Press.
Harkness L, Bennet-Clark HC (1978) The deep fovea as a focus indicator. Nature 272:814-816.
Harosi FI, MacNichol EF, Jr. (1974) Visual pigments of goldfish cones. Spectral properties and dichroism. J Gen Physiol 63:279-304.
Haug MF, Biehlmaier O, Mueller KP, Neuhauss SC (2010) Visual acuity in larval zebrafish: behavior and histology. Front Zool 7:8.
Hawryshyn CW, Arnold MG, Chaisson DJ, Martin PC (1989) The ontogeny of ultraviolet photosensitivity in rainbow trout (Salmo gairdneri). Vis Neurosci 2:247-254.
Hawryshyn CW, Moyer HD, Allison WT, Haimberger TJ, McFarland WN (2003) Multidimensional polarization sensitivity in damselfishes. J Comp Physiol A Neuroethol Sens Neural Behav Physiol 189:213-220.
Hendrickson A (1992) A morphological comparison of foveal development in man and monkey. Eye 6 (Pt 2):136-144.
Hendrickson AE, Yuodelis C (1984) The morphological development of the human fovea. Ophthalmology 91:603-612.
Hitchcock PF, Macdonald RE, VanDeRyt JT, Wilson SW (1996) Antibodies against Pax6 immunostain amacrine and ganglion cells and neuronal progenitors, but not rod precursors, in the normal and regenerating retina of the goldfish. J Neurobiol 29:399-413.
Hitchcock PF, Raymond PA (2004) The teleost retina as a model for developmental and regeneration biology. Zebrafish 1:257-271.
Hodel C, Neuhauss SCF (2008) Computer-Based Analysis of the Optokinetic Response in Zebrafish Larvae. Cold Spring Harbor Protocols 2008:pdb.prot4961.
Hodson S, Miller F, Riley M (1977) The electrogenic pump of rabbit corneal endothelium. Experimental Eye Research 24:249-253.
Hoke KL, Fernald RD (1997) Rod photoreceptor neurogenesis. Progress in Retinal and Eye Research 16:31-49.

Hoke KL, Fernald RD (1998) Cell death precedes rod neurogenesis in embryonic teleost retinal development. Developmental Brain Research 111:143-146.
Hollyfield JG (1972) Histogenesis of the retina in the killifish, Fundulus heteroclitus. J Comp Neurol 144:373-380.
Hughes A (1977) The topography of vision oin mammals. Berlin: Springer-Verlag.
Ito H, Murakami T (1984) Retinal ganglion cells in two teleost species, Sebastiscus marmoratus and Navodon modestus. J Comp Neurol 229:80-96.
James P, Heck Jr K (1994) The effects of habitat complexity and light intensity on ambush predation within a simulated seagrass habitat. Journal of Experimental Marine Biology and Ecology 176:187-200.
Jerlov NG (1976) Marine Optics: Elsevier Science.
Johns PR (1977) Growth of the adult goldfish eye. III. Source of the new retinal cells. The Journal of Comparative Neurology 176:343-357.
Johns PR (1982) Formation of photoreceptors in larval and adult goldfish. J Neurosci 2:178-198.
Johns PR, Easter SS, Jr. (1977) Growth of the adult goldfish eye. II. Increase in retinal cell number. J Comp Neurol 176:331-341.
Johns PR, Fernald RD (1981) Genesis of rods in teleost fish retina. Nature 293:141-142.
Julian D, Ennis K, Korenbrot JI (1998) Birth and fate of proliferative cells in the inner nuclear layer of the mature fish retina. J Comp Neurol 394:271-282.
Kamermans M, Hawryshyn C (2011) Teleost polarization vision: how it might work and what it might be good for. Philosophical Transactions of the Royal Society B: Biological Sciences 366:742-756.
Kaneko A (1970) Physiological and morphological identification of horizontal, bipolar and amacrine cells in goldfish retina. J Physiol 207:623-633.
Kaneko A (1973) Receptive field organization of bipolar and amacrine cells in the goldfish retina. J Physiol 235:133-153.
Kaneko A, Hashimoto H (1969) Electrophysiological study of single neurons in the inner nuclear layer of the carp retina. Vision Research 9:37-55.
Kock JH (1982) Neuronal addition and retinal expansion during growth of the crucian carp eye. J Comp Neurol 209:264-274.
Krauss A, Neumeyer C (2003) Wavelength dependence of the optomotor response in zebrafish (Danio rerio). Vision Res 43:1273-1282.
Kroger RH, Knoblauch B, Wagner HJ (2003) Rearing in different photic and spectral environments changes the optomotor response to chromatic stimuli in the cichlid fish Aequidens pulcher. J Exp Biol 206:1643-1648.
Kuiter RH (2000) The Marine Fish Families Series, Seahorses Pipefishes and their relatives, A comprehensive Guide to Syngnathiformes. Chorleywood, UK: TMC Publishing.
Land MF (1995) Fast-focus telephoto eye. Nature 373:658-659.
Land MF (1999) Visual optics: The sandlance eye breaks all the rules. Current biology : CB 9:R286-R288.
Li KT, Wetterer JK, Nelson G. Hairston, Jr. (1985) Fish Size, Visula Resolution, and Prey Selectivity. Ecology 66:1729-1735.
Li L, Dowling JE (1997) A dominant form of inherited retinal degeneration caused by a non-photoreceptor cell-specific mutation. Proceedings of the National Academy of Sciences 94:11645-11650.
Locket NA (1992) Problems of deep foveas. Aust New Zeal J Ophthalmol 20:281-295.
Loew ER, McFarland WN, Mills EL, Hunter D (1993) A chromatic action spectrum for planktonic predation by juvenile yellow perch, Perca flavescens. Canadian Journal of Zoology 71:384-386.
Losey GS, Cronin TW, Goldsmith TH, Hydes D, Marshall NJ, McFarland WN (1999) The UV vusyal world of fishes: A review. Journal of Fish Biology 54:921-943.
Losey GS, McFarland WN, Loew ER, Zamzow JP, Nelson PA, Marshall NJ, Montgomery WL (2003) Visual Biology of Hawaiian Coral Reef Fishes. I. Ocular Transmission and Visual Pigments. Copeia 2003:433-454.
Lyall AH (1957a) Cone Arrangements in Teleost Retinae. Quarterly Journal of Microscopical Science s3-98:189-201.

Lyall AH (1957b) The growth of the trout retina. Quarterly Journal of Microscopical Science 98:101-110.
Lythgoe JN (1979) The ecology of vision: Clarendon Press.
Lythgoe JN (ed.) (1980) Vision in fishes: ecological adaptations. New York: Premium Press.
Lythgoe JN (1984) Visual pigments and environmental light. Vision Research 24:1539-1550.
Lythgoe JN, Partridge JC (1989) Visual pigments and the acquisition of visual information. J Exp Biol 146:1-20.
Maaswinkel H, Li L (2003) Spatio-temporal frequency characteristics of the optomotor response in zebrafish. Vision Res 43:21-30.
Mack AF, Sussmann C, Hirt B, Wagner HJ (2004) Displaced amacrine cells disappear from the ganglion cell layer in the central retina of adult fish during growth. Invest Ophthalmol Vis Sci 45:3749-3755.
Mangrum WI, Dowling JE, Cohen ED (2002) A morphological classification of ganglion cells in the zebrafish retina. Visual Neuroscience 19:767-779.
Marchiafava PL (1976) Centrifugal actions on amacrine and ganglion cells in the retina of the turtle. J Physiol 255:137-155.
Marchiafava PL (1985) Cell Coupling in Double Cones of the Fish Retina. Proceedings of the Royal Society of London Series B Biological Sciences 226:211-215.
Marshak DW, Dowling JE (1987) Synapses of cone horizontal cell axons in goldfish retina. The Journal of Comparative Neurology 256:430-443.
Marshall J, Vorobyev M, Siebeck U (2006) What does a reef fish see when sees a reef fish? In: Communication in fishes (Kapoor, B. G. et al., eds) Enfield U.S.A.: Science Publisher Inc.
Marshall J, Vorobyev M (2003) The Design of Color Signals and Color Vision in Fishes. In: Sensory processing in aquatic environments (Collin, S. P. and Marshall, N. J., eds), pp 194-222 New York: Springer.
Marshall NJ, Jennings K, McFarland WN, Loew ER, Losey GS, Montgomery WL (2003) Visual Biology of Hawaiian Coral Reef Fishes. III. Environmental Light and an Integrated Approach to the Ecology of Reef Fish Vision. Copeia 2003:467-480.
Matthiessen L (1880) Untersuchungen über den Aplanatismus und die Periscopie der Krystalllinsen in den Augen der Fische. Pflügers Archiv European Journal of Physiology 21:287-307.
McFarland WN, Loew ER (1994) Ultraviolet visual pigments in marine fishes of the family pomacentridae. Vision Research 34:1393-1396.
Meyer RL (1978) Evidence from thymidine labeling for continuing growth of retina and tectum in juvenile goldfish. Experimental Neurology 59:99-111.
Miller T, Crowder L, Rice J (1993) Ontogenetic changes in behavioural and histological measures of visual acuity in three species of fish. Environmental Biology of Fishes 37:1-8.
Mitarai G, Goto T, Takagi S (1978) Receptive field arrangement of color-opponent bipolar and amacrine cells in the carp retina. Sens Processes 2:375-382.
Mö11er A (1950) Die Struktur des Auges bei Urodelen verschiedener K6rpergr6sse. Zool Jahrb Abt Allg Zool Physiol 62:138-182.
Moreland JD, Lythgoe JN (1968) Yellow corneas in fishes. Vision Research 8:1377-1380.
Morris AC, Scholz T, Fadool JM (2008) Rod Progenitor Cells in the Mature Zebrafish Retina Recent Advances in Retinal Degeneration. vol. 613 (Anderson, R. E. et al., eds), pp 361-368: Springer New York.
Mosk V, Thomas N, Hart NS, Partridge JC, Beazley LD, Shand J (2007) Spectral sensitivities of the seahorses Hippocampus subelongatus and Hippocampus barbouri and the pipefish Stigmatopora argus. Vis Neurosci 24:345-354.
Mueller KP, Neuhauss SC (2012) Automated visual choice discrimination learning in zebrafish (Danio rerio). J Integr Neurosci 11:73-85.
Mueller KP, Neuhauss SCF (2010) Quantitative measurements of the optokinetic response in adult fish. Journal of Neuroscience Methods 186:29-34.
Müller H (1952) Bau und Wachstum der Netzhaut des Guppy (Lebistes reticulatus). Zool Jb, Abt f allg Zool u Physiol 275–324.

Munk O (1975) On the eyes of 2 foveate notosudid teleosts scopelosaurus hoedti and ahliesaurus berryi. Videnskabelige Meddelelser fra Dansk Naturhistorisk Forening 138:87-125.
Murakami M, Shimoda Y (1977) Identification of amacrine and ganglion cells in the carp retina. J Physiol 264:801-818.
Neave DA (1984) The development of visual acuity in larval plaice (Pleuronectes platessa L.) and turbot (Scophthalmusmaximus L.). Journal of Experimental Marine Biology and Ecology 78:167-175.
Nelson R, Connaughton V (2013) Bipolar cell pathways in the vertebrate retina.
Neumeyer C (1986) Wavelength discrimination in the goldfish. J Comp Physiol A 158:203-213.
Neumeyer C (1992) Tetrachromatic color vision in goldfish: evidence from color mixture experiments. J Comp Physiol A 171:639-649.
Nguyen-Legros J, Hicks D (2000) Renewal of photoreceptor outer segments and their phagocytosis by the retinal pigment epithelium. Int Rev Cytol 196:245-313.
Niemeye G, Gouras P (1973) Rod and cone signals inS-potentials of the isolated perfused cat eye. Vision Research 13:1603-1612.
Northmore DP, Dvorak CA (1979) Contrast sensitivity and acuity of the goldfish. Vision Res 19:255-261.
Novales-Flamarique H, Hawryshyn C (1994) Ultraviolet photoreception contributes to prey search behaviour in two species of zooplanktivorous fishes. Journal of Experimental Biology 186:187-198.
O'Brien WJ, Browman HI, Evans BI (1990) Search strategies of foraging animals. Amer Sci 78:152-160.
Ollivier FJ, Samuelson DA, Brooks DE, Lewis PA, Kallberg ME, Komáromy AM (2004) Comparative morphology of the tapetum lucidum (among selected species). Veterinary Ophthalmology 7:11-22.
Orger MB, Baier H (2005) Channeling of red and green cone inputs to the zebrafish optomotor response. Vis Neurosci 22:275-281.
Orger MB, Gahtan E, Muto A, Page-McCaw P, Smear MC, Baier H (2004) Behavioral screening assays in zebrafish. Methods Cell Biol 77:53-68.
Otten E (1980) Vision During Growth of a Generalized Haplochromis Species: H. Elegans Trewavas 1933 (Pisces, Cichlidae). Netherlands Journal of Zoology 31:650-700.
Otteson DC, D'Costa AR, Hitchcock PF (2001) Putative Stem Cells and the Lineage of Rod Photoreceptors in the Mature Retina of the Goldfish. Developmental Biology 232:62-76.
Otteson DC, Hitchcock PF (2003) Stem cells in the teleost retina: persistent neurogenesis and injury-induced regeneration. Vision Res 43:927-936.
Pankhurst NW, Montgomery JC (1990) Ontogeny of vision in the Antarctic fish Pagothenia borchgrevinki (Nototheniidae). Polar Biology 10:419-422.
Pankhurst PM (1994) Age-related changes in the visual acuity of larvae of New Zealand snapper, Pagrus auratus. Journal of the Marine Biological Association of the United Kingdom 74:337-349.
Pankhurst PM, Pankhurst NW, Montgomery JC (1993) Comparison of behavioural and morphological measures of visual acuity during ontogeny in a teleost fish, Forsterygion varium, tripterygiidae (Forster, 1801). Brain Behav Evol 42:178-188.
Partridge JC (1990) The colour sensitivity and vision of fishes. In: Light and life in the sea (Herring, P. J. et al., eds), pp 167-184 Cambridge, England: Cambridge University Press.
Perlman I, Kolb H, Nelson R (2012) S-Potentials and Horizontal Cells. In: Webvision: The Organization of the Retina and Visual System.
Perry VH, Walker M (1980) Amacrine cells, displaced amacrine cells and interplexiform cells in the retina of the rat. Proc R Soc Lond B Biol Sci 208:415-431.
Peterson RE, Fadool JM, McClintock J, Linser PJ (2001) Müller cell differentiation in the zebrafish neural retina: Evidence of distinct early and late stages in cell maturation. The Journal of Comparative Neurology 429:530-540.
Pettigrew JD, Collin SP (1995) Terrestrial optics in an aquatic eye: The sandlance, *Limnichthytes fasciatus* (Creediidae, Teleostei). Journal of Comparative Physiology A: Neuroethology, Sensory, Neural, and Behavioral Physiology 177:397-408.

Pettigrew JD, Collin SP, Fritsches K (2000) Prey capture and accommodation in the sandlance, Limnichthyes fasciatus (Creediidae; Teleostei). J Comp Physiol [A] 186:247-260.
Pettigrew JD, Collin SP, Ott M (1999) Convergence of specialised behaviour, eye movements and visual optics in the sandlance (Teleostei) and the chameleon (Reptilia). Curr Biol 9:421-424.
Pignatelli V, Champ C, Marshall J, Vorobyev M (2010) Double cones are used for colour discrimination in the reef fish, Rhinecanthus aculeatus. Biol Lett 6:537-539.
Powers MK, Easter Jr SS (1978) Absolute visual sensitivity of the goldfish. Vision Research 18:1137-1147.
Powers MK, Easter Jr SS (1983) Behavioural significance of retinal structure and function in fishes In: Fish Neurobiology, vol. 1 (Northcutt, R. G. and Davis, R. E., eds), pp 377-404 Ann Arbor: University of Michigan Press.
ProjectSeahorse (1996-2013) Project Seahorse: Advancing marine conservation. The University of British Columbia.
Provis JM, Diaz CM, Dreher B (1998) Ontogeny of the primate fovea: a central issue in retinal development. Prog Neurobiol 54:549-580.
Pumphrey RJ (1948) The Theory of the Fovea. J Exp Biol 25:299-312.
Pushchin II, Podugolnikova TA, Kondrashev SL (2007) Morphology and spatial arrangement of large retinal ganglion cells projecting to the optic tectum in the perciform fish Pholidapus dybowskii. Vision Res 47:3212-3227.
Querubin A, Lee HR, Provis JM, Bumsted O'Brien KM (2009) Photoreceptor and ganglion cell topographies correlate with information convergence and high acuity regions in the adult pigeon (*Columba livia*) retina. The Journal of Comparative Neurology 517:711-722.
Rahmann H, Jeserich G, Zeutzius I (1979) Ontogeny of Visual Acuity of Rainbow Trout under Normal Conditions and Light Deprivation. Behaviour 68:315-322.
Raymond P, Barthel L, Bernardos R, Perkowski J (2006) Molecular characterization of retinal stem cells and their niches in adult zebrafish. BMC Developmental Biology 6:36.
Raymond PA (1985a) Cytodifferentiation of photoreceptors in larval goldfish: Delayed maturation of rods. The Journal of Comparative Neurology 236:90-105.
Raymond PA (1985b) The unique origin of rod photoreceptors in the teleost retina. Trends in Neurosciences 8:12-17.
Raymond PA, Reifler MJ, Rivlin PK (1988) Regeneration of goldfish retina: rod precursors are a likely source of regenerated cells. J Neurobiol 19:431-463.
Raymond PA, Rivlin PK (1987) Germinal cells in the goldfish retina that produce rod photoreceptors. Dev Biol 122:120-138.
Risner ML, Lemerise E, Vukmanic EV, Moore A (2006) Behavioral spectral sensitivity of the zebrafish (Danio rerio). Vision Research 46:2625-2635.
Schaerer S, Neumeyer C (1996) Motion detection in goldfish investigated with the optomotor response is "color blind". Vision Res 36:4025-4034.
Schmitt E, Kunz YW (1989) Retinal morphogenesis in the rainbow trout, Salmo gairdneri. Brain Behav Evol 34:48-64.
Scholes JH (1976) Neuronal Connections and Cellular Arrangement in the Fish Retina. In: Neural Principles in Vision (Zettler, F. and Weiler, R., eds), pp 63-93: Springer Berlin Heidelberg.
Schuster S, Amtsfeld S (2002) Template-matching describes visual pattern-recognition tasks in the weakly electric fish Gnathonemus petersii. J Exp Biol 205:549-557.
Schwassmann HO (1968) Visual projection upon the optic tectum in foveate marine teleosts. Vision Research 8:1337-IN1332.
Shand J (1997) Ontogenetic changes in retinal structure and visual acuity: a comparative study of coral-reef teleosts with differing post-settlement lifestyles. Environmental Biology of Fishes 49:307-322.
Shand J, Doving KB, Collin SP (1999) Optics of the developing fish eye: comparisons of Matthiessen's ratio and the focal length of the lens in the black bream Acanthopagrus butcheri (Sparidae, Teleostei). Vision Res 39:1071-1078.
Sharma SC, Ungar F (1980) Histogenesis of the goldfish retina. J Comp Neurol 191:373-382.

Siebeck UE, Marshall NJ (2001) Ocular media transmission of coral reef fish--can coral reef fish see ultraviolet light? Vision Res 41:133-149.
Siebeck UE, Wallis GM, Litherland L (2008) Colour vision in coral reef fish. J Exp Biol 211:354-360.
Sivak JG (1974) The refractive error of the fish eye. Vision Research 14:209-213.
Slonaker JR (1897) A comparative study of the area of acute vision in vertebrates. Journal of Morphology 13:445-502.
Steinberg RH (1985) Interactions between the retinal pigment epithelium and the neural retina. Documenta Ophthalmologica 60:327-346.
Stell WK (1967) The structure and relationships of horizontal cells and photoreceptor-bipolar synaptic complexes in goldfish retina. American Journal of Anatomy 121:401-423.
Stenkamp DL (2011) The rod photoreceptor lineage of teleost fish. Progress in Retinal and Eye Research 30:395-404.
Stenkamp DL, Barthel LK, Raymond PA (1997) Spatiotemporal coordination of rod and cone photoreceptor differentiation in goldfish retina. The Journal of Comparative Neurology 382:272-284.
Strauss O (2005) The retinal pigment epithelium in visual function. Physiol Rev 85:845-881.
Tappeiner C, Gerber S, Enzmann V, Balmer J, Jazwinska A, Tschopp M (2012) Visual acuity and contrast sensitivity of adult zebrafish. Front Zool 9:10.
Teller DY (1979) The forced-choice preferential looking procedure: A psychophysical technique for use with human infants. Infant Behavior and Development 2:135-153.
Tucker VA (2000) The deep fovea, sideways vision and spiral flight paths in raptors. J Exp Biol 203:3745-3754.
Utne-Palm AC, Bowmaker JK (2006) Spectral sensitivity of the two-spotted goby Gobiusculus flavescens (Fabricius): a physiological and behavioural study. J Exp Biol 209:2034-2041.
van der Meer HJ (1995) Visual resolution during growth in a cichlid fish: a morphological and behavioural case study. Brain Behav Evol 45:25-33.
Vilter V (1954) Differenciation foveale dans l'appareil visuel d'un poisson abyssal, le Bathylagus benedicti. Compte Rendu des Seances de la Societe de Biologie Paris 148.
Wagner HJ, Frohlich E, Negishi K, Collin SP (1998) The eyes of deep-sea fish. II. Functional morphology of the retina. Prog Retin Eye Res 17:637-685.
Wagner HJ, Wagner E (1988) Amacrine cells in the retina of a teleost fish, the roach (Rutilus rutilus): a Golgi study on differentiation and layering. Philos Trans R Soc Lond B Biol Sci 321:263-324.
Walls GL (1942) The vertebrate eye and its adaptive radiation. . Bloomfield Hills, Michigan: Cranbrook Institute of Science.
Wanzenbock J, Schiemer F (1989) Prey Detection in Cyprinids during Early Development. Can J Fish Aquat Sci 46:995-1001.
Wanzenböck J, Zaunreiter M, Wahl CM, Noakes DL (1996) Comparison of behavioural and morphological measures of visual resolution during ontogeny of roach (Rutilus rutilus) and yellow perch (Perca flavescens). Can J Fish Aquat Sci 53:1506–1512
Wassle H, Chun MH, Muller F (1987) Amacrine cells in the ganglion cell layer of the cat retina. J Comp Neurol 265:391-408.
Werblin FS (1970) Response of retinal cells to moving spots: intracellular recording in Necturus maculosus. J Neurophysiol 33:342-350.
Werblin FS, Dowling JE (1969) Organization of the retina of the mudpuppy, Necturus maculosus. II. Intracellular recording. J Neurophysiol 32:339-355.
West RW, Dowling JE (1972) Synapses onto different morphological types of retinal ganglion cells. Science 178:510-512.
Wikler KC, Szel A, Jacobsen AL (1996) Positional information and opsin identity in retinal cones. J Comp Neurol 374:96-107.
Witkovsky P, Dowling JE (1969) Synaptic relationships in the plexiform layers of carp retina. Z Zellforsch Mikrosk Anat 100:60-82.
Wu DM, Schneiderman T, Burgett J, Gokhale P, Barthel L, Raymond PA (2001) Cones regenerate from retinal stem cells sequestered in the inner nuclear layer of adult goldfish retina. Invest Ophthalmol Vis Sci 42:2115-2124.

Wunder W (1926) Ober den Bau der Netzhaut von Sfisswasser fischen, die in grosser Tiefe leben. Z Vergl Physiol 4:22-36.
Yazulla S, Studholme K, Wu JY (1986) Comparative distribution of 3H-GABA uptake and GAD immunoreactivity in goldfish retinal amacrine cells: a double-label analysis. J Comp Neurol 244:149-162.
Yuodelis C, Hendrickson A (1986) A qualitative and quantitative analysis of the human fovea during development. Vision Res 26:847-855.
Yurco P, Cameron DA (2005) Responses of Muller glia to retinal injury in adult zebrafish. Vision Res 45:991-1002.
Zhao XC, Yee RW, Norcom E, Burgess H, Avanesov AS, Barrish JP, Malicki J (2006) The Zebrafish Cornea: Structure and Development. Investigative Ophthalmology & Visual Science 47:4341-4348.
Zou SQ, Yin W, Zhang MJ, Hu CR, Huang YB, Hu B (2010) Using the optokinetic response to study visual function of zebrafish. J Vis Exp.
Zygar CA, Lee MJ, Fernald RD (1999) Nasotemporal asymmetry during teleost retinal growth: preserving an area of specialization. J Neurobiol 41:435-442.

Chapter Two

Morphological and behavioral limit of visual resolution in temperate (*Hippocampus abdominalis*) and tropical (*Hippocampus taeniopterus*) seahorses

This chapter is presented as shown in the publication:

Lee, H. R. and Bumsted O'Brien, K. M. (2011) "Morphological and behavioral limit of visual resolution in temperate (*Hippocampus abdominalis*) and tropical (*Hippocampus taeniopterus*) seahorses." Visual Neuroscience, 28(4):351-360.

Morphological and Behavioral Limit of Visual Resolution in Temperate (*Hippocampus abdominalis*) and Tropical (*Hippocampus taeniopterus*) Seahorses

Hie Rin Lee[1] and Keely M Bumsted O'Brien[1,2]

[1]ARC Centre of Excellence in Vision Science, [2] Research School of Biology,

The Australian National University, Canberra ACT 0200, Australia

Support:

Australian Research Council Centres of Excellence Program (CE0561903)

Morphological and Behavioral Limit of Visual Resolution in Temperate (*Hippocampus abdominalis*) and Tropical (*Hippocampus taeniopterus*) Seahorses

ABSTRACT

Seahorses are visually guided feeders that prey upon small fast-moving crustaceans. Seahorse habitats range from clear tropical to turbid temperate waters. How are seahorse retinae specialized to mediate vision in these diverse environments? Most species of seahorse have a specialization in their retina associated with acute vision, the fovea. The purpose of this study was to characterize the fovea of temperate *Hippocampus abdominalis* and tropical *H. taeniopterus* seahorses and to investigate their theoretical and behavioral limits of visual resolution. Their foveae were identified and photoreceptor (PR) and ganglion cell (GC) densities determined throughout the retina and topographically mapped. The theoretical limit of visual resolution was calculated using formulas taking into account lens radius and either cone PR or GC densities. Visual resolution was determined behaviorally using reactive distance. Both species possess a rod-free convexiclivate fovea. PR and GC densities were highest along the foveal slope, with a density decrease within the foveal center. Outside the fovea, there was a gradual density decrease towards the periphery. The theoretically calculated visual resolution on the foveal slope was poorer for *H. abdominalis* (5.25 min of arc) compared with *H. taeniopterus* (4.63 min of arc) based on PR density. Using GC density, *H. abdominalis* (9.81 min of arc) had a lower resolution compared with *H. taeniopterus* (9.04 min of arc). Behaviorally, *H. abdominalis* had a resolution limit of 1090.64 min of arc, while *H. taeniopterus* was much smaller, 692.86 min of arc. Although both species possess a fovea and the distribution of PR and GC is similar, *H. taeniopterus* has higher PR and GC densities on the foveal slope and better theoretical and behaviorally measured visual resolution compared to *H. abdominalis*. These data indicate that seahorses have a well-developed acute visual system and tropical seahorses have higher visual resolution compared to temperate seahorses.

Key words: vision, fish, fovea

INTRODUCTION

Seahorses (genus *Hippocampus*) are visually guided ambush predators. They wrap their prehensile tails around stationary objects and lie in wait for prey (James and Heck Jr, 1994, Foster and Vincent, 2004, Choo and Liew, 2006). Once a prey is visually detected, seahorses orient their eyes towards the prey and then reach forward to use a distinctive rapid suction mechanism to capture the prey (Bergert and Wainwright, 1997). This strategy depends on an acute visual system with the ability to detect small moving prey.

Seahorses are diurnal with the majority of their feeding behavior occurring during the daylight hours under photopic conditions (Kuiter, 2000). Seahorse habitats vary depending on the species; although within each species, their distribution is generally localized to a particular region. Within an area, most species are bottom dwellers inhabiting shallow waters near landmasses where they live amongst the vegetation (Kuiter, 2000). Seahorse species have been found in both tropical and temperate waters. The water in shallow tropical coral reefs has a broad spectrum of light including relatively large amounts of ultraviolet (less than 390 nm) and the far red (600-700 nm) wavelengths (Mosk et al., 2007). Temperate coastal habitats, also known as ”green water”, transmit a narrower spectrum with a maximum wavelength around 510-550 nm (Partridge, 1990).

Visual resolution under photopic conditions is determined by a number of factors, including the solid angle viewed by the eye, the cone photoreceptor (PR) spacing (Fernald, 1988), and the region of the retina stimulated. Related to these factors is the convergence of cones to higher order processing cells such as ganglion cells (GCs) with lower convergence values being associated with higher resolution (Campbell and Green, 1965, Collin and Pettigrew, 1989). In many vertebrate retinas, areae of high visual resolution are located in specialized regions surrounded by areae of lower resolution. These high-acuity areae range from local regions of higher GC density as observed in an *area centralis* to *fovea centralis*, which are not only characterized by a high ganglion and cone PR cell density but have a further morphological specialization of a small depression in the retina where inner retinal neurons are pushed to the

side forming a pit, called a fovea (Stone, 1965, Provis, 1979, Packer et al., 1989, Curcio et al., 1990, Garciá et al., 2005, Salinas-Navarro et al., 2009).

There are two general foveal morphologies: shallow, with a wide base (concaviclivate) and deep, with a narrow base (convexiclivate) (Slonaker, 1897, Walls, 1942, Fite and Rosenfield-Wessels, 1975). Primates and some bird retinas contain concaviclivate foveae [e.g., pigeons (*Columba livia*), northern blue jays (*Cyanocitta cristata*), and the ostrich (*Struthio camelus*)]. Certain species of raptors, lizards and fishes (including seahorses) have retinas containing convexiclivate foveae (Slonaker, 1897, Walls, 1942, Galifret, 1968, Fite and Lister, 1981, Collin and Collin, 1999, Boire et al., 2001, Mosk et al., 2007, Querubin et al., 2009). Convexiclivate foveae are funnel shaped with steep sides and a deep depression. A strong correlation has been reported between a convexiclivate fovea and predation, which involves the capture of moving prey (Fite and Rosenfield-Wessels, 1975), such as in observed with seahorses. It has been proposed that the convexiclivate fovea mediates visual resolution by magnifying retinal images (Walls, 1942), maintaining accurate fixation, and acting as a directional focus indicator (Harkness and Bennet-Clark, 1978).

The purpose of this study was to morphologically characterize the fovea and to functionally evaluate visual resolution in two seahorse species that inhabit visually diverse environments. *H. abdominalis* resides and feeds in temperate waters, which tend to be more turbid compared with tropical waters where *H. taeniopterus* is found. Are their retinae specialized for their habitats? We compared the fovea and visual resolution of *H. abdominalis* and *H. taeniopterus* by mapping the topography of PRs and cells in the ganglion cell layer (GCL) in the retina, calculating the theoretical limit of vision, and then behaviorally testing visual resolution. Investigating the topographic density of cells in the seahorse retina and how this compares to their behavior is important for understanding how their visual system is specialized to hunt small prey in a wide range of environments.

MATERIALS AND METHODS

H. abdominalis (n = 14) and *H. taeniopterus* (n = 19) seahorses (Fig. 1A and 1B) were obtained from Seahorse Australia, Beauty Point, Tasmania. The seahorses used in the study were between 11.5 and 18 cm, a size when they were considered sexually mature. All tissues were obtained and experiments conducted under the approved ethical protocols from the Australian National University animal care committee.

Reactive distance

The behavioral limit of visual resolution was determined by measuring the reactive distance (Wanzenbock and Schiemer, 1989, Job and Bellwood, 1996) in mature seahorses (n = 3; *H. abdominalis* and n = 10; *H. taeniopterus*). The fish were housed in 9/15 h light/dark cycle. The behavioral experiments were conducted at the beginning and towards the end of the light cycle. Food was withheld from the fish for 24 h prior to the commencement of the experiment. Ten minutes prior to the onset of testing, an individual seahorse was transferred to an experimental saltwater tank and allowed to acclimatize. Acclimatization to the tank was judged to have occurred after a decrease in gill movements and swimming was observed. Three of the tank walls and the bottom were covered with white paper. The tank was illuminated by a warm white energy saving petite spiral fluorescent lamp [3,100 lX; 240-V, 23-W (equivalent to 115-W) (Mirabella, Melbourne, Australia)] placed approximately 30 cm overhead. Video recordings were made from above and in front of the tank. Prior to the introduction of the prey (frozen mysid shrimp), preprey-capturing behavior was video recorded for 5 min. Frozen mysid shrimp of known sizes (6-12 mm) and high contrast (dark brown or red against white background) were dropped into the tank, and the feeding behavior of the seahorse was video recorded. From the video recordings, the reactive distance was determined by measuring the distance between the fish and the prey when the fish's eye oriented and the fish began to swim towards the prey. Reactions to prey were determined accurately by a sudden change in eye orientation and swimming direction. The reactive distance was measured in 10 trials per fish and the average reactive distance calculated. In order to calculate the angle an object (the prey) subtended on the fish retina, the following formula was used: Visual angle in minutes of arc = 2·[arc

tan(0.5·*h*/RD)], where *h* is prey size and RD was reactive distance (Wanzenbock and Schiemer, 1989, Miller et al., 1993, Job and Bellwood, 1996).

Tissue collection

Seahorses were anesthetized with clove oil (more than 2-6 drops in 1 L of seawater depending on the size of the fish) and then decapitated. The eyes were enucleated and immersion fixed in 4% paraformaldehyde in 0.1 $_{M}$ phosphate-buffered saline (1x PBS; pH 7.4) for 24 h to 6 months. After fixation, the cornea, lens, and vitreous were removed. For wholemounts, radial cuts were made at the retinal margin to relax the retina such that it would lie flat, and the retinal pigment epithelium was bleached as previously described (Hemmi and Grünert, 1999, Bumsted O'Brien et al., 2004). After bleaching, the tissue was either immediately mounted on glass slides and coverslipped or further processed for nuclear staining or immunocytochemistry. For cryosections, the eyes were cryoprotected in 30% sucrose in PBS at 4°C overnight. The retina was then frozen at a known orientation in equal parts of 30% sucrose solution in 1x PBS and Optimal Cutting Temperature (Tissue Tek, Sakura, Japan) mounting medium. The tissue was serially sectioned at 16 µm in a cryostat (Leica, Wetzlar, Germany). Tissue was collected on gelatinized-poly-$_{L}$-lysine-coated Superfrost Plus (Esco, Biolab Scientific Ltd., Scoresby, Australia) microscope slides, incubated overnight at 37°C and then stored in – 20°C.

Histology and immunolabeling

Retinal sections through the fovea were stained with propidium iodide (PI; Sigma; diluted 1:500 in PBS, Castle Hill, Australia). Sections and wholemounts were immunolabeled with an antibody to rod opsin [RET-P1 (Barnstable, 1980, Fekete and Barnstable, 1983); 1:200]. To block nonspecific bindings, tissue was preincubated in normal goat serum (Zymed Laboratories, South San Francisco, CA; 01-6101) diluted in 0.1% Triton X-100 in 1x PBS (1:10): sections for 1.5 h, while wholemounts were left for 2 days at 4°C. The cryosections were then incubated in the primary antibody overnight and wholemounts for 3-4 days at 4°C. After a thorough wash in 1x PBS, Alexa Fluor 488-conjugated goat antimouse (Molecular Probes Inc.,

Eugene, OR; A11029; 1:500), was applied for 3 h to sections and 2 days to wholemounts at room temperature followed by 1x PBS washes to decrease background. Sections and wholemounts were coverslipped with Aqua Poly/Mount (Polysciences Inc.,Warrington, PA; 18606). Immunolabeled sections were examined using a confocal Laser Scanning Microscope (LSM 5; Carl Zeiss AG, Oberkochen, Germany).

Sampling in wholemounts and cell counts

Cell density in retinal wholemounts was determined following the method of Querubin et al. (2009). Briefly, for PR cell sampling, the retina was mounted PR side up on a glass slide and coverslipped with 80% glycerol. The retinal axes were marked on the glass coverslip. PR inner segments at the fovea and every 500 µm eccentric to the fovea were photographed using a Zeiss Axio Imager M1 microscope with differential interference optics. The number of PR inner segment profiles (both rods and cones) was counted in ten 10 × 10 µm sampling boxes in a 250 µm wide field. The average number of inner segment profiles per square millimeter was calculated.

To determine GC densities, retinas were stained with PI (diluted 1:500 in PBS) for 1 h at room temperature, followed by two 15 min PBS washes and mounted GCL upwards. The fovea was located by finding a small circular depression, approximately 1 mm ventrotemporal from the optic disc (OD). The retinal axes were marked on the glass coverslip. A Zeiss Axio Imager M1 with a LSM 5 Pascal unit (Carl Zeiss AG) using a 40X objective lens and a He-Ne laser (LASOS Lasertechnik GmbH, Jena, Germany) was used in conjunction with PASCAL software (Release Version 4.0; Carl Zeiss AG) to obtain a series of confocal Z-stack images. Z-stacks were taken in the fovea and at 500 µm intervals from the fovea. Each Z-stack spanned the complete thickness of the GCL. The Z-stack images were opened in Adobe Photoshop CS3 and compiled into layers. All the GC nuclei in at least fifty 10 × 10 µm sampling boxes in the Z-stack images were counted. By counting only the newly appearing cells on the overlapping layers, it was assured that no cell was omitted or counted twice. The average number of cells per square millimeter was calculated.

Sampling in sections and cell counts

Cell density measures were also performed in serial 16-µm frozen cross sections covering the entire retina (Querubin et al., 2009). Starting at the ventral edge and ending at the dorsal edge, a series of sections approximately 320 µm apart was stained with PI solution (diluted 1:500 in PBS) for 3 min, followed by a 1 min PBS wash. Slides were coverslipped with Aqua Poly/Mount (Polysciences Inc.). In the central retina, the distance between sampled sections was decreased to approximately 160 µm to increase the amount of retina sampled. A Z-stack series of images centerd on the GCL were taken at each sampling location using a confocal LSM 5. The Z-stack images were opened in Adobe Photoshop CS3 and compiled into layers. By counting only the newly appearing cells on the overlapping layers, it was assured that no cell was omitted or counted twice. Cell counts were quantified by importing the data into Image J and using the "analyze particles" plug-in. To obtain the number of cells in square millimeter, the cell counts were multiplied by a factor taking into account the thickness of the section, Z-stack height, and width of the sampling window.

Rod density calculation

Rod density was determined using the same method to calculate total PR density in wholemounts; however, instead of counting inner segment profiles, the number of RET-P1-labeled rod outer segments was counted. The average rod PR density was subtracted from the total PR cell density at each retinal location to give an estimated cone PR density.

Topographic map construction

Topographic maps of the density of cells in the GCL and density of PRs were drawn from densities derived from *H. abdominalis* (n = 4) and *H. taeniopterus* (n = 4) retinas. The length of each section was measured using a stage micrometer, drawn to scale, and the X-Y coordinates of each sampling location were plotted on the drawing in Adobe Illustrator CS3. For wholemounts, the image of flattened retina was taken using a dissecting microscope (Zeiss – SteREO Discovery V12), and the retinal shape was traced in Adobe Illustrator CS3. Using the stage micrometer, X-Y coordinates of retinal landmarks were determined, and each sampling

location was plotted in the drawing. The calculated densities were added for each sampling point, and isodensity lines were drawn manually to connect regions of equivalent cell density.

Theoretical limit of seahorse visual resolution

Based on cone PR cell densities, the lens radius, and Matthiessen's ratio, the anatomical limit of visual resolution of seahorse vision was determined (Neave, 1984). The formula, $\sin \alpha = c/f$ was used where α was the minimum separable angle measured in minutes of arc, c was the distance between the centers of adjacent cones, and f was the focal length of the lens. The cone density (d) was estimated in number of cells per 1 mm length of retina, and therefore, the reciprocal of d gave the cone separation in millimeter. The focal length of the lens was calculated using Matthiessen's ratio, which states that the distance from center of the lens to the retina (posterior nodal distance, PND or the focal length of the lens) was 2.55 times the radius of the lens (r) (Matthiessen, 1880). The theoretical limit of acuity would normally be calculated using the formula: $\sin \alpha = 1/(d \times 2.55r)$; however, tissue shrinkage was approximately 10%. In order to take this into consideration when calculating the theoretical limit of acuity, a factor of 1.11 is included in the equation: $\sin \alpha = 1.11/(d \times 2.55r)$; $\sin \alpha = 0.43529/(dr)$.

The theoretical limit was also calculated based on the density of cells in the GCL (Collin and Pettigrew, 1989). The angle (α) subtending 1 mm on the retina was calculated by $\tan \alpha = 1$ mm/PND, and the spatial resolution was estimated by obtaining the number of cells subtended by 1 deg of visual arc, that is, cells per degree = cell density/PND. Since at least two GCs were needed to distinguish the light and dark boundaries forming one cycle of a grating of the highest resolvable frequency, the theoretical limit of visual resolution was calculated according to the equation: cycles per degree (cpd) = cells per degree/2. In order to make a direct comparison between theoretical and behavioral limits of visual resolution, the unit cpd was converted to minutes of arc. First, the value in cells per degree was converted to cells per minute of arc by dividing the number by 60 because 1 degree is equal to 60 min of arc. Then, the value of cells per minute of arc was inversed, 1/cells per minute of arc, to obtain the value in minutes of arc.

RESULTS

A comparison of *H. abdominalis* and *H. taeniopterus* showed that the eyes were similar in size although the length of the snout varied between species (Fig. 1). Both species had an avascular retina (data not shown) with the fovea evident macroscopically as a small depression located 1 mm ventrotemporal to the optic nerve (circle; Fig. 2A and 2B). Sections through the retinal region containing the *H. abdominalis* and *H. taeniopterus* fovea showed the presence of a distinctive convexiclivate pit demarcated with steep sloping edges. In the center of the pit, the GCL, inner nuclear layer (INL) and outer nuclear layer (ONL) were thinner compared with the foveal slope and more peripheral retinal regions. The retinal layers on the foveal slope were the thickest in the retina (Fig. 2C and 2D).

Rod PRs were observed as a segregated dense band of nuclei vitreal to the cones (data not shown). No rod nuclei or rod opsin immunoreactivity were detected in the fovea (Fig. 2 C-2F). The rod-free regions in *H. abdominalis* and *H. taeniopterus* were similar in size and were approximately twice the size of the morphologically defined convexiclivate pit. The rod-free zone was roughly circular (outlined in white), with a slight skewing along the horizontal meridian (Fig. 2E and 2F; Fig. 3A and 3B).

PR density

Changes in the topography of PR cell density were mapped in *H. abdominalis* and *H. taeniopterus* retina (Fig. 3A and 3B). A representative map for each species demonstrated that there was a region of elevated PR cell density around the fovea. In general, the overall pattern for the density of PRs was similar between species. PR densities reached a peak of 225,500 ± 6856 cells/mm^2 in *H. abdominalis* and 289,250 ± 6185 cells/mm^2 in *H. taeniopterus* on the foveal slope with a slight density decrease in the center of the pit (199,000 ± 4830cells/mm^2 and 241,500 ± 9147 cells/mm^2, respectively). Outside the fovea, cell density gradually declined to 165,409 ± 5040 cells/mm^2 and 120,500 ± 30,260 cells/mm^2 in the far periphery (Fig. 3A and 3B). Near the retinal edge, PR cell density increased slightly in the *H. taeniopterus* retina (Fig. 3B). Despite the similarities in overall pattern, *H. taeniopterus* retinas showed a statistically

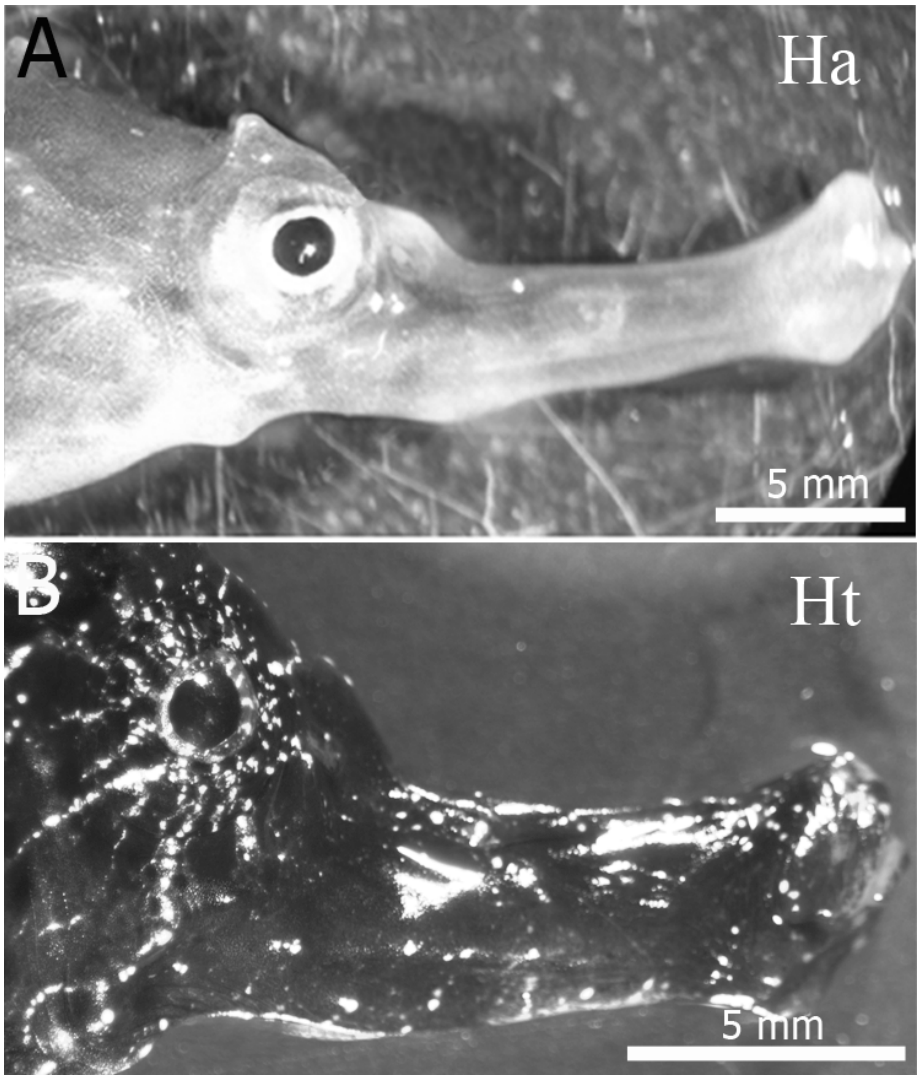

Fig. 1. A comparison of *Hippocampus abdominalis* (A) and *H. taeniopterus* (B) head morphology and eye size *in situ*. *H. abdominalis* (A) was lighter in coloration compared to the darkly pigmented *H. taeniopterus* (B). Note that the snout length is variable between species. Scale bar = 5 mm.

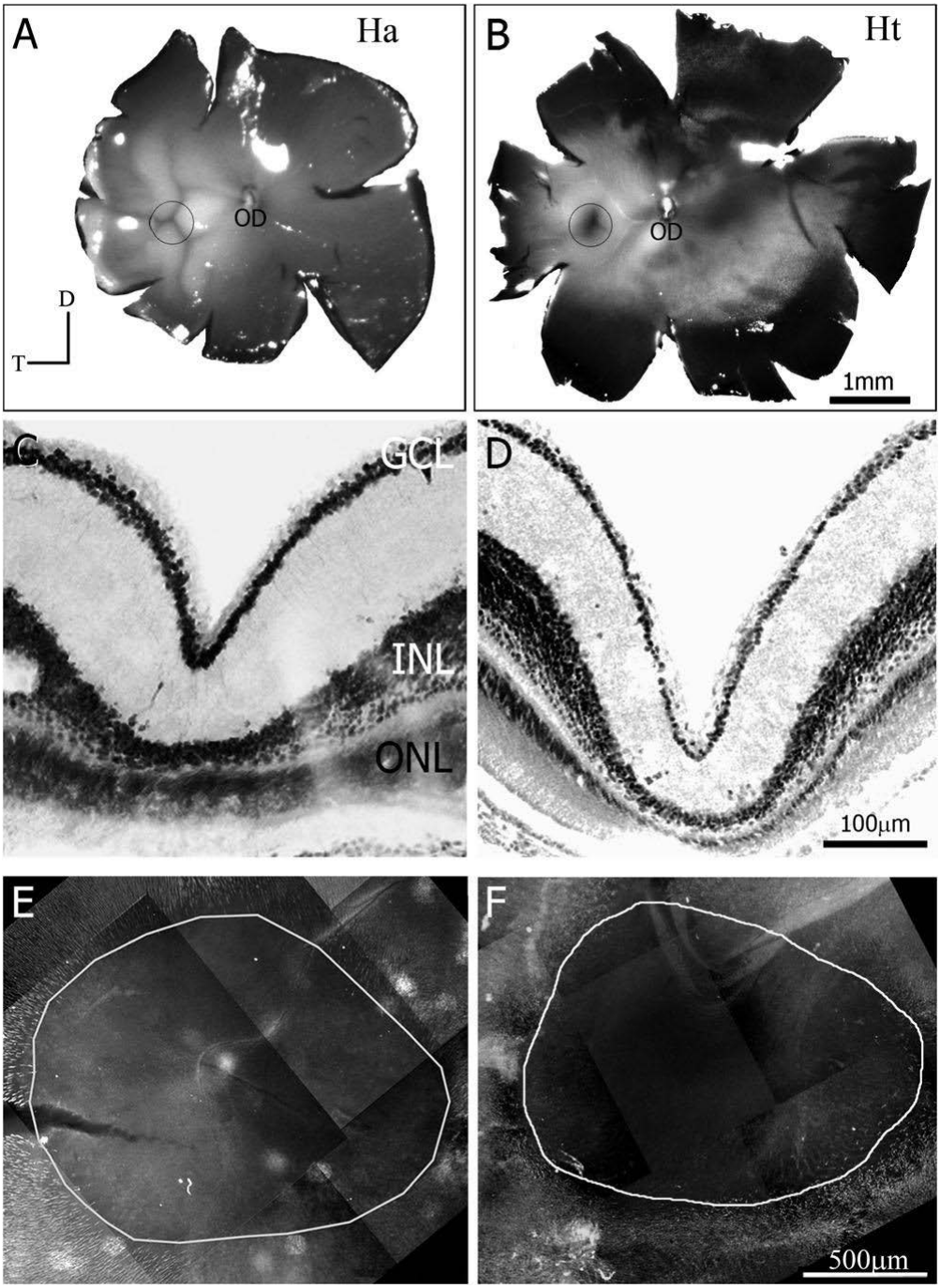

Fig. 2. The adult seahorse retina. *H. abdominalis* (Ha; A) and *H. taeniopterus* (Ht; B) flattened eye cup, in which the fovea (circle) was evident as a depression in the retinal surface temporal and slightly inferior to the OD. The *fovea centralis* in the *H. abdominalis* (C) and *H. taeniopterus* (D) was characterized by a convexiclivate pit, in which the retinal layers are thinned compared with the foveal slope. Rod PR outer segments labeled with a rod opsin antibody in a retinal flatmount (shown as white dots around the rod-free region outlined with a white line) were absent in the fovea, with the size of the rod-free region similar in *H. abdominalis* (E) and *H. taeniopterus* (F). Abbreviations: Dorsal (D), Temporal (T), ganglion cell layer (GCL), inner nuclear layer (INL), and outer nuclear layer (ONL). Scale bars for A-B = 1 mm, C-D = 100 μm, and E-F = 500 μm.

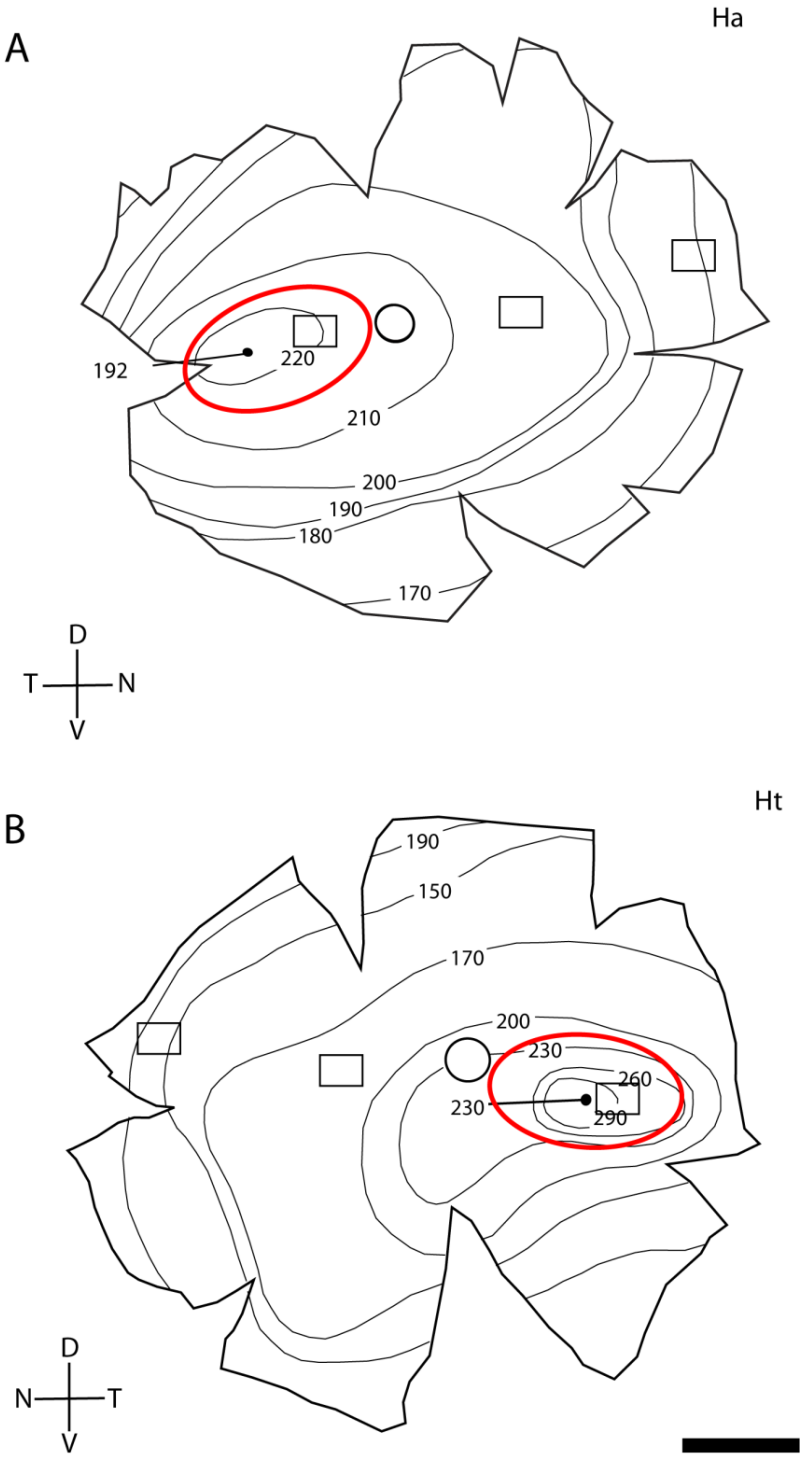

Fig. 3. Topographic maps of the total PR densities across the *H. abdominalis* (A) and *H. taeniopterus* (B) retinae. The numbers must be multiplied by 1000 to obtain cell density (cells/square millimeter). The fovea within rod-free zone (red circle) is indicated by a black dot. The OD is indicated by the open black circle. Boxed regions indicate the sampling area used to generate the graph of PR density in Fig. 4. Abbreviations: Dorsal (D), Ventral (V), Nasal (N), Temporal (T), *H. abdominalis* (Ha), and *H. taeniopterus* (Ht). Scale bars = 1 mm.

higher density of cones on the foveal slope (Fig. 4). In the mid periphery, the PR density appeared similar in both species. In the far periphery, the density was higher in *H. abdominalis*.

On the dorsal edge of the rod-free area in both species, rods comprised 17% of the PRs. The density of rods slowly increased towards the periphery. Nasal to the optic nerve, rods comprised 30% of the total PR density, with further density increases to 45% in the mid periphery and 55% of the total PR density in the far periphery. When the contribution of rods was taken into account in peripheral retina and subtracted from the total PR density, the cone densities rapidly decreased compared to those observed in the central retina.

GC density

Topographic maps of the density of cells in the GCL (Fig. 5A and 5B) showed that the highest density of cells in the GCL was located along the foveal slope (41,327 ± 3457 cells/mm^2, *H. abdominalis* and 48,500 ± 2517 cells/mm^2, *H. taeniopterus*). Within the foveal pit, the density of cells in the GCL declined to 25,215 ± 1279 cells/mm^2 and 25,500 ± 2887 cells/mm^2, respectively. Outside the fovea, the density of cells in the GCL decreased gradually to 9554 ± 973 cells/mm^2 and 9000 ± 1414 cells/mm^2 in the peripheral retina of each species. Although there was some individual variation, the overall pattern of the density of cells in the GCL was similar between retinal samples and species; however, the peak density of cells in the GCL obtained at the foveal slope in the *H. taeniopterus* retina was significantly higher compared with that of *H. abdominalis* (Fig. 6).

The ratio of PRs to cells in the GCL across the retina, as a measure of convergence in the retinal circuitry, indicated that *H. abdominalis* had a lower convergence ratio in the fovea (7.9 PRs for every GC; 7.9:1) and along the foveal slope (5.5:1) compared with *H. taeniopterus* (9.5:1 and 6.0:1, respectively). The differences between species for both ratios were not statistically significant. Outside the fovea where rods start to appear, *H. taeniopterus* had lower convergence ratio in the mid periphery (7.7:1) and far periphery (13.4:1), compared with *H. abdominalis* (8.2:1 and 17.3:1, respectively). It was only with the ratio at the far periphery that the difference was considered to be statistically significant ($P = 0.0112$).

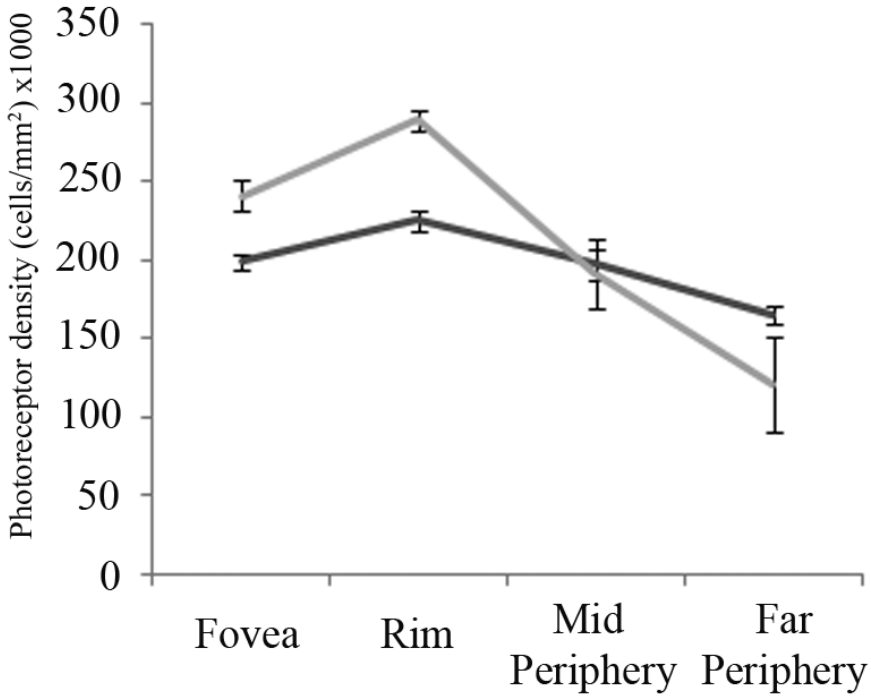

Fig. 4. PR cell density along the horizontal meridian from the fovea to the far periphery in *Hippocampus abdominalis* (n = 4; dark line) and *H. taeniopterus* (n=3; gray line) retinae. The mean densities of PRs ± $_{S.D.}$ are plotted.

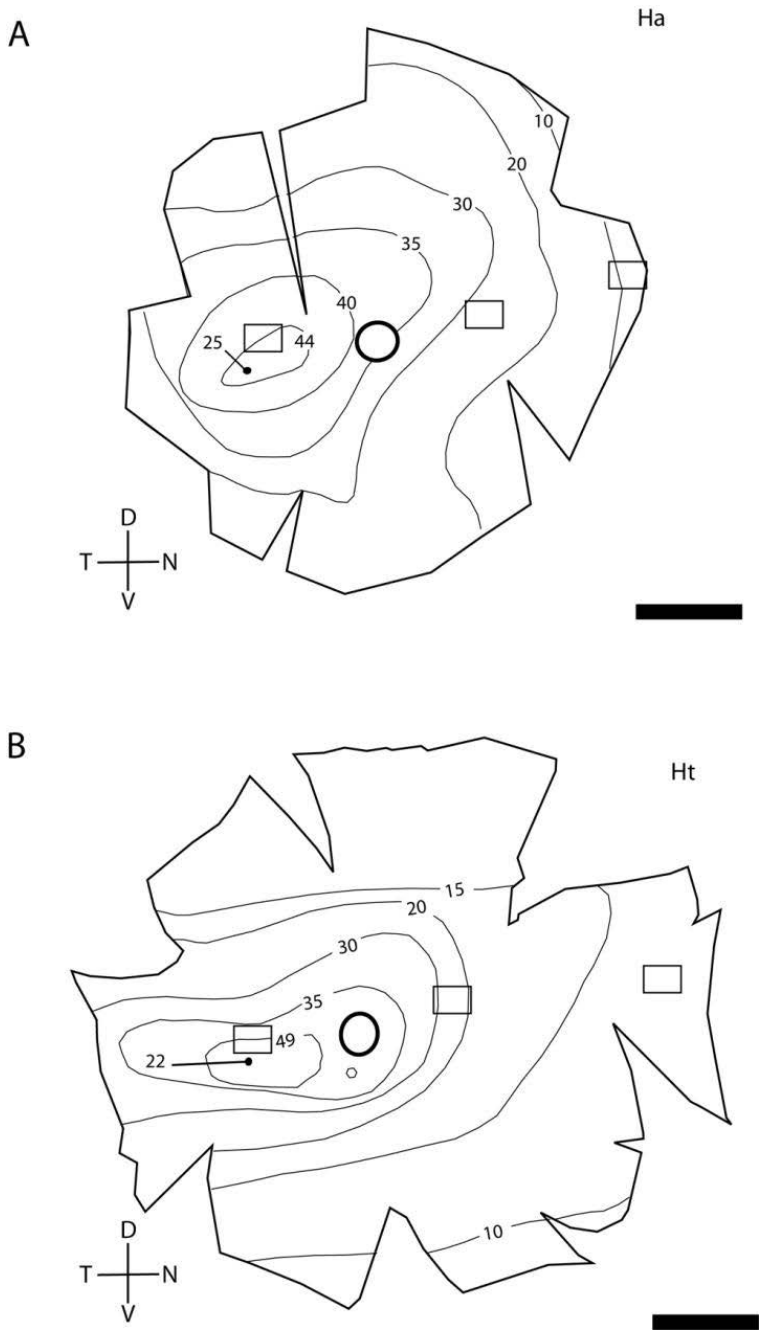

Fig. 5. Topographic maps showing the GC densities across the *Hippocampus abdominalis* (A) and *H. taeniopterus* (B) retinae. The numbers must be multiplied by 1000 to obtain cell density (cells/square millimeter). The fovea is indicated by a black dot and the OD by an open black circle. Boxed regions indicate the sampling area used to generate a graph of GC density shown in Fig. 6. Abbreviations: Dorsal (D), Ventral (V), Nasal (N) and Temporal (T), *H. abdominalis* (Ha), and *H. taeniopterus* (Ht). Scale bars for A-B = 1 mm.

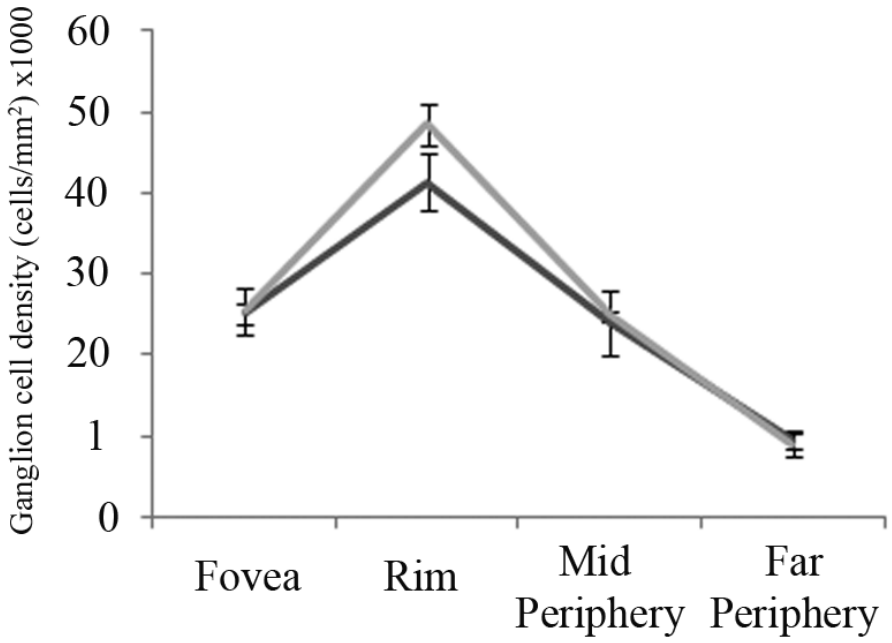

Fig. 6. GC density along the horizontal meridian from the fovea to the far periphery in *Hippocampus abdominalis* (n = 4; dark line) and *H. taeniopterus* (n=3; gray line) retinae. The mean densities of GCs ± $_{S.D.}$ are plotted.

Theoretical limit of visual performance

For *H. abdominalis*, based on an average lens radius of 0.6 mm and the PR density (199,000 cells/mm^2 in the fovea and 225,500 cells/mm^2 on the foveal slope), the calculated theoretical limit of visual resolution in the adult seahorse, *H. abdominalis* was 5.59 ± 0.07 min of arc in the fovea and 5.25 ± 0.08 min of arc on the foveal slope. For *H. taeniopterus*, the lens radius was 0.6 mm. The PR densities were 241,500 cells/mm^2 in the fovea and 289,250 cells/mm^2 on the foveal slope. The calculated limits of visual acuity were 5.08 ± 0.10 and 4.64 ± 0.05 min of arc, respectively. The theoretical limit of visual resolution in *H. taeniopterus* was significantly lower compared to that of *H. abdominalis* on the foveal slope ($P < 0.0001$). This suggested that the tropical species, *H. taeniopterus* had a better theoretically estimated visual resolution and was able to resolve smaller prey at the same distance compared with *H. abdominalis*.

Using a formula which takes into account the densities of cells on the GCL (25,215 cells/mm^2 in the fovea and 41,327 cells/mm^2 on the foveal slope), the spatial resolution of *H. abdominalis* was calculated to be 4.79 ± 0.12 cells per degree in the fovea and 6.12 ± 0.26 cells per degree on the foveal slope. Hence, the calculated theoretical limit of visual resolution was 2.39 ± 0.06 cpd in the fovea and 3.06 ± 0.13 cpd on the foveal slope or 12.54 ± 0.32 min of arc in the fovea and 9.81 ± 0.43 min of arc on the foveal slope (Table 1). For *H. taeniopterus*, the foveal density of cells on the GCL was 25,500 cells/mm^2. The calculated spatial resolution (4.81 ± 0.27 cells per degree) and theoretical limits of visual resolution (2.40 ± 0.14 cpd or 12.51 ± 0.72 min of arc) were similar to that of *H. abdominalis*. The higher density of the cells the GCL on the foveal slope (48,500 cells/mm^2) resulted in a higher spatial resolution on the foveal slope (6.64 ± 0.17 cells per degree), which leads to a higher theoretical limits of visual resolution (3.32 ± 0.09 cpd or 9.04 ± 0.24 min of arc). The difference in the theoretical limits of *H. taeniopterus* estimated at the foveal slope was considered to be statistically significant compared with that in *H. abdominalis* (*P* value= 0.0214; Table 1).

Table 1. Theoretical limits of visual resolution calculated based on ganglion cell densities.

	Fovea (cpd)	Foveal slope (cpd)	Fovea (minutes of arc)	Foveal slope (minutes of arc)
H. abdominalis	2.39 ± 0.06	3.06 ± 0.13	12.54 ± 0.32	9.81 ±0.43
H. taeniopterus	2.40 ± 0.14	3.32 ± 0.09	12.51 ± 0.72	9.04 ± 0.24

Behavioral limit of visual resolution

The sizes of the prey were variable, which lead to variable reactive distances. In general, a larger prey resulted in a longer reactive distance. The visual angle measured behaviorally in minutes of arc was greater with *H. abdominalis* (1090.64 ± 70.44 min of arc) compared to the *H. taeniopterus* (692.86 ± 198.36 min of arc) under the same experimental conditions. This indicated that *H. taeniopterus* was able to detect smaller prey. Behaviorally, *H. taeniopterus* had a statistically better visual resolution compared with *H. abdominalis* ($P = 0.0068$). Compared with the theoretical limit of visual resolution calculated from the PR cell or cells in the GCL densities, both fish perform more poorly than predicted; however, it was consistent that *H. taeniopterus* had lower theoretical and behavioral limits of acuity, which translates to a greater degree of visual resolution compared with *H. abdominalis*.

DISCUSSION

This is the first report of the topographic distribution of PRs and GCs across the *H. abdominalis* and *H. taeniopterus* retina, which also includes a comparison of the theoretical limit of visual resolution with the feeding behavior of the seahorse. Our data show that both species possess a distinct rod-free convexiclivate *fovea centralis* in the ventrotemporal retina. PR cell densities were highest at the foveal slope with lower densities within the foveal center. Beyond the foveal slopes, cell density gradually decreased towards the periphery. The density of cells in the GCL varied in accordance with the PR densities. Overall, *H. taeniopterus* had a higher density peak of PR and cells in the GCL on the foveal slope compared with *H. abdominalis*. The theoretical limit of acuity suggested that *H. taeniopterus* was able to detect statistically smaller targets compared to *H. abdominalis*. The behavioral measurement of visual resolution, reactive distance, was consistent with the theoretical estimation of visual resolution in that *H. taeniopterus* was able to detect smaller prey at the same distance.

Foveal morphology

Seahorses belong to the family *Syngnathidae*, which means "jaw fused". Within this family, there are 55 genera including more than 320 species. The family *Syngnathidae* can be divided into four subfamilies based on their shared features; *Syngnathinae* (pipefishes), *Hippocampinae* (seahorses and pygmy pipefishes), *Solegnathinae* (seadragons and pipehorses) and *Doryrhamphinae* (free swimming pipefishes). Some immediately related taxa of the seahorse include the pipefishes which share some retinal characteristics (Collin and Collin, 1999, Kuiter, 2000). All of the members of the *Syngnathidae* family that have been studied contain a foveal specialization in their retina, except *H. kuda* (Easter, 1992).

The presence of a fovea in the teleost retina was first reported by Slonaker (1897), but it was not until 1942 that Walls reported the presence of a *fovea centralis* in the seahorse retina. The current study is in agreement with Walls (1942) who described the seahorse fovea as a convexiclivate structure; however, we observed that the fovea was located in the ventrotemporal retina rather than the central retina as described previously. The temporal location of *fovea centralis* has been observed in a variety of teleosts with laterally displaced eyes such as the

pipefish, *Corythoichthyes paxtoni* (Collin and Collin, 1999). It has been postulated that the temporal fovea mediates increased spatial resolving power in the binocular regions of the visual field. The temporal location of the seahorse fovea may also be essential in binocular depth judgment, especially when capturing prey.

Many other fish species have been shown to possess a fovea, although the morphologies are variable. Collin and Collin (1999) classified the teleost fovea into four distinct types based on their morphology citing differences in depth, degree of inner retinal neuron displacement, and presence of radial fibers in the fovea. According to this classification, both the *H. abdominalis* and *H. taeniopterus* temporal foveae are categorized as Type I, similar to the previously described fovea of the pipefish (*C. paxtoni*), deep-snouted pipefish (*Syngnathus typhle*), the bass *(Paralabrax nebulifer*) and the barred sand perch (*Parapercis nebulosis*) (Schwassmann, 1968, Easter, 1992, Collin and Collin, 1999). Type I foveae are characterized by a deep convexiclivate retinal depression without the lateral displacement of the inner retinal layers, the exclusion of rods, and an increase in PR and GC densities (Collin and Collin, 1999).

Easter (1992) reported that a tropical species of seahorse, *H. kuda* did not possess a *fovea centralis*; instead, the retina contained an *area centralis* (Easter, 1992). Our personal observations were in agreement that the *H. kuda* does not have a fovea but rather has a rod-free *area centralis* with the increased retinal thickness at the corresponding region in the ventrotemporal retina (unpublished data). The fovea of *H. abdominalis* and *H. taeniopterus,* however, are distinctly convexiclivate, lack rod PRs, and possess increased PR and ganglion GC densities, similar to other syngnathids. At least two other species of seahorse, *H. subelongatus* and *H. barouri* have been reported to possess a foveate retina (Mosk et al., 2007). Our analysis of two additional species of seahorse (*H. abdominalis* and *H. taeniopterus)* indicated that the presence of a *fovea centralis* is the norm rather than the exception in seahorses.

Although the functions of a convexiclivate fovea still remain to be explained further, it was possible that seahorses use their fovea as an image magnifier to promote high resolution and provide a mechanism for maintaining accurate fixation by increasing sensitivity to small angular movements due to distortion of the retinal image (Walls, 1942, Pumphrey, 1948,

Harkness and Bennet-Clark, 1978). The idea that the convexiclivate fovea is useful for detecting motion is consistent with our behavioral data. Although due to the experimental conditions, the most common prey capture event occurred with stationary prey, we observed that both species of seahorses were able to detect mobile prey more rapidly and at a greater distance with higher sensitivity (data not shown). Our data strongly suggest that unlike in primates where motion detection and visual acuity are processed in different visual pathways (Merigan and Maunsell, 1993), the seahorse visual system is attuned to movement detection as opposed to acuity.

Topographic variation in PR and GC density and visual acuity

Both the *H. abdominalis* and *H. taeniopterus* retinae have a rod-free region that extends beyond the *fovea centralis*. The function of the rod-free zone in fish is not completely clear. Because visual acuity is usually measured in photopic conditions when the rods are less active, their contribution to acuity is likely minimal. It has been postulated that without the rods, cones are able to pack together at higher density as is the case with the type I fovea of the pipefish *C. paxtoni* (Collin and Collin, 1999). The cone PRs within the foveal region form the square mosaic with a probable role in the perception of movement of small approaching prey in conjunction with high visual acuity provided by an increased PR cell density. The cone PRs function best in photopic conditions and again their very presence would support that the seahorse is specialized for perceiving finer detail.

A common feature in foveate retinae is the topographical variation in cell density across the retina, with the highest densities of both PRs and GCs located in the foveal region. In teleosts, cone PRs are added at the retinal margin during growth, whereas new rods are generated throughout the retina and integrated into the existing retinal circuitry, which results in the maintenance of rod density. This may induce a differential distribution pattern of rod PR topography to that of total PRs (Fernald, 1985). Our results on the rod PR densities at various locations in the retina support this differential distribution pattern. The density values increase gradually from the margin of the rod-free region towards the far nasal periphery, which is the opposite pattern to the topography of total PRs.

It is also interesting to note the reversed pattern of the PR cell density in the far periphery, where *H. abdominalis* has higher density compared with *H. taeniopterus* retina. A possible explanation for this increased PR cell density in the far peripheral retina of *H. abdominalis* is that these size-matched seahorses from each species could be at different developmental stages even at mature ages. The fish eye grows in size throughout the lifetime with mechanisms of stretching and adding new cells generated at the far peripheral margin (Fernald, 1985).

In order to estimate GC density, all cells in the GCL were counted. The GCL is often composed of other cell types including glial cells and displaced amacrine cells; therefore, GC densities obtained in this study may be inflated. The degree of amacrine cell displacement varies across species. For example, 49% in elasmobranch (Collin, 1988) and 24% in three species of reef fish (Collin and Pettigrew, 1988c) of the cells in the GCL were amacrine cells. The influence of overestimated density calculations would be an increased visual acuity estimated from the lower convergence ratio between cone PRs and GCs. Mack et al. (2004) postulated changes in the proportion of displaced amacrine cells in GCL as the fish mature. They have concluded that the displaced amacrine cells are eliminated from the GCL in the more central retina during growth of the eye. Although we have not counted the number of displaced amacrine cells in GCL of the adult seahorse retinas in this study, the inflation of GC counts may be smaller in the central retina compared to the periphery if displaced amacrine cells decrease with age.

Visual resolution: theoretical versus behavioral

Various studies investigating the acuity of teleost fish have concluded that the behavioral estimate of acuity is poorer than the theoretical estimate of acuity, as determined from retinal cell densities (Miller et al., 1993, Pankhurst et al., 1993). The theoretical limit calculated in the current study is based on the quantitative morphological data such as PR or GC densities. The theoretical limit signifies the maximum limit of visual acuity, which can be achieved at the cellular level in the retina. On the other hand, the behavioral limit of visual resolution was obtained experimentally; therefore, the resulting behavior includes other factors

influencing visual processing including neural processing in the brain. Browman et al. (1990) reported that behavioral measures of visual acuity are likely to yield a more accurate estimate of an animal's visual abilities.

Different kinds of acuity assessments have variable sensitivities, which means that a comparison to the theoretical limit is an important factor in analyzing visual function (Dobson and Teller, 1978, Hodos et al., 2002). For theoretical limit calculation, we have used a formula, which takes into account the intercone spacing and lens radius and hence focal length of the lens. To obtain the focal length of the lens, the average Matthiessen's ratio (2.55) was used (Browman et al., 1990). It has been shown that the ratios could vary within the range of 2.4-2.82 depending on the variety of fish species (Pankhurst et al., 1993).

It has been suggested that the behavioral limit of visual detection in teleosts is set by the convergence ratios of cones to higher processing cells such as GCs, the resolving power of the lens, and the accommodative state of the eye. Is it the intercone spacing or the density of the GCs that is the limiting factor for visual acuity (Fernald, 1988)? Collin and Pettigrew (1989) proposed that the spatial distribution of the retinal GCs places an upper limit on the spatial resolving power, and therefore, the least separable visual angle approximates the angle subtended by one GC. In other words, the spatial resolving power of the eye needs to be calculated from the inter-GC distances in area of highest GC density. In this region, there is a low convergence ratio of cones to a GC, and because each GC possesses a separate conductive axon to higher brain centers *via* the optic nerve, the retinal GC mosaic provides the only link between the eye and behavioral output (Collin and Pettigrew, 1989).

Why are the theoretical and behavioral limits of visual resolution higher in the tropical species, *H. taeniopterus*? Morphologically, their retina and, especially, the fovea bear a resemblance to each other, except that the cell densities are higher in *H. taeniopterus*. Considering that visual acuity can be limited by the spatial resolution of PR packing density and the types of connections made to GCs *via* bipolar cells, the observed increase in cell density, PR cell density in particular, in the foveal region is thought to subserve higher visual acuity. A low convergence ratio between GCs and PRs ensures an increased sampling of light information for

direct transmission of information centrally. Although convergence ratios are only an indirect indication of the circuitry responsible for high acuity and other visual functions, they have been widely applied for this purpose (Boycott and Wassle, 1999). In the far periphery, *H. taeniopterus* had lower convergence ratios compared with *H. abdominalis*. We did not take into account the resolving power of the lens from each species.

Influence of habitat

The light conditions in their natural habitats are quite different as *H. abdominalis* is a temperate fish, whereas *H. taeniopterus* is a tropical fish. In nature, seahorses are found in a diverse range of aquatic environments with differing light intensities and spectral radiance distributions from ”blue water” coral reefs and ”green water” coastal habitats (Foster and Vincent, 2004, Mosk et al., 2007). Cone PR pigment properties could be different in these two species of seahorse. Mosk et al. (2007) have measured the spectral absorption characteristics of visual pigments in the retinal PRs using microspectrophotometry technique. They reported that a tropical seahorse *H. barbouri* has greater transmission of short wavelengths of light and an additional short wavelength specific pigment present, allowing an extended spectral range available for vision. Sensitivity to shorter wavelengths in the shallow coral reef habitat is beneficial to this species compared to temperate seahorse, *H. subelongatus*. It may be possible that the increased visual resolution enhances the ability of *H. taeniopterus* to capture prey in the blue water of the tropical environment. Although the difference observed between *H. abdominalis* and *H. taeniopterus* foveal morphology, theoretical limit of visual resolution and reactive distance were statistically significant, further experiments with increased number of animals will give better outcomes and predictions of their visual and behavioral ecology.

Conclusions

The syngnathids are a group of fishes that feed on small crustaceans, with individual prey items detected and tracked visually prior to capture (Bergert and Wainwright, 1997). The presence of a convexiclivate fovea is an advantage for capturing their prey in many species, which inhabit a wide variety of environments.

References

Barnstable CJ (1980) Monoclonal antibodies which recognize different cell types in the rat retina. Nature 286:231-235.

Bergert BA, Wainwright PC (1997) Morphology and kinematics of prey capture in the syngnathid fishes Hippocampus erectus and Syngnathus floridae. Marine Biology 127:563-570.

Boire D, Dufour JS, Theoret H, Ptito M (2001) Quantitative analysis of the retinal ganglion cell layer in the ostrich, Struthio camelus. Brain Behav Evol 58:343-355.

Boycott B, Wassle H (1999) Parallel processing in the mammalian retina: the Proctor Lecture. Invest

Browman HI, Gordon WC, Evans BI, O'Brien WJ (1990) Correlation between histological and behavioral measures of visual acuity in a zooplanktivorous fish, the white crappie (Pomoxis annularis). Brain Behav Evol 35:85-97.

Bumsted O'Brien KM, Cheng H, Jiang Y, Schulte D, Swaroop A, Hendrickson AE (2004) Expression of photoreceptor-specific nuclear receptor NR2E3 in rod photoreceptors of fetal human retina. Invest Ophthalmol Vis Sci 45:2807-2812.

Campbell FW, Green DG (1965) Optical and retinal factors affecting visual resolution. J Physiol 181:576-593.

Choo CK, Liew HC (2006) Morphological development and allometric growth patterns in the juvenile seahorse Hippocampus kuda Bleeker. Journal of Fish Biology 69:426-445.

Collin SP (1988) The retina of the shovel-nosed ray, Rhinobatos batillum (Rhinobatidae): morphology and quantitative analysis of the ganglion, amacrine and bipolar cell populations. Experimental biology 47:195-207.

Collin SP, Collin HB (1999) The foveal photoreceptor mosaic in the pipefish, Corythoichthyes paxtoni (Syngnathidae, Teleostei). Histol Histopathol 14:369-382.

Collin SP, Pettigrew JD (1988b) Retinal Topography in Reef Teleosts, I. Some Species with Well-Developed Areae but Poorly-Developed Streaks. Brain Behav Evol 31:269-282.

Collin SP, Pettigrew JD (1988c) Retinal Topography in Reef Teleosts, II. Some Species with Prominent Horizontal Streaks and High-Density Areae. Brain Behav Evol 31:283-295.

Collin SP, Pettigrew JD (1989) Quantitative Comparison of the Limits on Visual Spatial Resolution Set by the Ganglion Cell Layer in Twelve Species of Reef Teleosts. Brain Behav Evol 34:184-192.

Curcio CA, Sloan KR, Kalina RE, Hendrickson AE (1990) Human photoreceptor topography. J Comp Neurol 292:497-523.

Dobson V, Teller DY (1978) Visual acuity in human infants: A review and comparison of behavioral and electrophysiological studies. Vision Research 18:1469-1483.

Easter SS, Jr. (1992) Retinal growth in foveated teleosts: nasotemporal asymmetry keeps the fovea in temporal retina. J Neurosci 12:2381-2392.

Fekete DM, Barnstable CJ (1983) The subcellular localization of rat photoreceptor-specific antigens. J Neurocytol 12:785-803.

Fernald RD (1985) Growth of the teleost eye: novel solutions to complex constraints. Environmental Biology of Fishes 13:113-123.

Fernald RD (1988) Aquatic adaptations in fish eyes. In: Sensory Biology of Aquatic Animals (Atema, J. et al., eds), pp 435-466 Berlin: Springer.

Fite KV, Lister BC (1981) Bifoveal vision in anolis lizards. Brain Behav Evol 19:144-154.

Fite KV, Rosenfield-Wessels S (1975) A Comparative Study of Deep Avian Foveas. Brain, Behavior and Evolution 12:97-115.

Foster SJ, Vincent ACJ (2004) Life history and ecology of seahorses: implications for conservation and management. Journal of Fish Biology 65:1-61.

Galifret Y (1968) Les diverses aires fonctionnelles de la retine du pigeon. Z Zellforsch Mikrosk Anat 86:535–545.

Garciá M, Ruiz-Ederra J, Hernández-Barbáchano H, Vecino E (2005) Topography of pig retinal ganglion cells. J Comp Neurol 486:361-372.

Harkness L, Bennet-Clark HC (1978) The deep fovea as a focus indicator. Nature 272:814-816.

Hemmi JM, Grünert U (1999) Distribution of photoreceptor types in the retina of a marsupial, the tammar wallaby (Macropus eugenii). Visual Neuroscience 16:291-302.
Hodos W, Ghim MM, Potocki A, Fields JN, Storm T (2002) Contrast sensitivity in pigeons: a comparison of behavioral and pattern ERG methods. Doc Ophthalmol 104:107-118.
James P, Heck Jr K (1994) The effects of habitat complexity and light intensity on ambush predation within a simulated seagrass habitat. Journal of Experimental Marine Biology and Ecology 176:187-200.
Job SD, Bellwood DR (1996) Visual acuity and feeding in larval *Premnas biaculeatus*. Journal of Fish Biology 48:952-963.
Kuiter RH (2000) The Marine Fish Families Series, Seahorses Pipefishes and their relatives, A comprehensive Guide to Syngnathiformes. Chorleywood, UK: TMC Publishing.
Mack AF, Fernald RD (1997) Cell movement and cell cycle dynamics in the retina of the adult teleost Haplochromis burtoni. J Comp Neurol 388:435-443.
Mack AF, Sussmann C, Hirt B, Wagner HJ (2004) Displaced amacrine cells disappear from the ganglion cell layer in the central retina of adult fish during growth. Invest Ophthalmol Vis Sci 45:3749-3755.
Matthiessen L (1880) Untersuchungen über den Aplanatismus und die Periscopie der Krystalllinsen in den Augen der Fische. Pflügers Archiv European Journal of Physiology 21:287-307.
Merigan WH, Maunsell JHR (1993) How Parallel are the Primate Visual Pathways? Annual Review of Neuroscience 16:369-402.
Miller T, Crowder L, Rice J (1993) Ontogenetic changes in behavioural and histological measures of visual acuity in three species of fish. Environmental Biology of Fishes 37:1-8.
Mosk V, Thomas N, Hart NS, Partridge JC, Beazley LD, Shand J (2007) Spectral sensitivities of the seahorses Hippocampus subelongatus and Hippocampus barbouri and the pipefish Stigmatopora argus. Vis Neurosci 24:345-354.
Neave DA (1984) The development of visual acuity in larval plaice (Pleuronectes platessa L.) and turbot (Scophthalmusmaximus L.). Journal of Experimental Marine Biology and Ecology 78:167-175.
Packer O, Hendrickson AE, Curcio CA (1989) Photoreceptor topography of the retina in the adult pigtail macaque (Macaca nemestrina). J Comp Neurol 288:165-183.
Pankhurst PM, Pankhurst NW, Montgomery JC (1993) Comparison of behavioural and morphological measures of visual acuity during ontogeny in a teleost fish, Forsterygion varium, tripterygiidae (Forster, 1801). Brain Behav Evol 42:178-188.
Partridge JC (1990) The colour sensitivity and vision of fishes. In: Light and life in the sea (Herring, P. J. et al., eds), pp 167-184 Cambridge, England: Cambridge University Press.
Provis JM (1979) The distribution and size of ganglion cells in the regina of the pigmented rabbit: a quantitative analysis. J Comp Neurol 185:121-137.
Pumphrey RJ (1948) The Theory of the Fovea. J Exp Biol 25:299-312.
Querubin A, Lee HR, Provis JM, Bumsted O'Brien KM (2009) Photoreceptor and ganglion cell topographies correlate with information convergence and high acuity regions in the adult pigeon (<I>Columba livia)</I> retina. The Journal of Comparative Neurology 517:711-722.
Salinas-Navarro M, Mayor-Torroglosa S, Jimenez-Lopez M, Aviles-Trigueros M, Holmes TM, Lund RD, Villegas-Perez MP, Vidal-Sanz M (2009) A computerized analysis of the entire retinal ganglion cell population and its spatial distribution in adult rats. Vision Res 49:115-126.
Schwassmann HO (1968) Visual projection upon the optic tectum in foveate marine teleosts. Vision Research 8:1337-IN1332.
Slonaker JR (1897) A comparative study of the area of acute vision in vertebrates. Journal of Morphology 13:445-502.
Stone J (1965) A quantitative analysis of the distribution of ganglion cells in the cat's retina. J Comp Neurol 124:337-352.
Walls GL (1942) The vertebrate eye and its adaptive radiation. . Bloomfield Hills, Michigan: Cranbrook Institute of Science.

Wanzenbock J, Schiemer F (1989) Prey Detection in Cyprinids during Early Development. Can J Fish Aquat Sci 46:995-1001.

Chapter Three

Development of the Fovea and Visual Resolution in the Tropical Seahorse (*Hippocampus taeniopterus*)

Development of the Fovea and Visual Resolution in the Tropical Seahorse (*Hippocampus taeniopterus*)

Hie Rin Lee[1,2] **and Keely M Bumsted O'Brien**[1,2]

[1]ARC Centre of Excellence in Vision Science, [2] John Curtin School of Medical Research, The Australian National University, Canberra ACT 0200, Australia

Support:

Australian Research Council Centres of Excellence Program (CE0561903)

Development of the Fovea and Visual Resolution in the Tropical Seahorse (*Hippocampus taeniopterus*)

ABSTRACT

The tropical seahorse species *Hippocampus taeniopterus* has a convexiclivate, rod-free fovea located at the centre of gaze. Currently, the morphological development of the fovea and visual acuity is unknown. As a result, we do not have a good grasp of the variables affecting visual acuity, which is critical to enabling young seahorses to detect and ingest prey. In this study, we analysed the developmental changes in foveal morphology, cell density and Reactive Distance - a behavioural measure of visual resolution. In three increasingly large size groups of tropical *H. taeniopterus* seahorses, visual resolution was measured, followed by photoreceptor and ganglion cell density measures. Morphologically, the depression of the foveal pit enlarged as the fish grew. The area of rod-free zone also increased with fish size. The photoreceptor and ganglion cell densities increased with fish size at the foveal slope, although there was a decrease in cone and ganglion cell density at the foveal centre with age. Outside the foveal region, cell densities gradually decreased towards the periphery. Both theoretically and behaviourally determined visual resolution improved with increasing fish size, with larger fish being able to detect prey of a fixed size at a greater distance. The behaviourally measured increased visual function correlates with changes in morphology with fish size.

Key words: vision, seahorse, fish, fovea

INTRODUCTION

Under photopic conditions high visual resolution is associated with various factors including the solid angle viewed by the eye, the cone photoreceptor spacing across the retina (Neave, 1984, Fernald, 1988), and the region of the retina stimulated. A lower convergence ratio from cones to higher-order processing cells such as ganglion cells is related to higher resolution (Campbell and Green, 1965, Fernald, 1988, Collin and Pettigrew, 1989). Hence, images projected onto a larger retinal area where cone photoreceptors are tightly packed results in higher resolution. In many vertebrate retinas, this area of high visual resolution is located in a specialised region known as an *area centralis* or *visual streak* (Walls, 1942, Stone, 1965, Hughes, 1971, Stone and Johnston, 1981, Rapaport and Stone, 1984, Collin and Collin, 1988b, Collin and Pettigrew, 1988a, Juliusson et al., 1994, Shand et al., 2000, Garciá et al., 2005, Salinas-Navarro et al., 2009). These regions are characterised by higher cone photoreceptor and ganglion cell densities. In some cases, a further morphological specialisation is present as a small depression in the retina, called a *fovea centralis* (Packer et al., 1989, Curcio et al., 1990, Collin and Collin, 1999, Querubin et al., 2009, Lee and Bumsted O'Brien, 2011).

Seahorses are visually guided feeders as well as ambush predators, who use high visual resolution to detect and capture prey (Lee and Bumsted O'Brien, 2011). The adult seahorse retina contains a ventro-temporally located convexiclivate *fovea centralis* that is characterised by the absence of rod photoreceptors and an increased density of cones, interneurons and ganglion cells at the foveal slope (Walls, 1942, Collin and Collin, 1999, Fritsches and Marshall, 2002, Lee and Bumsted O'Brien, 2011). It has been postulated that a convexiclivate fovea plays a role in achieving high visual resolution by magnifying retinal images (Walls, 1942), maintaining accurate fixation, detecting small angular movements (Pumphrey, 1948) and acting as a directional focus indicator (Harkness and Bennet-Clark, 1978). Furthermore, the presence of a convexiclivate fovea appears to be strongly correlated with the capture of moving prey (Fite and Rosenfield-Wessels, 1975, Lee and Bumsted O'Brien, 2011).

It has been reported that juvenile seahorses are able to feed immediately after birth, which suggests that they have sufficiently good vision to detect moving prey (Van Wassenbergh

et al., 2009). How does this compare with other foveate creatures where an increase in visual resolving power is correlated with the refinement of foveal structure: increased cell density and the formation of a depression in the retina? In primates, the fovea starts to mature over a protracted timeframe during which visual acuity improves (Hendrickson and Yuodelis, 1984, Yuodelis and Hendrickson, 1986). Fish have the added feature of continued eye growth throughout life (Fernald, 1988, Fadool, 2003, Hitchcock and Raymond, 2004, Morris et al., 2008). The eye increases in the size, and the functional aspects of the vision improve as the fish grows. During growth, the cone to ganglion cell ratio has been reported to remain constant (e.g. the cichlid fish, *Haplochromis sauvagei*)(van der Meer, 1994); therefore, with the increased number of cones per unit visual angle, larger fish likely have better photopic resolution, approaching the best theoretically achievable visual acuity (Otten, 1980, Kock, 1982, Neave, 1984, Browman et al., 1990).

Does the juvenile seahorse retina contain a well-developed fovea and is their vision as acute as compared with that observed in the mature seahorse? To address this question, the current study characterised the development of the seahorse fovea morphologically and functionally evaluated whether visual resolution improves with age in the tropical seahorse, *Hippocampus taeniopterus.* The overall development of the retina, with particular reference to the *fovea centralis* was determined by morphological analysis of the fovea and mapping the topography of photoreceptors and ganglion cell densities in three different age groups. The theoretical limit of visual resolution was calculated from the cell densities estimated. Visual resolution was also measured behaviourally using Reactive Distance techniques. The resulting data indicate that the seahorse fovea develops both morphologically and functionally as the fish grows in size.

MATERIALS AND METHODS

Tropical *H. taeniopterus* (n = 21) seahorses were obtained from Seahorse Australia, Beauty Point, Tasmania. The fish were categorised into the three groups according to their body lengths: group 1 (n = 6) 5.82 ± 0.26 cm, group 2 (n = 5) 9.70 ± 0.33 cm, and group 3 (n = 10) 14.56 ± 0.77 cm. All tissue collection and experiments were conducted under approved ethical protocols from the Australian National University animal care committee.

Reactive Distance

The reactive distance technique was adapted for estimating the behavioural limit of visual resolution in the above seahorses (n = 21) (Wanzenbock and Schiemer, 1989, Job and Bellwood, 1996, Lee and Bumsted O'Brien, 2011). The detailed procedure has been described previously (Lee and Bumsted O'Brien, 2011). In brief, the fish was starved for 24 hours prior to the commencement of the experiment. Following the acclimatisation to the experimental tank and video recording of pre-prey capturing behaviour, frozen mysid shrimp of known sizes (6-12 mm) and high contrast (dark brown or red against a white background) were dropped into the tank. Video recordings of the feeding behaviour were made from above and in front of the tank.

From the video recordings, the reactive distance was determined by measuring the distance (in cm) between the fish and the prey at the time when the fish's eye oriented and the fish began to swim towards the prey. Reactions to prey were determined accurately by a sudden change in eye orientation, swimming direction and the pulling back of the snout. The reactive distance was measured in approximately ten trials per fish and the average reactive distance was calculated. The angle that the prey subtended on the fish retina, the formula was calculated as: Visual angle in minutes of arc = $2 \cdot (\arctan(0.5 \cdot h/\mathrm{RD}))$, where h is prey size, RD was reactive distance (Wanzenbock and Schiemer, 1989, Miller et al., 1993, Job and Bellwood, 1996, Lee and Bumsted O'Brien, 2011).

Tissue Collection

Following behavioural vision testing, the seahorses were anesthetised with clove oil (more than 2-6 drops in 1 L of seawater depending on the size of the fish) and then decapitated.

The eyes were enucleated and immersion fixed in 4% paraformaldehyde (PFA) in 0.1 M phosphate buffered saline (1x PBS; pH 7.4) until processed for flatmounting.

Following eye-lens diameter measurements, the retina from one eye was prepared as a wholemount. Using the distinct pigmentation on the ventral iris as a landmark, orientation marks were cut into the dorsal and ventral poles according to the body axes of the intact animal so that the orientation of the eye was preserved through subsequent processing. Following the removal of cornea, lens, and sclera, additional radial relaxation cuts were made. The retinal pigment epithelium (RPE) was bleached in freshly prepared solution made of 5 mL of purified and deionised water, 1 mL of 9% sodium chloride (NaCl), 4 mL of 30% hydrogen peroxide (H_2O_2) and 1 drop of ammonia (NH_3) (Hemmi and Grünert, 1999, Bumsted O'Brien et al., 2004, Lee and Bumsted O'Brien, 2011). After bleaching, the tissue was processed for nuclear staining with propidium idodide (PI) (Sigma; diluted 1:500 in 1X PBS) or for immunocytochemical labeling with antibodies.

The other eye was processed for cryosectioning, by removal of cornea, lens and sclera. The retina was immersed in a 30% sucrose in 1x PBS solution overnight, and then frozen at a known orientation in equal parts of 30% sucrose solution and Optimum Cutting Temperature (Tissue Tek, Sakura, Japan) mounting medium. Transverse retinal sections were cut at 10 or 16 μm thickness and prepared for immunolabeling and/or nuclear staining.

Immunolabeling

Retinal wholemounts were immunolabeled with an antibody to rod opsin (RET-P1, (Barnstable, 1980, Fekete and Barnstable, 1983); 1:200). To block non-specific bindings, tissue was pre-incubated in normal goat serum (Zymed Laboratories, South San Francisco, CA, 01-6101) diluted in 0.1% Triton X-100 in 1x PBS (TPBS) (1:10) for two days at 4℃, then incubated in the primary antibody for 3-4 days at 4℃. After a thorough wash in 1x PBS, Alexa Fluor 488 conjugated with goat anti-mouse (Molecular Probes Inc., Eugene, OR, A11029; 1:500) was applied for two days at room temperature, and 1x PBS washes were followed to decrease background. For retinal sections, the same reagents were used, but with shorter incubation and

washing periods, blocking was done in a humidified chamber for one hour, for the primary antibody in the fridge for overnight, and for the secondary antibody for two hours at room temperature. The wholemounted retina and retinal sections were coverslipped with 80% glycerol. Immunolabeled retinas were examined and images of a rod-free zone (RFZ) were taken using a Zeiss Axio Imager M1 microscope with DIC optics.

Sampling in Wholemounts and Cell counts

Cell density in retinal wholemounts was determined as described in recent publications (Querubin et al., 2009, Lee and Bumsted O'Brien, 2011) with slight modifications. Briefly, for total photoreceptor cell sampling, the retina was mounted photoreceptor side up on a glass slide and coverslipped with 80% glycerol. Using a Zeiss Axio Imager M1 microscope with DIC optics, photoreceptor inner segments were photographed at the fovea, 500 μm eccentric to the fovea, and then at 1 mm intervals until the peripheral edge of the retina was reached. The number of total photoreceptor inner segment profiles (both rods and cones) was counted in ten randomly selected 10 μm × 10 μm sampling boxes in a 250 μm-wide field. The average number of inner segment profiles per mm^2 was then calculated.

To determine ganglion cell density, retinas were stained with PI (Sigma; diluted 1:500 in 1X PBS) for 1 hour at room temperature, followed by two 15 minute 1X PBS washes. The retina was mounted ganglion cell layer (GCL) upwards on a glass slide. The fovea was located by identifying a small circular depression in the ventro-temporal retina of the optic disc (Figure 1). To obtain a series of confocal Z-stack images through the complete thickness of the GCL in the fovea, and at 500 μm intervals from the fovea to the retinal margins in the nasal, temporal, dorsal and ventral orientations, a Zeiss Axio Imager M1 with a LSM 5 Pascal unit (Carl Zeiss AG) and He-Ne laser (LASOS Lasertechnik GmbH, Jena, Germany) was used in conjunction with PASCAL software (Release Version 4.0, Carl Zeiss AG). The Z-stack images were opened in Adobe Photoshop CS3 and compiled into layers. All the ganglion cell nuclei in an average of 16 (10 μm × 10 μm) sampling boxes were counted through all Z-stacks. By counting only the

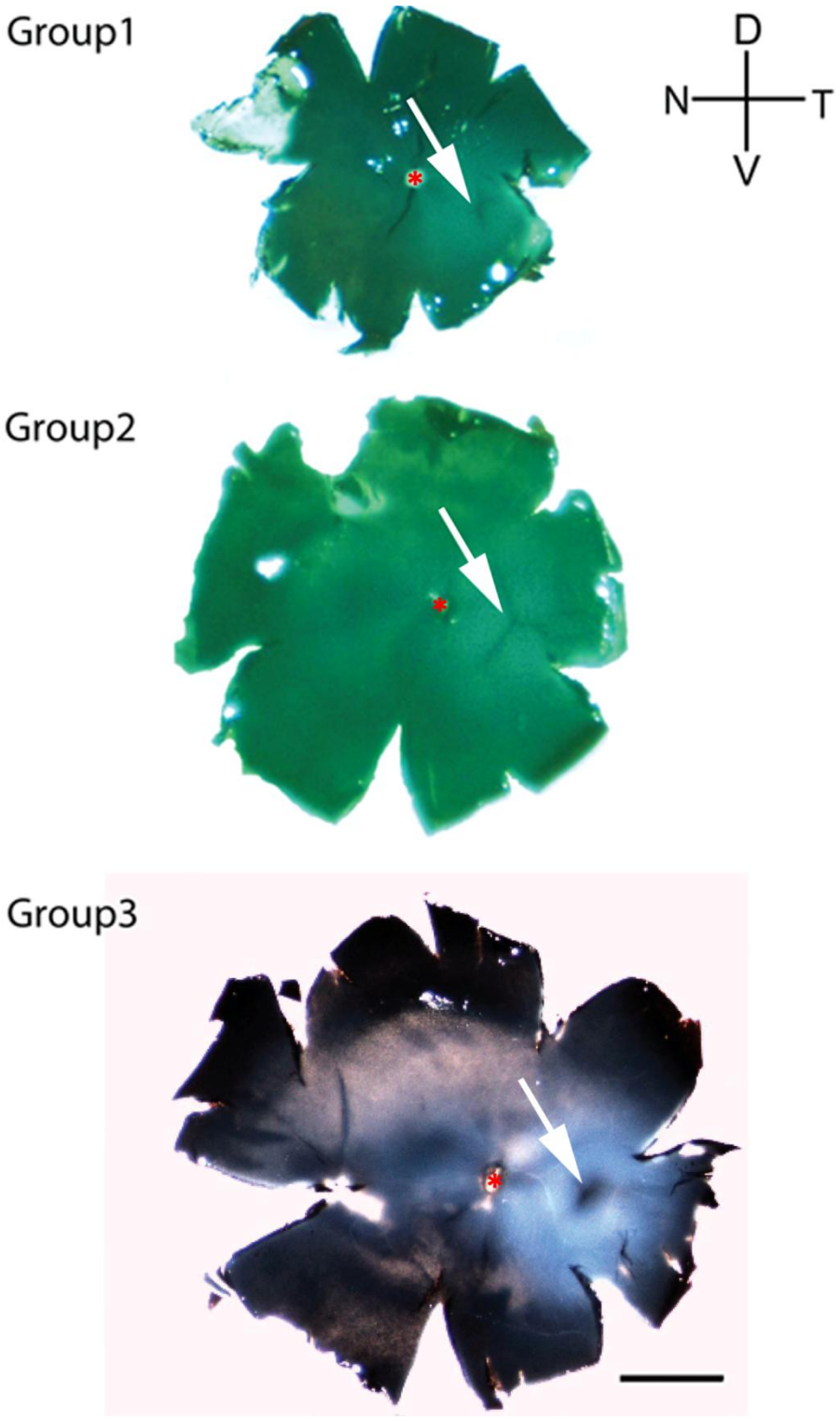

Figure 1: The location of fovea relative to the optic nerve

Flat-mounted eyecups. A convexiclivate fovea is located in the region ventro-temporal to the optic nerve (*) and remains the same relative location during development. It is marked by slightly raised area (foveal slope) with an indentation at the centre (fovea), arrow. Scale bar = 1 mm.

only the newly appearing cells on the overlapping layers, it was assured that no cell was omitted or counted twice. The average number of cells per mm^2 was then calculated.

Topographic Map Construction

Topographic maps of the GCL and total photoreceptor density were constructed from *H. taeniopterus* retinas where the number of retinas processed was: group 1 (n = 5), group 2 (n = 5), and group 3 (n = 2). The image of each flattened retina was taken using a dissecting microscope (Zeiss SteREO Discovery.V12, Jena, Germany or Leica MZ 16A, Leica Microsystems, Heerbrugg, Switzerland) and the retinal shape was traced in Adobe Illustrator CS3. Using the stage micrometer, X-Y coordinates of retinal landmarks were determined and each sampling location was plotted. Using the calculated densities for each sampling point, isodensity lines were drawn manually to connect regions of equivalent cell density.

Theoretical Limit of Seahorse Visual Resolution

We adopted the same calculation methods previously discussed in depth to determine the theoretical limit of seahorse visual resolution (Neave, 1984, Collin and Pettigrew, 1989, Lee and Bumsted O'Brien, 2011). The theoretical limit was calculated using two different methods taking either cone photoreceptor density or ganglion cell density into account. Neave (1984) determined the anatomical limit of visual resolution using cone photoreceptor cell densities, the lens radius and Matthiessen's ratio. The formula used was $\sin \alpha = c/f$, where α was the minimum separable angle measured in minutes of arc, c was the distance between the centres of adjacent cones, and f was the focal length of the lens. The cone spacing distance (c) in mm was obtained from the reciprocal of the cone density (d), which was estimated in number of cells per 1 mm length of retina. The focal length of the lens was calculated using Matthiessen's ratio, which states that the distance from centre of the lens to the retina (posterior nodal distance, PND or the focal length of the lens, f) was 2.55 times the radius of the lens (r) (Matthiessen, 1880). A formula to calculate the theoretical limit of acuity was modified to: $\sin \alpha = 1/(d \times 2.55r)$, however, tissue shrinkage was calculated to be approximately 10%. In order to take this into

consideration when calculating the theoretical limit of acuity, a factor of 1.11 is included in the equation: $\sin \alpha = 1.11/(d \times 2.55r)$; $\sin \alpha = 0.43529/(dr)$.

Another method to calculate the theoretical limit was introduced by Collin and Pettigrew (1989) using the density of cells in the GCL (Collin and Pettigrew, 1989). The angle (α) subtending 1 mm on the retina was calculated by $\tan \alpha = 1$ mm/PND and the spatial resolution was estimated by obtaining the number of cells subtended by one degree of visual arc, i.e. cells per degree = cell density/PND. Since at least two ganglion cells were needed to distinguish the light and dark boundaries forming one cycle of a grating of the highest resolvable frequency, the theoretical limit of visual resolution was calculated according to the equation: Cycles per degree (cpd) = cells per degree/2. In order to make a direct comparison between theoretical and behavioural limits of visual resolution, the unit cpd was converted to minutes of arc/cell by: 1/(cells/degree · degrees/60 minutes) = minutes/cell.

Statistical analysis was conducted by an Analysis of variance (ANOVA) and Linear Mixed Models (Restricted Maximum Likelihood (REML) methods) using GenStat software. Coefficient of determination (R^2) which indicates how well the data points fit a statistical model was calculated using the Excel function for the correlation coefficient (CORREL) and square it.

RESULTS

The average length of fish (Table 1) was statistically significantly different between groups ($P < 0.001$). With the increase in body length, the average naso-temporal diameter of *H. taeniopterus* eyes increased (Table 1). Larger fish had a statistically significant larger naso-temporal diameter ($P < 0.001$).

Morphological Development of the Fovea and Rod-Free Zone (RFZ)

All *H. taeniopterus* reported in this study possessed a convexiclivate foveal pit in the ventro-temporal retina characterised by a steep foveal slope with a thin narrow foveal centre that contained all the nuclear layers (Figure 2a, 2c and 2e). The basic shape of the foveal pit was similar in all age groups; however, there was a trend for the pit to be deeper and wider as the eye enlarged.

In addition to a fovea, a RFZ located in the ventro-temporal retina was present in all age groups. The RFZ included the convexiclivate *fovea centralis* and surrounding retina. Initially, the shape of RFZ was slightly skewed towards the optic nerve (group 1, Figure 2b). With age, the RFZ shape became more circular (groups 2 and 3, Figure 2d and 2f). The area of the RFZ increased with age from 0.557 ± 0.11 mm^2 (group 1, n = 5), 0.808 ± 0.10 mm^2 (group 2, n = 5) to 1.213 ± 0.06 mm^2 (group 3, n = 2) ($R^2 = 0.860$). Hence, the largest fish had the largest RFZ. The relative size of the RFZ in comparison to the whole retina decreased during development: the ratio of RFZ area to retinal area was 0.064 in group 1, 0.056 in group 2, to 0.054 in group 3. The distance between the centre of the RFZ and the optic nerve also increased with increasing fish size (Figure 2). These changes occurred mostly between groups 2 and 3. Furthermore, the distance between the nasal margins of the RFZ to the optic nerve increased with increasing fish size.

Total Photoreceptor Cell Density and Topography Maps

The overall pattern of total photoreceptor cell density in *H. taeniopterus* was similar at all ages (Figure 4) in that there was an area with an elevated photoreceptor cell density, which coincided with the foveal rim. Photoreceptor density decreased at the centre of the fovea and

Table 1: Average body length and eye diameter of *H. taeniopterus* in all age groups

Size Group	Body length (mean ± SD, cm)		Naso-temporal eye diameter (mean ± SD, mm)	
	N		N	
1	6	5.82 ± 0.26	11	2.62 ± 0.11
2	5	9.70 ± 0.33	7	3.33 ± 0.14
3	10	14.56 ± 0.77	21	4.17 ± 0.23

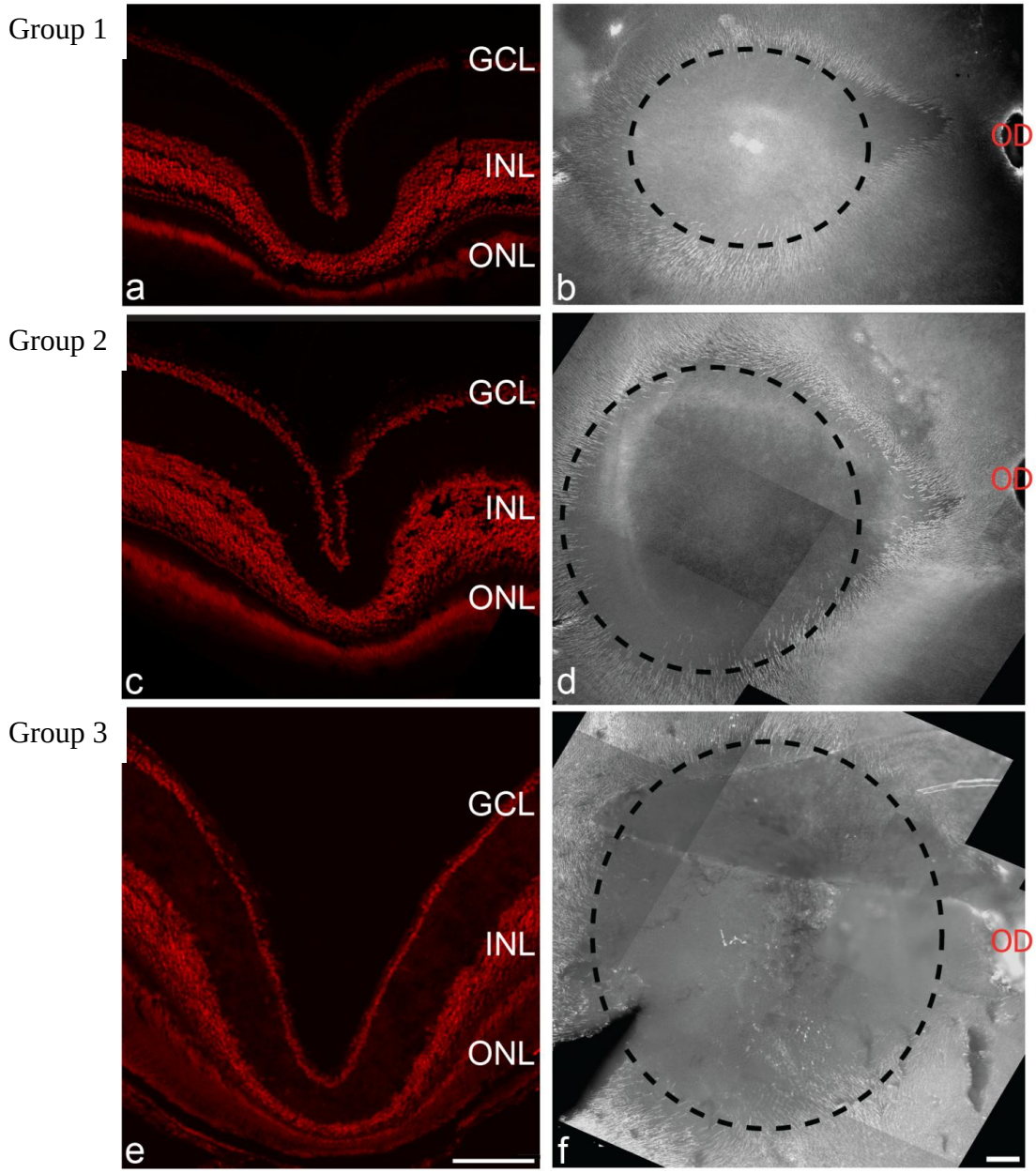

Figure 2: The changes of foveal pit and RFZ during development
Left column: A retinal section through the fovea demonstrates a convexiclivate foveal pit in a developing *H. taeniopterus* (a,c,e). The retinal section was nuclear stained with PI (red). The foveal pit enlarged as fish grew in size. Right column: Wholemount retinas of developing *H. taeniopterus* were immunolabeled with an antibody to rod opsin (RET-P1; white dots and lines labeling rod photoreceptor outer segments). The region where rod photoreceptors were absent (RFZ) was demarcated with black dashed lines. The RFZ increased its size with increasing fish size and its shape became more circular. GCL = ganglion cell layer, INL = inner nuclear layer, ONL = outer nuclear layer, OD = optic disc. Scale bar = 100 μm.

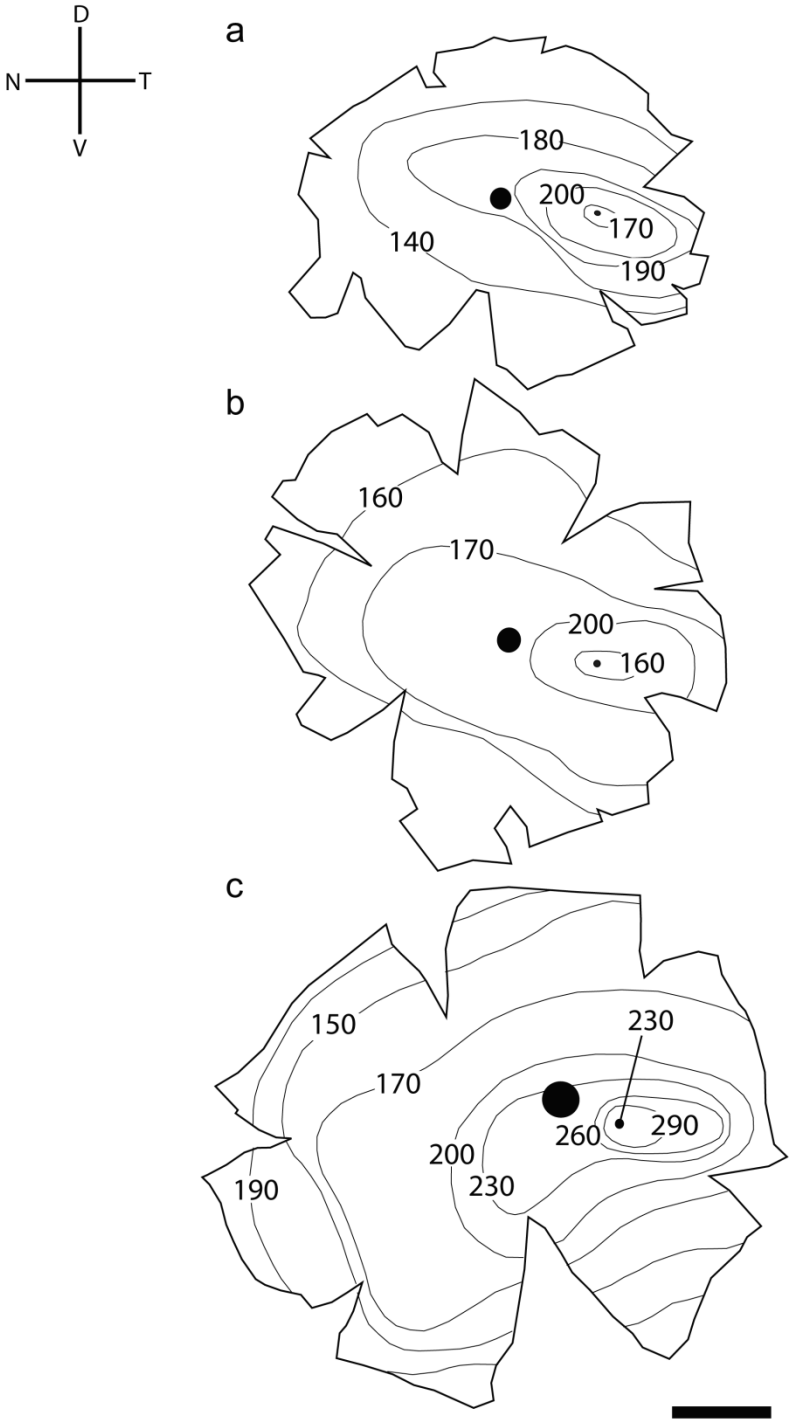

Figure 3: Topography maps of total photoreceptor cells in developing *H. taeniopterus*
Topographic density maps show that the overall pattern of photoreceptor cell density in *H. taeniopterus* was similar at all age groups. The density was highest at the foveal rim and dropped within the foveal center. Towards the periphery, it decreased gradually. Scale bar = 1 mm. Dorsal (D), Temporal (T), Nasal (N), and Ventral (V).

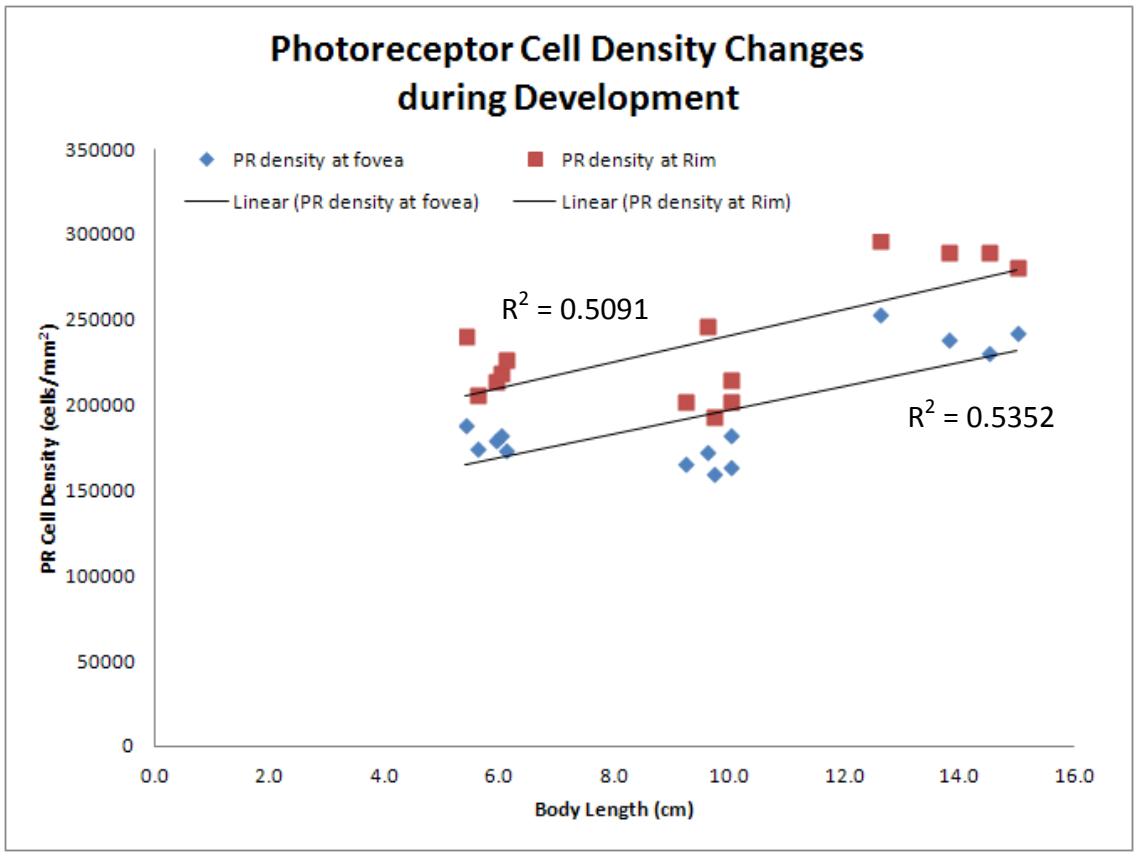

Figure 4: Total photoreceptor cell density changes during development

The total photoreceptor cell densities at the foveal centre and the rim increased as fish grew in size. This suggests that the cone photoreceptor cell density increased at the foveal region during the ocular enlargement since there are no rod photoreceptors in this region. The vertical axis indicates the cell densities (cells/mm^2) and the horizontal axis indicates the body length of fish in centimetres.

into the periphery; however, with increasing size there was a significant increase in photoreceptor and ganglion cell density on the foveal slope. The average peak photoreceptor density (Figure 3 and 4) increased with fish size from 221,200 ± 5,809 cells/mm^2 in group 1 (n = 5) to 289,250 ± 3,092 cells/mm^2 in group 3 (n = 4). This change was statistically significant ($P < 0.001$, $R^2 = 0.509$). In group 2, the peak photoreceptor density was 211,600 ± 9,288 cells/mm^2 (n = 5), which was not statistically different to the photoreceptor density of group 1 at 5% level of significance. The difference in photoreceptor density between group 2 and group 3 was statistically significant, with group 3 having an increased photoreceptor density.

The densities at the centre of the foveal pit (Figure 3 and 4) increased from 180,200 ± 2,746 cells/mm^2 (group 1, n=5), 169,200 ± 4,042 cells/mm^2 (group 2, n=5), to 241,500 ± 4,573 cells/mm^2 (group 3, n=4) ($P < 0.001$, $R^2 = 0.535$). Similar to the peak density values, the differences in photoreceptor density between group 1 and group 2 were not statistically significant. Differences in photoreceptor density between group 2 and group 3, as well as groups 1 and 3 were statistically significant ($P < 0.001$). The average photoreceptor densities at the periphery decreased with age from 150,200 ± 7,172 cells/mm^2 (group 1, n=5), 136,000 ± 7,823 cells/mm^2 (group 2, n=5) to 120,500 ± 15,130 cells/mm^2 (group 3, n=4) (Figure 3 and 4). These changes were not statistically significant ($P = 0.162$).

Ganglion Cell Density and Topography Maps

Figure 5 shows a representative retinal ganglion cell topography map from each age group. The overall ganglion cell density pattern was similar at all stages of development (Figure 5). The highest ganglion cell densities were observed at the foveal slope with slightly decreased ganglion cell densities in the foveal centre. Beyond the foveal slope, the ganglion cell densities gradually decreased towards the edge of the retina. When the highest ganglion cell densities calculated were compared amongst the size groups (Figure 6), the ganglion cell density decreased as fish grew in size. Group 1 (n = 5) had the highest retinal ganglion cell density (69,800 ± 6304 cells/mm^2), group 2 (n = 5) (53,400 ± 7474 cells/mm^2) ganglion cell density was intermediate and group 3 (n = 6) retinas (50,000 ± 1265 cells/mm^2) ganglion cell densities were the lowest. This decrease was statistically significant ($P = 0.047$, $R^2 = 0.324$).

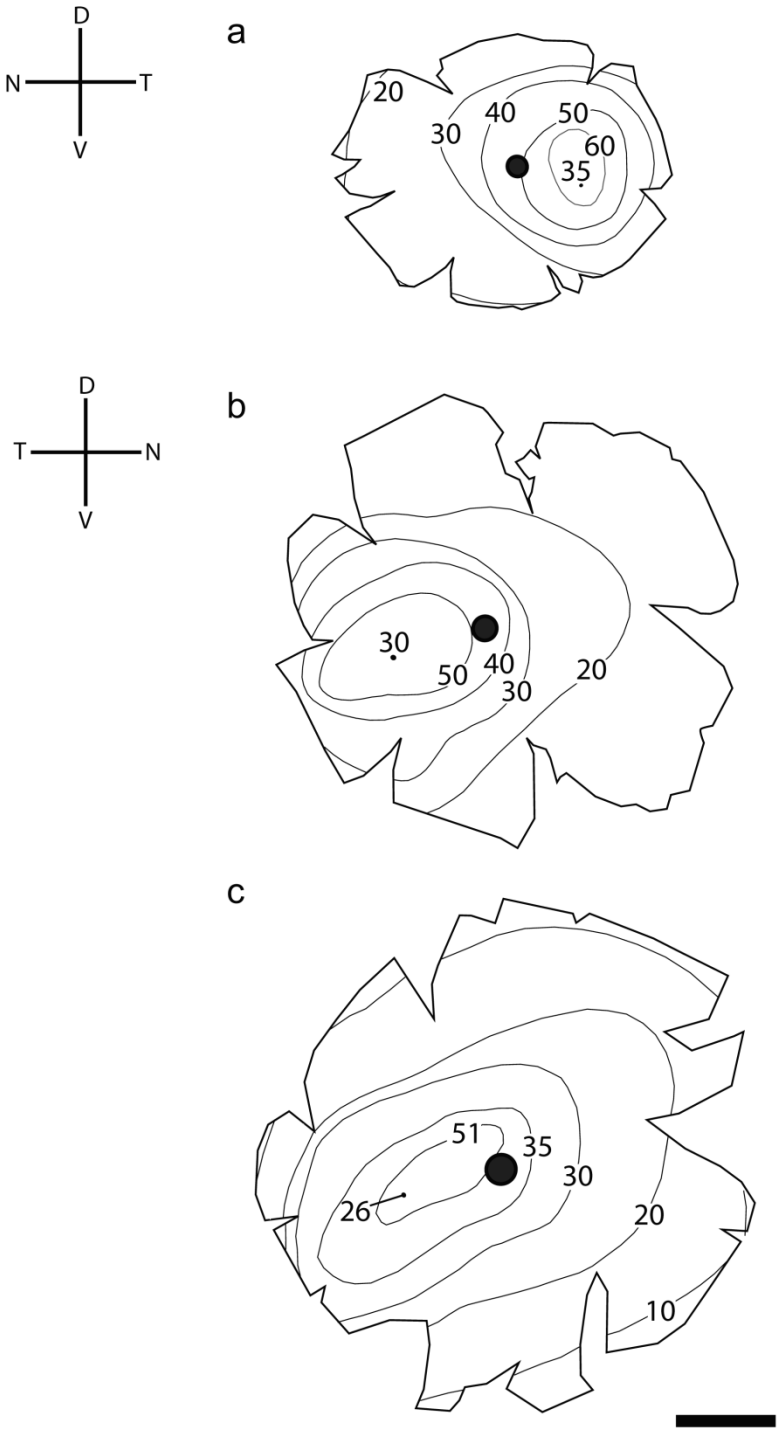

Figure 5: Topography maps of ganglion cells in developing *H. taeniopterus*
Topographic maps of ganglion cell density indicate that the overall pattern of ganglion cell density in *H. taeniopterus* was similar at all age groups. The pattern is also similar to that of total photoreceptor cells (Figure 3). The density was highest at the foveal rim and dropped within the foveal centre. Towards the periphery, it decreased gradually. Scale bar = 1 mm. Dorsal (D), Temporal (T), Nasal (N), and Ventral (V).

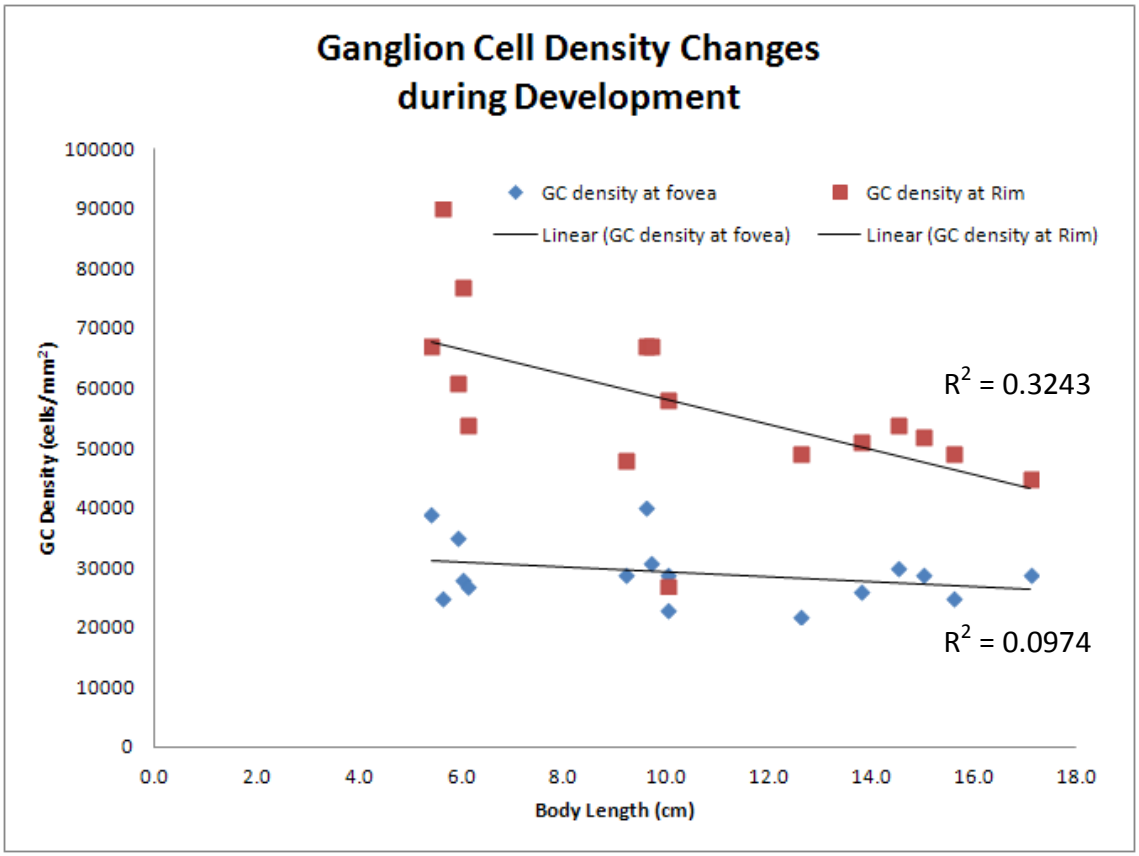

Figure 6: Ganglion cell density changes during development

The ganglion cell densities at the foveal centre did not change significantly (R^2 = 0.097), whereas those at the rim decreased as fish grew in size (R^2 = 0.324). The changes occurred at the foveal centre deviated from the general rule of teleost retinal growth. The vertical axis indicates the cell densities (cells/mm^2) and the horizontal axis indicates the body length of fish in centimetres.

At the centre of the fovea, the average ganglion cell densities were 30,800 ± 2653 cells/mm^2 (group 1, n = 5), 30,400 ± 2750 cells/mm^2 (group 2; n = 5) and 26,833 ± 1249 cells/mm^2 (group 3; n = 6) (Figure 6). These changes in ganglion cell density between age groups were not statistically significant ($P = 0.385$, $R^2 = 0.097$). At the far periphery, the ganglion cell densities were 19,000 ± 1225 cells/mm^2, 16,800 ± 917 cells/mm^2, and 14,667 ± 1584 cells/mm^2, respectively. Again, the changes were not statistically significant ($P = 0.102$).

Theoretical Visual Resolution

The average lens radius showed a statistically significant increase with increasing fish size from 0.43 ± 0.01 mm (group 1, n = 12), to 0.56 ± 0.01 mm (group 2, n = 7) and to 0.69 ± 0.04 mm (group 3, n = 24; $P < 0.001$). The theoretical visual resolution based on the cone photoreceptor cell densities at the foveal slope and the lens radius improved from 7.42 ± 0.10 minutes of arc in group 1, to 5.78 ± 0.12 minutes of arc in group 2, and to 4.04 ± 0.02 minutes of arc in group 3 (Figure 7). This change was statistically significant ($P < 0.001$, $R^2 = 0.950$). The theoretical visual resolution calculated from the density values in the foveal centre yielded 8.21 ± 0.06 minutes of arc in group 1, 6.45 ± 0.08 minutes of arc in group 2 and 4.43 ± 0.04 minutes of arc in group 3 (Figure 7). These data indicated that the best theoretically achievable seahorse resolution significantly improved with increasing fish size ($P < 0.001$, $R^2 = 0.962$).

The theoretical visual resolution was also calculated using a formula taking the ganglion cell densities into account (Figure 7). From the average highest ganglion cell density values estimated at the foveal slope, the calculated theoretical visual resolution was 9.75 ± 0.96 minutes of arc in group 1, 9.40 ± 1.94 minutes of arc in group 2, and 7.97 ± 0.25 minutes of arc in group 3. These changes were not statistically significant between groups ($P = 0.065$, $R^2 = 0.273$). This indicated that the spatial visual resolution that the seahorse could achieve theoretically based on the ganglion cell density were similar in different size groups studied.

In constrat, the theoretical visual resolution calculated from the ganglion cell densities at the foveal centre was 14.65 ± 1.35 minutes of arc, 12.11 ± 1.19 minutes of arc, and 10.91 ± 0.66 minutes of arc, respectively. These differences were statistically significant ($P < 0.001$, $R^2 =$

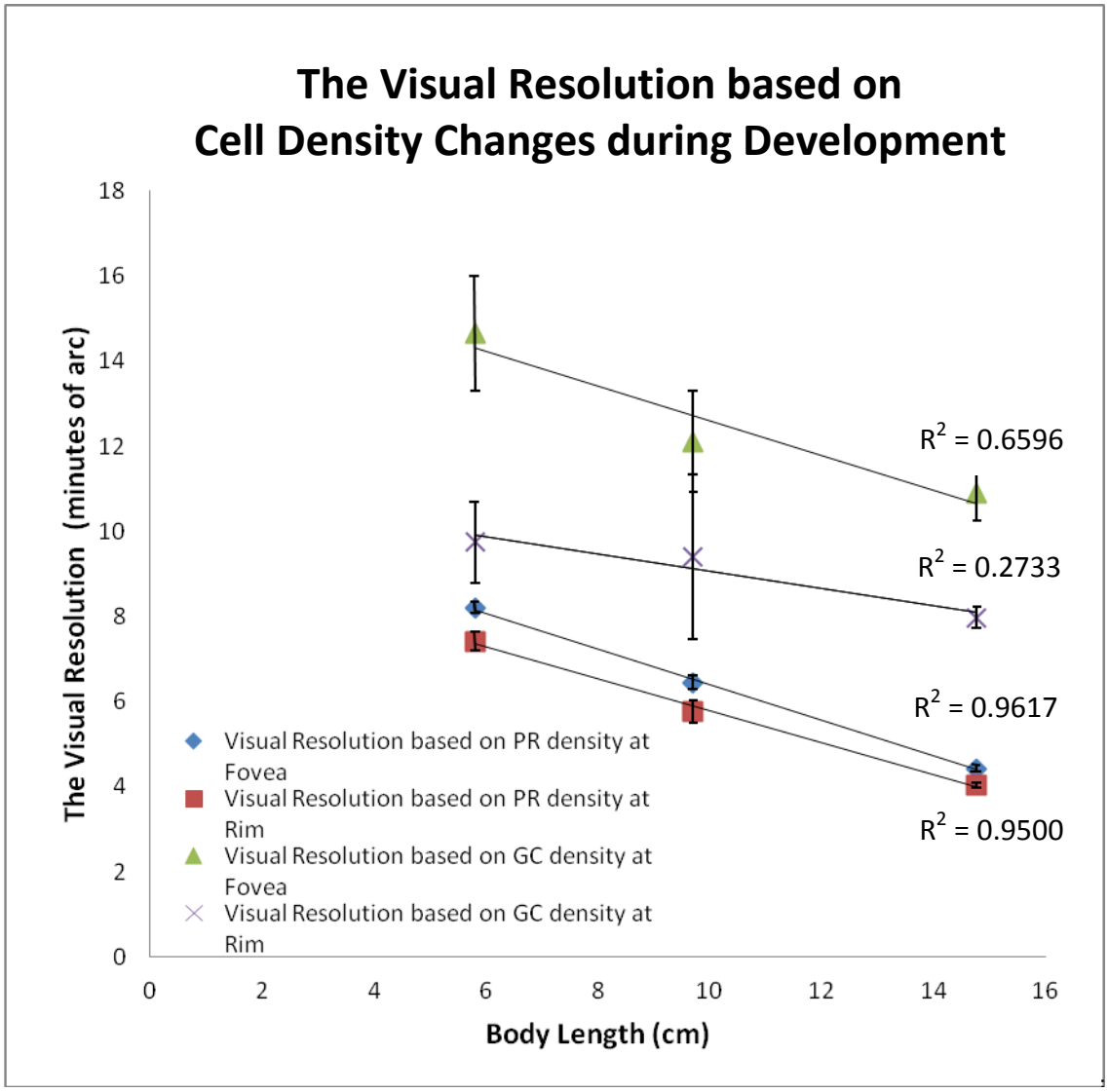

Figure 7: Theoretical visual resolution based on the cell densities

The theoretical visual resolution based on the cone photoreceptor and ganglion cell densities significantly improved at the foveal centre during development. The results demonstrated that the fish can resolve smaller objects as they grow, and hence, has better visual resolution. The visual resolution was poorer when calculated with the ganglion cell densities. The vertical axis indicates the visual resolution in minutes of arc and the horizontal axis indicates the body length of fish in centimetres. The error bars indicate standard deviation.

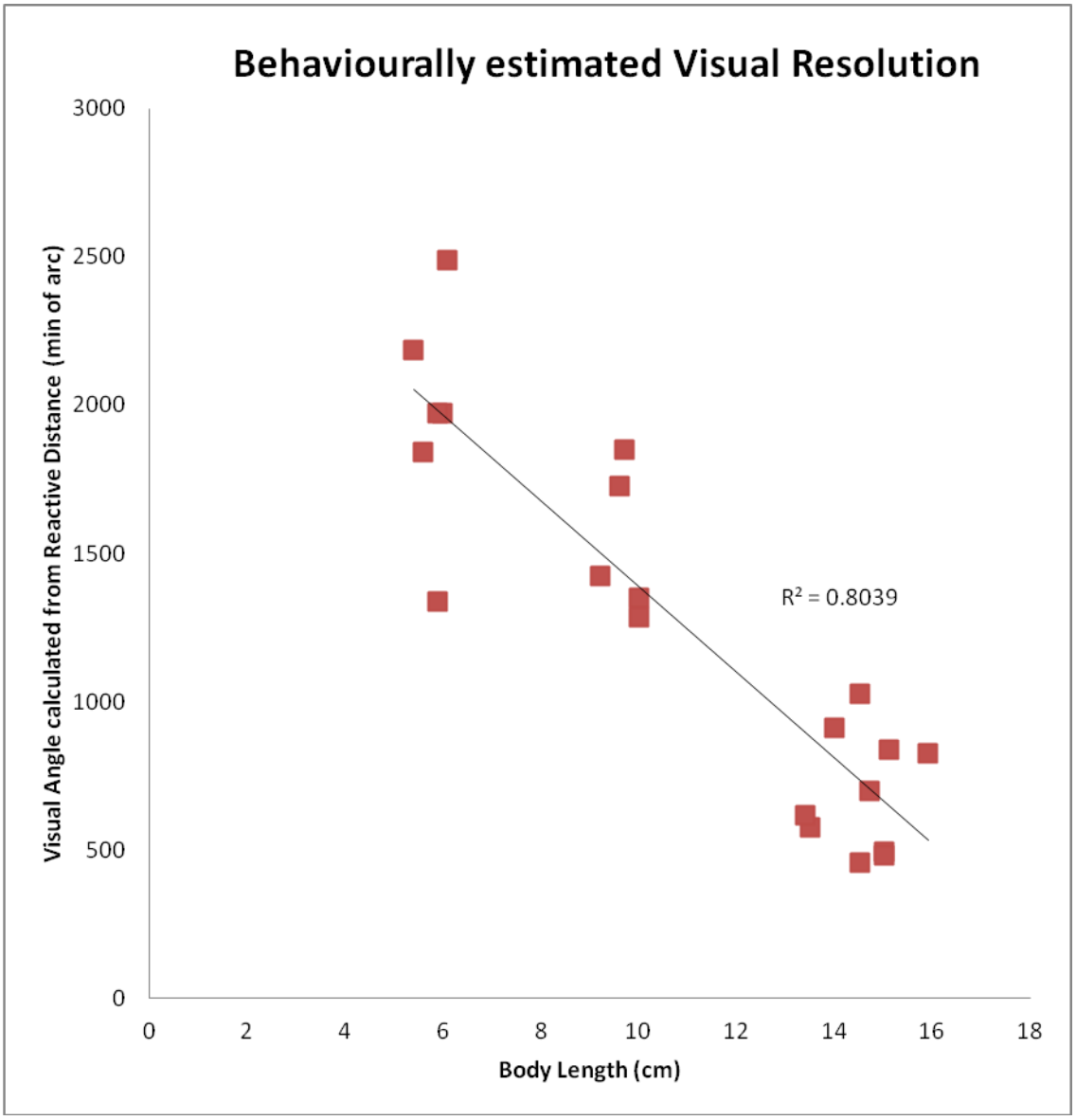

Figure 8: Behaviourally estimated visual resolution

Individual data for behaviourally estimated visual resolution demonstrated a linear relationship with the body length of *H. taeniopterus* (R^2 = 0.804). The vertical axis indicates the visual resolution estimated from the reactive distance (minutes of arc) and the horizontal axis indicates the body length of fish (centimetres).

0.660). These data indicated that the theoretically achievable visual resolution at ganglion cell level at the foveal centre becomes better as the seahorse grows larger.

Behaviourally estimated Visual Resolution

Larger seahorses (group 3, n=10) had smaller visual angles measured behaviourally in minutes of arc (692.86 ± 198.36 min of arc), compared to the smaller groups (1966.47 ± 382.67 min of arc; group 1 (n=6), 1527.20 ± 246.81 min of arc; group 2 (n=5)) (Figure 8). This indicated that the larger seahorses (group 3) were able to detect prey of smaller size, and therefore, had a significantly better visual resolution, compared to the smaller fish ($P < 0.001$, $R^2 = 0.804$).

DISCUSSION

This study demonstrated that the seahorse *fovea centralis* changes as the fish grows. Morphologically, the *fovea centralis* became wider and deeper pit during development. Photoreceptor cell densities at the foveal centre and slope showed a statistically significant increase with fish size. Ganglion cell densities, on the other hand, decreased within the foveal centre, and did not change on the slope as the fish grew. The density changes occurred mostly between groups 2 and 3, which correlated with a larger change in fish size compared with the difference in size between groups 1 and 2. The observed morphological changes during development correlated with functional changes, although there was an exception with the visual resolution calculated from the ganglion cell densities. The theoretical visual resolution calculated from the cone photoreceptor cell densities were always higher compared with those calculated from the ganglion cell densities; however, both the theoretical limits of visual resolution improved as the fish grew. In every case, the theoretical visual resolution calculated from both cone photoreceptor and ganglion cell densities was higher than the behaviourally onserved visual resolution.

The Development of the fovea in Teleosts

The association between the morphological development of the fovea and improvements in visual resolution has been studied in various teleost species (Browman et al., 1990, Pankhurst et al., 1993, van der Meer, 1995). In the current study, a morphologically distinct fovea was present in the smallest seahorse age group studied. With increasing fish size, the foveal region displayed developmental changes, which included an increased pit definition including an increase in width and depth. I suggest that these changes are associated with the enlargement of the eye. Seahorse eyes, like all fish eyes, continue to grow throughout life. In most fish, eye growth rate is relative to body growth depending on the importance of vision to the animal (Fernald, 1988). The enlargement of the teleost retina is attributable to two different mechanisms; the addition of new neurons 1) at the retinal margins and from the rod progenitor cells interspersed across the entire retina and 2) the spreading of existing neural elements as the retina stretches (Müller, 1952, Johns, 1977, Johns and Easter, 1977, Johns, 1981, Fernald, 1985,

Pankhurst et al., 1993, Otteson and Hitchcock, 2003, Hitchcock and Raymond, 2004, Morris et al., 2008). As the retina stretches during enlargement, the pit may be mechanically stretched resulting in it becoming wider. Furthermore, asymmetrical cell addition within a temporal retinal specialisation (Cameron, 1995) may result in thicker retinal layers in the temporal region, which may function to deepen the foveal pit.

How does the ocular enlargement influence the development of teleost retinae with an emphasis on a retinal specialisation? New neurons including cone photoreceptor, bipolar and ganglion cells are added circumferentially at the retinal margin (circumferential germinal zone, CGZ) (Raymond and Rivlin, 1987, Fernald, 1988, Otteson and Hitchcock, 2003, Hitchcock and Raymond, 2004, Moshiri et al., 2004, Raymond et al., 2006). The densities of these newly generated and added retinal neurons decreases during development although the total number of cells increases (Johns, 1977, Johns and Easter, 1977, Johns and Fernald, 1981, Fernald, 1985, Fernald, 1988, Pankhurst et al., 1993, van der Meer, 1995). The mechanism suggested for this oserved density decrease and cell number increase was retinal stretching. The increased stretch force applied to the retina out-paced the addition of new neurons. New rod photoreceptors are an exception because they are generated and integrated into the existing outer nuclear layer across the retina (Otteson and Hitchcock, 2003, Hitchcock and Raymond, 2004, Morris et al., 2008). Newly generated rods are added at a faster rate compared with newly formed cells at the retinal margin; therefore, eye stretching does not directly contribute to the observed rod photoreceptor density increases with age (Fernald, 1988, Pankhurst et al., 1993). According to previous literature, increased total photoreceptor cell density is due to the addition of rod photoreceptor cells across the entire differentiated retina. This mechanism would likely not play a role in the increased cone photoreceptor densities observed on the foveal slope with increasing fish size because the fovea lies within the RFZ, a region where rods were never detected.

Asymmetrical retinal growth (Easter, 1992, Cameron, 1995, 1996, Zygar et al., 1999) may play a role in the location of the RFZ as the fish grows. In order to preserve the relative location of the temporally positioned fovea in teleosts possessing a fovea, the retina may grow asymmetrically along the naso-temporal axis (Easter, 1992). A proposed mechanism would be a

decreased retinal growth rate between the optic nerve and the fovea as compared with retina temporal to the foveal pit. Considering the naso-temporal asymmetry in growth, the sampling from 500 μm eccentricity from the centre of the fovea on the nasal side of the foveal centre in older fish may include rod photoreceptors. Also, this sampling window may include rod photoreceptors in group 1 retinas where the radius of RFZ was smaller. Hence, the increased rod densities in these sampling windows may affect the total photoreceptor cell density changes. This pattern of growth is different to primates where the distance between the foveal centre and the optic nerve does not change during development (Packer et al., 1990, Hendrickson, 1992). This may be due to the fact that the ocular enlargement is not as dramatic during their growth and is often finite.

My data do not completely exclude cell migration towards the fovea during retinal development. The mechanism that mediated the increased photoreceptor cell densities on the foveal slope and at the foveal centre is unknown. Previous authors (Hendrickson and Yuodelis, 1984, Yuodelis and Hendrickson, 1986, Diaz Araya and Provis, 1992, Provis et al., 1998) have shown that the foveal depression in primates begins to form just before mid-gestation. This is the time that ganglion cells accumulate at the centre of the incipient fovea to form the thickened GCL at fetal week (Fwk) 14-15 in human and at 90 fetal days (Fd) in macaque monkeys (Provis et al., 1998). At Fwk 24 in humans and Fd 110 in macaque monkeys, centrifugal displacement of the cells in GCL and INL in the region of the incipient fovea is first observed. The early fovea is observable as a shallow depression that becomes deeper with age, eventually leading to a depression in which only the ONL is present. At the same time that the fovea is forming, there is an increase in cone photoreceptor cell density and corresponding elongation of the fibers of Henle follows (Diaz Araya and Provis, 1992).

Unlike well-studied primate foveal development, my study did not include seahorses prior to hatching, nor did I include newly hatched searhoses in my analysis. In the smallest seahorse analysed, a fovea was detected. This means that if early seahorse development is similar to the primate, pit formation must be occurring prior to hatching. In addition, the observation that the foveal depression becomes wider and deeper as the fish grows suggests

some similarity with primate foveal development; however, because the seahorse eye enlarges throughout its lifetime (unlike in primates) there must be distinct differences. One major difference between the seahorse and primate foveas is that in the groups investigated, all the nuclear layers are present within the foveal region. Despite these differences between the primate and seahorse, it is still possible that the increased cone photoreceptor density in the fovea is mediated by a similar mechanism that remains unknown.

The peak ganglion cell density values of the seahorse retina followed the general pattern of fish eye growth as well (Easter Jr et al., 1977, Collin and Pettigrew, 1989). Despite the increase of the total number of the ganglion cells, the density decreased as the retina enlarged during development. These density values are less than the peak ganglion cell density of 15.0 x 10^4 cells per mm^2 in the sandlance *Limnichthyes fasciatus* (Collin and Collin, 1988b) that is known to possess a fovea and independent ocular movements similar to the seahorse. In human, the ganglion cell density at the central retina was estimated to be 3.2 x 10^4 – 3.8 x 10^4 cells per mm^2 (Curcio and Allen, 1990), less than the peak ganglion cell density of the seahorse retina. This is an interesting point as the human has higher visual resolution compared to the seahorse. Ganglion cell densities at the foveal centre, however, did now show statistically significant changes in contrast to the general rule.

The Developmental Changes of Retinal Topography

The cell density topography patterns for both total photoreceptors and ganglion cells in *H. taeniopterus* demonstrated a single fovea in the ventro-temporal retina with a concentric arrangement of isodensity lines around the fovea (Figure 3 and 5). A similar topographic pattern was observed in the sandlance *L. fasciatus* (Collin and Collin, 1988b). The Terrain Theory (Hughes, 1977) suggested that the topography of ganglion cells across the retina depends on the symmetry or openness of the perceived world. For instance, horizontal streaks were found in several open-water teleost species, which enabled the fish to scan a broad horizon, without distinctive eye movements (Collin and Pettigrew, 1988c, b). Ambush predators including the clown triggerfish, *Balistoides conspicillum* and the painted flute mouth, *Aulostoma chinensis* take advantage of those horizontal streaks, which minimise whole body movements. In contrast,

species inhabiting closed environments possess retinal specialisations; single or multiple areas with increased cell densities. Most seahorses inhabit algal or sponge reefs in 5 to 30 m depth (Kuiter, 2000). Therefore, the presence of a fovea is not a surprise. Furthermore, independently moving eyes are used to scan continuously across their surroundings. This peculiarity of independent eye movements may compensate the lack of a horizontal streak in seahorses, as ambush predators.

Foveal location depends on the position of the eyes in the head (Collin and Collin, 1988b, Collin, 1999). In general, teleosts have laterally displaced eyes, and hence, possess temporal retinal specialisations. Various functions of these temporal retinal specialisations have been suggested. A fovea is believed to give fish an advantage with acute binocular vision at near distances. This may imply that the fish can judge the prey size using binocular cues as well as from the visual angle subtended. Collin and Pettigrew (1988c) suggested that this acute zone is associated with feeding more than surveillance of potential predators (Collin and Pettigrew, 1988c). Kahmann's study also suggested that the temporal retinal specialisation may also be used for monocular vision in addition to binocular vision (Kahmann, 1934, Collin and Collin, 1999). The topography pattern remains the same throughout life in seahorses, whereas, in some fish these topography changes from a larval stage to an adult (Bozzano and Catalán, 2002). It may be due to the different visual needs depending on the different environmental habitat available during development. This agrees with the 'terrian theory' (Hughes, 1977).

The Development of Visual Resolution

In this study, the theoretical visual resolution in seahorse were determined using both cone photoreceptor and ganglion cell densities (Neave, 1984, Collin and Pettigrew, 1989). Cone photoreceptor cell density has been most frequently used for calculating the visual resolution as the inter-cone spacing determines the finest resolution for retinal images (Neave, 1984). According to the calculation involving cone photoreceptor densities, the visual resolution in seahorses improved during development both at the foveal centre and slopes (Otten, 1980, Miller et al., 1993). Hence, larger seahorses have better spatial visual resolution.

Better visual resolution also requires a higher angular density of cones. In general, the actual cone densities decreased during teleost development. Nevertheless, increasing eye and lens size with a corresponding longer focal length, allow a larger retinal area to be exposed, and therefore a larger number of cones per visual angle to be stimulated (Guma'a, 1982, Pankhurst et al., 1993). Hence, retinal images are magnified as the eye grows (Easter et al., 1977, Collin and Pettigrew, 1989). In our results, the total photoreceptor cell densities at the foveal slope as well as the cone densities at the foveal centre increased as fish grew in size. The gradual increase in cone packing density in the fovea is consistent with improved visual functions including visual acuity and contrast sensitivity (Breck and Gitter, 1983, Boothe et al., 1985, Pankhurst et al., 1993).

Collin and Pettigrew (1989) used ganglion cell density instead for the calculation of the visual resolution (Collin and Pettigrew, 1989). They suggested that the spatial distribution of the retinal ganglion cells place an upper limit on the spatial resolving power of the animal because the retinal ganglion cell mosaic provides the only link between the eye and behavioural output (Collin and Pettigrew, 1989). In seahorses, the visual resolution determined from ganglion cell densities improved at the foveal centre during development. Considering that the ganglion cell densities at a foveal centre remained statistically constant, improvement in visual resolution may be due to the increase in angular density as fish eye enlarges during growth. On the foveal slope where the ganglion cell density decreased as fish grew, the calculated visual resolution did not have statistically significant changes. These data agree with previous literature that have reported that acuities vary directly with eye size and lens diameter and that ganglion cell densities play less of a role in determining visual acuity (Hairston et al., 1982, Collin and Pettigrew, 1989). From the calculation based on the ganglion cell densities, Collin and Pettigrew (1989) demonstrated that the teleost species with larger eye sizes had better visual resolution regardless of the ganglion cell densities (Collin and Pettigrew, 1989). A positive correlation between intraspecific eye size and visual prey detection were also demonstrated in behavioural studies (Hairston et al., 1982, Breck and Gitter, 1983, Li et al., 1985, Pankhurst et al., 1993). Our data also demonstrated that the larger sized seahorses had the lowest ganglion cell densities

at the foveal slope, but had better behavioural spatial visual resolution. The theoretical visual resolution in the largest seahorses calculated from ganglion cell density (around 2.76 cpd) are poorer than most reef teleost species studies by Collin and Pettigrew (1989) (Collin and Pettigrew, 1989). This may be due to the smaller sized eyes in *H. taeniopterus*.

The behaviourally measured visual resolution in seahorses improved during development as well. Various methods have been conducted to determine the functional aspects of teleost vision involving the optokinetic or optomotor responses to visual stimuli of vertical gratings presented on a rotating drum (Fritsches and Marshall, 2002, Fleisch and Neuhauss, 2006, Mueller and Neuhauss, 2010), and the training of the fish to distinguish a visual stimulus from background (positive reinforcements) (van der Meer, 1995, Siebeck et al., 2008) as a function of retinal growth. In general, the visual stimuli are gratings with various spatial frequencies and the background is a uniform grey target. Seahorses do not behave the same way as other teleosts. As an ambush predator, they await the prey in a stationary position. Using their independent eye movements, they scan across their surroundings for their prey as well as their predators. They do not possess consistent optomotor responses in that they do not swim consistently to the direction of visual stimulus (personal observation). With independent eye movements, they possess extended asynchronous optokinetic responses to a single whole-field stimulus similar to that observed in the sandlance and pipefish (Fritsches and Marshall, 2002). Therefore, in this study, for consistently and more reliable results we have used a method known as “Reactive Distances”.

The ‘reaction’ or ‘pursuit distance’ has been commonly used in zooplanktivores to measure a fish’s ability to locate prey (O'Brien, 1979, Lazzaro, 1987, Wanzenbock and Schiemer, 1989). Reactive distance is defined as the distance between predator and prey at which the predator first ‘notices’ or reacts to the prey (Browman et al., 1990). Pursuit distance is defined as the distance of the repositioning movement that precedes an attack on a prey item. This reaction or pursuit distance to detect the prey is used to define the limits of the fish’s search space by integrating it into a formula to calculate visual resolution (O'Brien, 1979, Lazzaro, 1987, Browman et al., 1990). The behaviourally determined visual resolution improved as the

seahorse grew, and hence, the result is consistent with the theoretical calculation that larger fish have better visual resolution.

In general, behaviourally determined visual resolution has been reported to be poorer than theoretical visual resolution (Northmore and Dvorak, 1979). It is also true for the seahorse. The mismatch between the theoretical and behavioural visual resolution in *H. taeniopterus* is 50 to 100 times. The theoretical visual resolution estimates the visual angle whereas, the behaviourally measured visual resolution involves actual recognition of the prey in that the fish resolves features of the object in the way we recognise faces (Ransom-Hogg and Spillmann, 1980, Anstis and Harris, 1987, Costen et al., 1994). In addition, seahorses have binocular vision with a fovea. It is possible that searhoses use stereopsis for the determination of the prey distance. The determination of size likely involves more than resolving just the angular substance of the prey independent of distance. Seahorse must recognise an object as prey before striking. This means painting a picture of it across an array of many ganglion cell receptive fields. Therefore, the angular size is much bigger than that which would be determined by ganglion cell size (Anstis and Harris, 1987).

The visual resolution calculated from the cone photoreceptor cell densities also resulted in smaller minimum resolvable angles compared to those calculated using the ganglion cell densities. These differences may be due to the size of ganglion receptive fields combined with the convergence of cones onto ganglion cells, as well as the additional computations inherent in higher order processing centres (Browman et al., 1990, Pankhurst et al., 1993). The visual resolution estimated using the cone photoreceptor cell densities determines the finest resolution for retinal images whereas, the visual resolution calculated from the ganglion cell density is more practical (Browman et al., 1990, Pankhurst et al., 1993). Despite the differences among the methods to determine the visual resolution in seahorses, the results from the theoretical visual resolution and morphological measures are correlated; larger seahorses resolve smaller targets, and therefore, have better visual resolution compared with smaller fish.

A possible reason for improved vision may be the more developed retinal structures including neuronal circuitry as well as the projections in visual pathways up to higher-order

processing centres. These factors have been suggested to contribute to the rapid development of behavioural acuity during the early free-swimming phases of teleost fishes (Rahmann et al., 1979, Schmitt and Kunz, 1989, Pankhurst et al., 1993). Contrasting theories postulate that the developmental changes of retinal structure are necessary for preserving a constant visual capability, rather than an actual improvement of visual abilities (Fernald, 1988).

Another factor that may contribute to the improved visual resolution in fish is a mature foveal morphology. From our observations during the behavioural tests, it seemed that the youngest seahorse was able to detect mobile prey faster and more efficiently compared to stationary prey (data not shown, personal observations). In the youngest age, the fovea may act as a motion detector, rather a high visual resolution display. In fact, it has been postulated that the convexiclivate fovea functions as a motion detector (Fite and Rosenfield-Wessels, 1975, Lee and Bumsted O'Brien, 2011). As the fish grows, and therefore, the fovea becomes more mature, the detecting ability of the fish for both mobile and stationary prey at a same distance apart becomes similar (personal observation).

Also, considering that the convergence ratio between cone photoreceptors and ganglion cells remains constant during growth (van der Meer, 1994), the increasing number of cone photoreceptors per visual angle would theoretically result in an enhanced photopic resolution and therefore, visual acuity (Guma'a, 1982, Neave, 1984, Browman et al., 1990, Zaunreiter et al., 1991). Along with the increased angular cone density, the diameter of cone photoreceptor outer segments increased as the fish grew (Blaxter and Jones, 1967, Guma'a, 1982, Pankhurst and Montgomery, 1990, Pankhurst et al., 1993). Enlarged cone photoreceptor outer segments have the advantage of increased chances of photon capture. Therefore, sensitivity is enhanced (Pankhurst et al., 1993) and the fish have better visual resolution. Other studies suggested that as the fish grows, the inter-cone spacing decreases. This also increases angular density and therefore, visual resolution improves. However, there is a limit to the further improvement in spatial acuity as further decrease in size can result in light spill into adjacent photoreceptors (Lythgoe, 1980).

The refractive state changes during development may also contribute to the improvement in behavioural acuity (Pankhurst et al., 1993). In larval fish stage, due to the underdeveloped accommodative system, the fish is not able to compensate for potential refractive errors (myopia) caused by Matthiessen's ratio (Wanzenbock and Schiemer, 1989, Pankhurst et al., 1993, Pankhurst, 1994). Furthermore, the fovea of an elliptical eye has a longer lens-to-retina distance making the fovea more myopic, whereas elsewhere the retina would be hypermetropic (Collin, 1999). Although Easter and Nicola (1996) demonstrated that the larval zebrafish is initially hyperopic (Shand et al., 1999), these refractive errors, both myopia and hyperopia would result in smaller fish performing worse than predictions based on cone cell density and lens diameter. However, as the fish matured, they become more emmetropic (Pankhurst et al., 1993, Pankhurst, 1994, Shand et al., 1999) and have better behavioural visual resolution (Wanzenbock and Schiemer, 1989). This is due to a well-developed accommodative system (Pankhurst, 1994) including the stabilisation of Matthiessen's ratio and maturation of the retractor lentis muscle (Shand et al., 1999).

In summary, morphological changes occurring during the development of *H. taeniopterus* are correlated with the functional changes. Photoreceptor cell density in the region of a retinal specialisation increases as the fish grows. This increase suggests the presence of a unique mechanism for foveal development in *H. taeniopterus*, which is also associated with the improvement in their visual resolution.

REFERENCES

Anstis S, Harris J (1987) Magnification factor for adaptation of a visual transient mechanism. J Opt Soc Am A 4:1688-1698.

Barnstable CJ (1980) Monoclonal antibodies which recognize different cell types in the rat retina. Nature 286:231-235.

Blaxter JHS, Jones MP (1967) The Development of the Retina and Retinomotor Responses in the Herring. Journal of the Marine Biological Association of the United Kingdom 47:677-697.

Boothe RG, Dobson V, Teller DY (1985) Postnatal development of vision in human and nonhuman primates. Annu Rev Neurosci 8:495-545.

Bozzano A, Catalán IA (2002) Ontogenetic changes in the retinal topography of the European hake, Merluccius merluccius : implications for feeding and depth distribution.

Breck JE, Gitter MJ (1983) Effect of fish size on the reactive distance of bluegill (Lepomis macrochirus) sunfish. Can J Fish Aquat Sci 40:162-167.

Browman HI, Gordon WC, Evans BI, O'Brien WJ (1990) Correlation between histological and behavioral measures of visual acuity in a zooplanktivorous fish, the white crappie (Pomoxis annularis). Brain Behav Evol 35:85-97.

Bumsted O'Brien KM, Cheng H, Jiang Y, Schulte D, Swaroop A, Hendrickson AE (2004) Expression of photoreceptor-specific nuclear receptor NR2E3 in rod photoreceptors of fetal human retina. Invest Ophthalmol Vis Sci 45:2807-2812.

Cameron DA (1995) Asymmetric retinal growth in the adult teleost green sunfish (Lepomis cyanellus). Vis Neurosci 12:95-102.

Cameron DA (1996) Asymmetric retinal growth: evidence for regulation by a retinotopic mechanism. Vis Neurosci 13:493-500.

Campbell FW, Green DG (1965) Optical and retinal factors affecting visual resolution. J Physiol 181:576-593.

Collin SP (1999) Behavioural ecology and retinal cell topography. In: Adaptive Mechanisms in The Ecology of Vision (Archer, S. N. et al., eds), pp 509-535 Dordrecht: Kluwer Academic Publishers.

Collin SP, Collin HB (1988b) Topographic analysis of the retinal ganglion cell layer and optic nerve in the sandlance Limnichthyes fasciatus (Creeiidae, Perciformes). J Comp Neurol 278:226-241.

Collin SP, Collin HB (1999) The foveal photoreceptor mosaic in the pipefish, Corythoichthyes paxtoni (Syngnathidae, Teleostei). Histol Histopathol 14:369-382.

Collin SP, Pettigrew JD (1988a) Retinal ganglion cell topography in teleosts: a comparison between Nissl-stained material and retrograde labelling from the optic nerve. J Comp Neurol 276:412-422.

Collin SP, Pettigrew JD (1988b) Retinal Topography in Reef Teleosts, I. Some Species with Well-Developed Areae but Poorly-Developed Streaks. Brain Behav Evol 31:269-282.

Collin SP, Pettigrew JD (1988c) Retinal Topography in Reef Teleosts, II. Some Species with Prominent Horizontal Streaks and High-Density Areae. Brain Behav Evol 31:283-295.

Collin SP, Pettigrew JD (1989) Quantitative Comparison of the Limits on Visual Spatial Resolution Set by the Ganglion Cell Layer in Twelve Species of Reef Teleosts. Brain Behav Evol 34:184-192.

Costen NP, Parker DM, Craw I (1994) Spatial content and spatial quantisation effects in face recognition. Perception 23:129-146.

Curcio CA, Allen KA (1990) Topography of ganglion cells in human retina. J Comp Neurol 300:5-25.

Curcio CA, Sloan KR, Kalina RE, Hendrickson AE (1990) Human photoreceptor topography. J Comp Neurol 292:497-523.

Diaz Araya C, Provis JM (1992) Evidence of photoreceptor migration during early foveal development: A quantitative analysis of human fetal retinae. Visual Neuroscience 8:505-514.

Easter Jr SS, Johns PR, Baumann LR (1977) Growth of the adult goldfish eye—I: Optics. Vision Research 17:469-477.

Easter SS, Jr. (1992) Retinal growth in foveated teleosts: nasotemporal asymmetry keeps the fovea in temporal retina. J Neurosci 12:2381-2392.
Easter SS, Jr., Nicola GN (1996) The development of vision in the zebrafish (Danio rerio). Dev Biol 180:646-663.
Fadool JM (2003) Development of a rod photoreceptor mosaic revealed in transgenic zebrafish. Developmental Biology 258:277-290.
Fekete DM, Barnstable CJ (1983) The subcellular localization of rat photoreceptor-specific antigens. J Neurocytol 12:785-803.
Fernald RD (1985) Growth of the teleost eye: novel solutions to complex constraints. Environmental Biology of Fishes 13:113-123.
Fernald RD (1988) Aquatic adaptations in fish eyes. In: Sensory Biology of Aquatic Animals (Atema, J. et al., eds), pp 435-466 Berlin: Springer.
Fite KV, Rosenfield-Wessels S (1975) A Comparative Study of Deep Avian Foveas. Brain, Behavior and Evolution 12:97-115.
Fleisch VC, Neuhauss SC (2006) Visual behavior in zebrafish. Zebrafish 3:191-201.
Fritsches KA, Marshall NJ (2002) Independent and conjugate eye movements during optokinesis in teleost fish. J Exp Biol 205:1241-1252.
Garciá M, Ruiz-Ederra J, Hernández-Barbáchano H, Vecino E (2005) Topography of pig retinal ganglion cells. J Comp Neurol 486:361-372.
Guma'a SA (1982) Retinal development and retinomotor responses in perch, Perca fluviatilis L. Journal of Fish Biology 20:611-618.
Hairston NG, Jr., Li KT, Easter SS, Jr. (1982) Fish vision and the detection of planktonic prey. Science 218:1240-1242.
Hamann S (2002) Molecular mechanisms of water transport in the eye. In: International Review of Cytology, vol. Volume 215 (Thomas Zeuthen, W. D. S., ed), pp 395-431: Academic Press.
Harkness L, Bennet-Clark HC (1978) The deep fovea as a focus indicator. Nature 272:814-816.
Hemmi JM, Grünert U (1999) Distribution of photoreceptor types in the retina of a marsupial, the tammar wallaby (Macropus eugenii). Visual Neuroscience 16:291-302.
Hendrickson A (1992) A morphological comparison of foveal development in man and monkey. Eye 6 (Pt 2):136-144.
Hendrickson AE, Yuodelis C (1984) The morphological development of the human fovea. Ophthalmology 91:603-612.
Hitchcock PF, Raymond PA (2004) The teleost retina as a model for developmental and regeneration biology. Zebrafish 1:257-271.
Hughes A (1971) Topographical relationships between the anatomy and physiology of the rabbit visual system. Documenta Ophthalmologica 30:33-159.
Hughes A (1977) The topography of vision oin mammals. Berlin: Springer-Verlag.
Job SD, Bellwood DR (1996) Visual acuity and feeding in larval *Premnas biaculeatus*. Journal of Fish Biology 48:952-963.
Johns PR (1977) Growth of the adult goldfish eye. III. Source of the new retinal cells. The Journal of Comparative Neurology 176:343-357.
Johns PR (1981) Growth of Fish Retinas. American Zoologist 21:447-458.
Johns PR, Easter SS, Jr. (1977) Growth of the adult goldfish eye. II. Increase in retinal cell number. J Comp Neurol 176:331-341.
Johns PR, Fernald RD (1981) Genesis of rods in teleost fish retina. Nature 293:141-142.
Juliusson B, Bergström A, Röhlich P, Ehinger B, van Veen T, Szél A (1994) Complementary cone fields of the rabbit retina. Investigative Ophthalmology & Visual Science 35:811-818.
Kahmann H (1934) ijber die Vorkommen einer Fovea centralis im Knochenfischauge. Zool Anz 106:49-55.
Kock JH (1982) Neuronal addition and retinal expansion during growth of the crucian carp eye. J Comp Neurol 209:264-274.
Kuiter RH (2000) The Marine Fish Families Series, Seahorses Pipefishes and their relatives, A comprehensive Guide to Syngnathiformes. Chorleywood, UK: TMC Publishing.
Lazzaro X (1987) A review of planktivorous fishes: Their evolution, feeding behaviours, selectivities, and impacts. Hydrobiologia 146:97-167.

Lee HR, Bumsted O'Brien KYM (2011) Morphological and behavioral limit of visual resolution in temperate (Hippocampus abdominalis) and tropical (Hippocampus taeniopterus) seahorses. Visual Neuroscience 28:351-360.
Li KT, Wetterer JK, Nelson G. Hairston, Jr. (1985) Fish Size, Visula Resolution, and Prey Selectivity. Ecology 66:1729-1735.
Lythgoe JN (ed.) (1980) Vision in fishes: ecological adaptations. New York: Premium Press.
Matthiessen L (1880) Untersuchungen über den Aplanatismus und die Periscopie der Krystalllinsen in den Augen der Fische. Pflügers Archiv European Journal of Physiology 21:287-307.
Miller T, Crowder L, Rice J (1993) Ontogenetic changes in behavioural and histological measures of visual acuity in three species of fish. Environmental Biology of Fishes 37:1-8.
Morris AC, Scholz T, Fadool JM (2008) Rod Progenitor Cells in the Mature Zebrafish Retina Recent Advances in Retinal Degeneration. vol. 613 (Anderson, R. E. et al., eds), pp 361-368: Springer New York.
Moshiri A, Close J, Reh TA (2004) Retinal stem cells and regeneration. Int J Dev Biol 48:1003-1014.
Mueller KP, Neuhauss SCF (2010) Quantitative measurements of the optokinetic response in adult fish. Journal of Neuroscience Methods 186:29-34.
Müller H (1952) Bau und Wachstum der Netzhaut des Guppy (Lebistes reticulatus). Zool Jb, Abt f allg Zool u Physiol 275–324.
Neave DA (1984) The development of visual acuity in larval plaice (Pleuronectes platessa L.) and turbot (Scophthalmusmaximus L.). Journal of Experimental Marine Biology and Ecology 78:167-175.
Northmore DP, Dvorak CA (1979) Contrast sensitivity and acuity of the goldfish. Vision Res 19:255-261.
O'Brien WJ (1979) The Predator-Prey Interaction of Planktivorous Fish and Zooplankton: Recent research with planktivorous fish and their zooplankton prey shows the evolutionary thrust and parry of the predator-prey relationship. American Scientist 67:572-581.
Otten E (1980) Vision During Growth of a Generalized Haplochromis Species: H. Elegans Trewavas 1933 (Pisces, Cichlidae). Netherlands Journal of Zoology 31:650-700.
Otteson DC, Hitchcock PF (2003) Stem cells in the teleost retina: persistent neurogenesis and injury-induced regeneration. Vision Res 43:927-936.
Packer O, Hendrickson AE, Curcio CA (1990) Development redistribution of photoreceptors across the Macaca nemestrina (pigtail macaque) retina. J Comp Neurol 298:472-493.
Packer O, Hendrickson AE, Curcio CA (1989) Photoreceptor topography of the retina in the adult pigtail macaque (Macaca nemestrina). J Comp Neurol 288:165-183.
Pankhurst NW, Montgomery JC (1990) Ontogeny of vision in the Antarctic fish Pagothenia borchgrevinki (Nototheniidae). Polar Biology 10:419-422.
Pankhurst PM (1994) Age-related changes in the visual acuity of larvae of New Zealand snapper, Pagrus auratus. Journal of the Marine Biological Association of the United Kingdom 74:337-349.
Pankhurst PM, Pankhurst NW, Montgomery JC (1993) Comparison of behavioural and morphological measures of visual acuity during ontogeny in a teleost fish, Forsterygion varium, tripterygiidae (Forster, 1801). Brain Behav Evol 42:178-188.
Provis JM, Diaz CM, Dreher B (1998) Ontogeny of the primate fovea: a central issue in retinal development. Prog Neurobiol 54:549-580.
Pumphrey RJ (1948) The Theory of the Fovea. J Exp Biol 25:299-312.
Querubin A, Lee HR, Provis JM, Bumsted O'Brien KM (2009) Photoreceptor and ganglion cell topographies correlate with information convergence and high acuity regions in the adult pigeon (<I>Columba livia)</I> retina. The Journal of Comparative Neurology 517:711-722.
Rahmann H, Jeserich G, Zeutzius I (1979) Ontogeny of Visual Acuity of Rainbow Trout under Normal Conditions and Light Deprivation. Behaviour 68:315-322.
Ransom-Hogg A, Spillmann L (1980) Perceptive field size in fovea and periphery of the light- and dark-adapted retina. Vision Research 20:221-228.

Rapaport DH, Stone J (1984) The area centralis of the retina in the cat and other mammals: Focal point for function and development of the visual system. Neuroscience 11:289-301.
Raymond P, Barthel L, Bernardos R, Perkowski J (2006) Molecular characterization of retinal stem cells and their niches in adult zebrafish. BMC Developmental Biology 6:36.
Raymond PA, Rivlin PK (1987) Germinal cells in the goldfish retina that produce rod photoreceptors. Dev Biol 122:120-138.
Salinas-Navarro M, Mayor-Torroglosa S, Jimenez-Lopez M, Aviles-Trigueros M, Holmes TM, Lund RD, Villegas-Perez MP, Vidal-Sanz M (2009) A computerized analysis of the entire retinal ganglion cell population and its spatial distribution in adult rats. Vision Res 49:115-126.
Schmitt E, Kunz YW (1989) Retinal morphogenesis in the rainbow trout, Salmo gairdneri. Brain Behav Evol 34:48-64.
Shand J, Chin SM, Harman AM, Moore S, Collin SP (2000) Variability in the Location of the Retinal Ganglion Cell Area Centralis Is Correlated with Ontogenetic Changes in Feeding Behavior in the Black Bream, Acanthopagrus butcheri (Sparidae, Teleostei). Brain, Behavior and Evolution 55:176-190.
Shand J, Doving KB, Collin SP (1999) Optics of the developing fish eye: comparisons of Matthiessen's ratio and the focal length of the lens in the black bream Acanthopagrus butcheri (Sparidae, Teleostei). Vision Res 39:1071-1078.
Siebeck UE, Wallis GM, Litherland L (2008) Colour vision in coral reef fish. J Exp Biol 211:354-360.
Stone J (1965) A quantitative analysis of the distribution of ganglion cells in the cat's retina. J Comp Neurol 124:337-352.
van der Meer HJ (1994) Ontogenetic change of visual thresholds in the cichlid fish Haplochromis sauvagei. Brain Behav Evol 44:40-49.
van der Meer HJ (1995) Visual resolution during growth in a cichlid fish: a morphological and behavioural case study. Brain Behav Evol 45:25-33.
Van Wassenbergh S, Roos G, Genbrugge A, Leysen H, Aerts P, Adriaens D, Herrel A (2009) Suction is kid's play: extremely fast suction in newborn seahorses. Biology Letters 5:200-203.
Walls GL (1942) The vertebrate eye and its adaptive radiation. . Bloomfield Hills, Michigan: Cranbrook Institute of Science.
Wanzenbock J, Schiemer F (1989) Prey Detection in Cyprinids during Early Development. Can J Fish Aquat Sci 46:995-1001.
Yuodelis C, Hendrickson A (1986) A qualitative and quantitative analysis of the human fovea during development. Vision Res 26:847-855.
Zaunreiter M, Junger H, Kotrschal K (1991) Retinal morphology of cyprinid fishes: A quantitative histological study of ontogenetic changes and interspecific variation. Vision Research 31:383-394.
Zygar CA, Lee MJ, Fernald RD (1999) Nasotemporal asymmetry during teleost retinal growth: preserving an area of specialization. J Neurobiol 41:435-442.

Chapter Four

Mechanisms of Foveal and Visual Development in the Tropical Seahorse, *Hippocampus taeniopterus*: Cell Proliferation and Cell Death

Mechanisms of Foveal and Visual Development

in the Tropical Seahorse, *Hippocampus taeniopterus*:

Cell Proliferation and Cell Death

Hie Rin Lee[1,2] **and Keely M Bumsted O'Brien**[1,2]

[1]ARC Centre of Excellence in Vision Science, [2] John Curtin School of Medical Research, The Australian National University, Canberra ACT 0200, Australia

Support:

Australian Research Council Centres of Excellence Program (CE0561903)

Mechanisms of Foveal and Visual Development in the Tropical Seahorse, *Hippocampus taeniopterus*: Cell Proliferation and Cell Death

ABSTRACT

Seahorses possess a convexiclivate fovea characterised by a rod-free depression. In this study, I analysed the developmental changes in the morphology of the fovea and rod-free zone, reactive distance, a behavioural measure of visual resolution, and the contribution of cell death and proliferation on foveal development. Five size groups of tropical *H. taeniopterus* seahorses were analysed ranging in size from 6-15 cm in length. Following reactive distance measurements, BrdU was injected intravetreally. Eyes were processed for frozen sections or flat-mounted. Wholemounts were stained with propidium iodide and immunolabeled with an anti-BrdU antibody. Cell death was examined using a terminal deoxynucleotidyl transferase (TdT)-mediated dUTP-biotin nick end labeling (TUNEL) assay on frozen sections. The behaviourally measured visual resolution improved with age, which meant that bigger fish were able to detect the prey of a fixed size at greater distances. Morphologically, the area of the rod-free zone increased as fish grew in size. From our previous studies, it was observed that the cone photoreceptor cell densities increased at the foveal region during development; however, BrdU labeling showed the absence of neuroretinal cell addition in the ONL, but the presence of dividing cells in the INL within the rod-free zone. A TUNEL assay confirmed the lack of programmed large-scale photoreceptor cell death in and around the rod-free zone during development. Taken together, our data could not rule out the possibility of cone photoreceptor cell generation from INL stem cells within the rod-free zone. The data indicate that the cell death is not likely to be a major mechanism in foveal development. Future studies will be designed to determine the underlying mechanism in the establishment of the adult rod-free zone.

Key words: vision, fish, fovea

INTRODUCTION

The adult seahorse retina contains a convexiclivate fovea that shares common features with the primate fovea including a pit, lack of rod photoreceptors and increased cone photoreceptor and ganglion cell densities; however, there are also very distinct differences such as the shape of the pit and the presence of inner retinal neurons in the fovea, the lack of inner retinal vasculature in the seahorse. Does the seahorse fovea develop in a similar manner compared with the primate fovea? In some respects our data indicate common themes in seahorse and primate foveal development; however, fish eye development has certain peculiarities not present in mammalian retinas.

During fish life, their eyes increase in size and the retinal area increases proportionally to their body size (Fernald, 1988, Fadool, 2003, Hitchcock and Raymond, 2004, Morris et al., 2008). In fish, the retina undergoes two different growth mechanisms; 1) addition of new neurons at the retinal margins, and 2) a lifelong expansion of the existing retinal tissues (Fadool, 2003, Otteson and Hitchcock, 2003, Morris et al., 2008). All types of retinal neurons are generated and integrated into the differentiated retina at the circumferential germinal zone (CGZ) located at the retinal margin between the neural retina and the iris epithelium (Fadool, 2003, Otteson and Hitchcock, 2003, Morris et al., 2008). It has been suggested that rate of new cell addition is comparatively slower than retinal stretching resulting in a decrease in cell density as the fish grows, despite an increase of total cell number (Fadool, 2003, Otteson and Hitchcock, 2003, Morris et al., 2008). Rod photoreceptors are the exception to the rule that no new cells are generated in differentiated retina. Rods are added into the outer nuclear layer (ONL) of more differentiated central retina by rod progenitor cells which originate from retinal stem cells in the inner nuclear layer (INL) (Raymond et al., 1988, Fadool, 2003, Otteson and Hitchcock, 2003, Morris et al., 2008). Their addition outpaces the rate of retinal expansion, which means that although most other cell densities decrease during development, rod photoreceptor densities remain constant (Fernald, 1985, Hoke and Fernald, 1997, Mueller and Neuhauss, 2010).

My previous study demonstrated that smaller seahorses possess a less mature convexiclivate fovea within a rod-free zone (RFZ) (2nd Result Chapter). The fovea becomes wider and deeper pit as the fish grows while preserving its relative location within the retina (2nd Result Chapter). Furthermore, cone photoreceptor cell densities in the foveal region increase during development, which may result in the retinal thickening and improvement of behaviourally measured vision. However, the exact mechanism of how the seahorse fovea develops still remains to be elucidated.

In this chapter, I investigated changes in seahorse fovea and vision at five different developmental stages by testing their vision behaviourally. Furthermore, the morphological changes of the fovea and RFZ were investigated by testing two null hypotheses; 1) new cone photoreceptor cells are added within the RFZ, and 2) pre-existing rod photoreceptors die around the margin of the RFZ. Unlike in the primate fovea, I have shown previously that the area of RFZ containing the *fovea centralis* increased along with an increase in cone photoreceptor cell densities with all three nuclear layers remaining during development of seahorse retina. I showed that the newly generated cells in the ONL as well as the apoptotic cells are absent in and around the RFZ. Nevertheless, the improved behaviourally measured vision and the increased in cone photoreceptor densities within the foveal region suggested the existence of a unique mechanism for the seahorse foveal development.

MATERIALS AND METHODS

Tropical *H. taeniopterus* (n = 22) seahorses were obtained from Seahorse Australia, Beauty Point, Tasmania. The fish were categorised into the five groups according to their body lengths; group 1 (n = 10) 6.03 ± 0.38 cm, group 2 (n = 5) 8.48 ± 0.36 cm, group 3 (n = 9) 9.8 ± 0.27 cm, group 4 (n = 5) 12.26 ± 0.42 cm, and group 5 (n = 14) 14.98 ± 1.03 cm. All tissues were obtained and experiments were conducted under the approved ethical protocols from the Australian National University animal care committee.

Behavioural Testing for Visual Resolution

The modified "Reactive Distance" technique (Wanzenbock and Schiemer, 1989, Job and Bellwood, 1996) used in this study for measuring the visual spatial resolution of seahorses was precisely described in the previous paper (Lee and Bumsted O'Brien, 2011). In brief, the experimental saltwater tank covered with white paper at the bottom and three walls was set up and illuminated by a warm white energy saving petite spiral fluorescent lamp (3,100 lx; 240-V, 23-W (equivalent to 115-W) (Mirabella, Melbourne, Australia)) placed approximately 30cm overhead. Food was withheld from the fish for 24 h prior to the commencement of the experiment. Fish were initially acclimatised in the experimental saltwater tank for ten minutes. Frozen mysid shrimps of known sizes (7-12 mm) and high contrast (dark brown or red against white background) were introduced into the tank one at a time. The feeding behaviour of the seahorse was video recorded from above and in front of the tank.

From the video recordings, the reactive distance (cm) was measured when the fish first reacted to the prey by suddenly changing the eye orientation, starting to swim towards the prey and pulling back of the snout. The reactive distance was measured in more than ten trials per fish. The angle that an object (the prey) subtended on the fish retina was calculated using the formula involving the average reactive distance: Visual angle in minutes of arc = $2 \cdot (\arctan(0.5 \cdot h/\mathrm{RD}))$, where h was prey size and RD was Reactive distance (Wanzenbock and Schiemer, 1989, Miller et al., 1993, Job and Bellwood, 1996).

5-bromo-2'-deoxyuridine (BrdU) labeling

Following the behavioural tests, BrdU was injected into the fish eye to label proliferative cells in the retina (Cameron, 1995, Stenkamp et al., 1997, Cameron, 2000, Wu et al., 2001). The fish were anesthetised with clove oil (2-6 drops in 1 L of seawater depending on the size of the fish), wrapped in wet tissues on a petri-dish, and placed on the stage of an operating microscope. A small incision was made on the superior limbus for the right eye and temporal limbus for the left eye through the skin and sclera using a microknife. BrdU in 0.1M phosphate- buffered saline (PBS) was injected into the vitreal cavity (n=5 each age group) with a blunt-tipped, 33-gauge needle attached to a microsyringe (Hamilton Company, Reno, NV). The amount of BrdU solution injected was determined to achieve intraocular concentration of 20μM. The concentration was estimated as published by Raymond et al. (1988). Injections were conducted immediately prior to the onset of the dark cycle to allow maximal BrdU uptake (Chiu et al., 1995).

Tissue Collection

The next morning, after body length was recorded and fish were dark adapted, fish were sacrificed. Dark adapted facilitated the separation of the neural retina from the pigmented epithelium (Wu et al., 2001). Following the anesthetisation in clove oil (more than 2-6 drops in 1 L of seawater depending on the size of the fish, once the gill movements had stopped, the fish were decapitated. Then, both eyes were enucleated and immersion fixed in 4% paraformaldehyde (PFA) in 0.1 M phosphate-buffered saline (1x PBS; pH 7.4) at 4℃ for overnight (Lee and Bumsted O'Brien, 2011).

The nasotemporal diameter of the globe and lens diameter were recorded. For whole-mount preparations, the cornea and lens were removed under a dissecting microscope. Using the distinct pigmentation on the ventral sclera as a landmark, the distinguishing cuts were made at the dorsal and ventral poles according to the body axes of the intact animal so that the orientation of the eye was preserved through subsequent processing. Then, the sclera, choroid,

and optic nerve stump were removed and additional radial relaxation cuts were made on the nasal and temporal margins.

For cryosectioning, following the fixation in 4% PFA and removal of the cornea, lens and sclera, the retina was immersed in 30% sucrose solution in 1x PBS for overnight and frozen at a known orientation in equal parts of 30% sucrose solution and Optimum Cutting Temperature (Tissue Tek, Sakura, Japan) mounting medium. Transverse retinal sections were cut at 10 or 16 μm thickness and prepared for immunolabeling nuclear staining, and/or Terminal deoxynucleotidyl transferase (TdT)-mediated dUTP-biotin nick end labeling (TUNEL). Polysine adhesion slides (Thermo Fisher Scientific Inc., Scorsby, Australia) were used to mount the retinal sections.

Immunocytochemistry

Immunolocalisation of BrdU in whole-mounted tissue was carried out according to the procedure published by Cameron (1995) with the following modifications. For permeabilisation, the tissue was treated with 0.5% Triton-X100 in 0.2M PBS (PBS/Tx), and then immersed in 2*N* HCl(hydrochloric acid)/PBS/Tx for 1 hr. Following PBS/Tx washes, in order to block nonspecific bindings, the tissue was pre-incubated in 10% normal goat serum (Zymed Laboratories, South San Francisco, CA; 01-6101) diluted in PBS/Tx for 1 hour. The tissue was then incubated in 10% anti-BrdU rat monoclonal antibody (Bul/75, Accurate Chemical & Scientific Cooperation, Westbury, NY, USA) (Julian et al., 1998) in PBS/Tx at 4℃ for 24 hours. After thorough washes in 1x PBS, Alexa fluor 488 (green) conjugated goat anti-rat secondary antibody (Invitrogen, Life Technologies Cooperation, Mulgrave, Australia; A11006) in 1x PBS (1:200) was applied for 24 hours at 4℃. The reacted whole-mounts were washed in 1x PBS to decrease background, and then, incubated in propidium iodide (PI; 1:500; Sigma, Castle Hill, Australia) for 15 minutes for nuclear staining. Following extra washes in 1x PBS, it was converslipped on either a gelatinised poly-L-lysine-coated Superfrost Plus (Esco, Biolab Scientific Ltd., Scoresby, Australia) microscope slide or a Polysine adhesion slides (Thermo

Fisher Scientific Inc., Scorsby, Australia) with 80% glycerol in phosphate buffer, and visualised with a confocal Laser-Scanning Microscope (LSM 5; Carl Zeiss AG, Oberkochen, Germany).

DNA Nick End Labeling on Retinal Sections

TUNEL (Gavrieli et al., 1992, Maslim et al., 1997) was used to detect the cells and their locations undergoing apoptosis. Following the consecutive washes with 70% Ethanol for 15 minutes, with distilled water twice for five minutes each, and with 1x TdT buffer for ten minutes, the retinal sections were incubated in reaction mixture (1060 μL of distilled water, 125 μL of 10x TdT buffer, 3 μL of biotin-dUTP, and 1.5 μL of Terminal Transferase Enzyme) in a humid container for exactly 1 hour at 37 ℃. Then, the reaction was stopped by washing in 2x saline sodium citrate (SSC) buffer for 15 minutes. The slides were blocked with 10% normal goat serum in 1x PBS for 10 minutes and incubated again in diluted Strep Alexa 594 (1:1000) in 1x PBS in a humid container for one hour at 37 ℃. The slides were washed twice with 1x PBS for five minutes each and incubated with bisbenzimide (1:10,000; Calbiochem, La Jolla, CA, USA) for exactly two minutes and washed again with 1x PBS twice for five minutes each. The slides were then coverslipped with Aqua Poly/Mount (Polysciences Inc., Warrington, PA, 18606). The labeled cells were viewed under the inverted microscope (Inverted Axiovert, Carl Zeiss, Jena, Germany).

Statistical analysis was conducted using an Analysis of variance (ANOVA) test and a Linear Mixed Model (Restricted Maximum Likelihood (REML) methods) using GenStat software. The coefficient of determination (R^2), which indicates how well the data fit a statistical model, was calculated using the Excel function for the correlation coefficient (CORREL).

RESULTS

Enlargement of the Seahorse Eye and Lens with Increasing Body Length

Figure 1 shows the increase in eye size as the fish grows larger, such that the difference in eye size between the smallest and the largest fish was on average 1.56 mm (Table 1). When lens diameter was measured, the increase in size was less dramatic compared with the eye size; however, there was a statistically significant increase in lens diameter with increasing fish size ($P < 0.001$, Figure 1).

Increase in Visual Resolution with Increasing Body Length

Visual Resolution data from individual fish of all sizes indicated there was a clear linear relationship between the visual resolution and the body length (Figure 2, $R^2 = 0.556$). The behaviourally measured visual resolution improved as seahorses grew in size (Figure 2). This indicated that larger fish have increased visual resolution. Data from each size group also demonstrated that the average visual resolution increased as the fish grew (Table 2). The smallest group of fish (group 1) had the largest resolvable visual angle subtended on the retina. These fish had the shortest reactive distance, indicating that the smallest fish had the poorest vision. The largest fish (group 5) had the smallest visual angle subtended on the retina ($P < 0.001$). Larger fish were able to resolve smaller prey compared with smaller fish. In other words, larger fish were able to detect the same sized prey at the further distances Indicating that larger fish had the best visual resolution (Figure 2).

Cell Proliferation in Central and Peripheral Retina Compared with Body Length

In the CGZ, BrdU labeled proliferating cells were present in all layers of the retina from all age groups (top panels in Figure 3-7 (green), black arrows). The nasal margin contained the thickest band of BrdU labeled cells compared with the other retinal margins (wholemount retina in the middle of Figure 3-7). Qualitatively, the amount of proliferation detected by BrdU decreased with increasing body length, with group 5 fish having very few labeled cells at the margin. In the nasal mid-periphery, BrdU labeled cells were found in both GCL and INL in

Table 1.: Average eye and lens diameter of *H. taeniopterus* in all age groups

Size Group	Body Lengths (mean ± S.D., cm)		Nasotemporal Eye Diameter (mean ± S.D., mm)		Lens Diameter (mean ± S.D., mm)	
	N		N		N	
1	10	6.03 ± 0.38	11	2.62 ± 0.11	12	0.87 ± 0.03
2	5	8.48 ± 0.36	6	2.97 ± 0.10	6	1.00 ± 0.03
3	9	9.80 ± 0.27	7	3.33 ± 0.14	7	1.13 ± 0.03
4	5	12.26 ± 0.42	10	3.62 ± 0.17	10	1.28 ± 0.06
5	14	14.98 ± 1.03	21	4.17 ± 0.23	24	1.38 ± 0.08

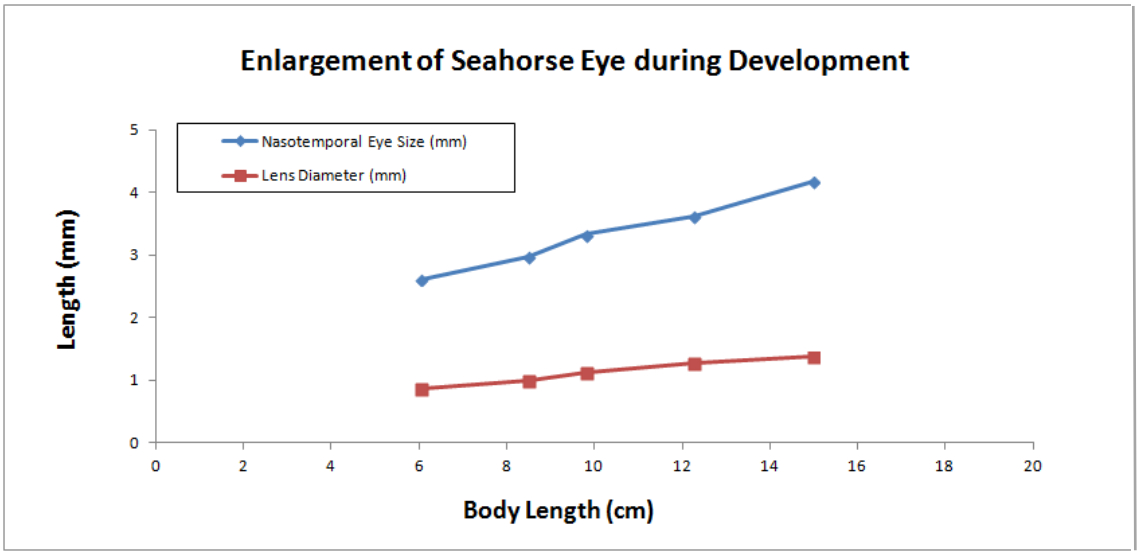

Figure 1.: Enlargement of seahorse eye during development
The increase in eye and lens sizes is correlated with the increase in body length during the development of *H. taeniopterus*. The vertical axis indicates the nasotemporal diameter of an eye and a lens (mm) and the horizontal axis indicates the total body length (cm).

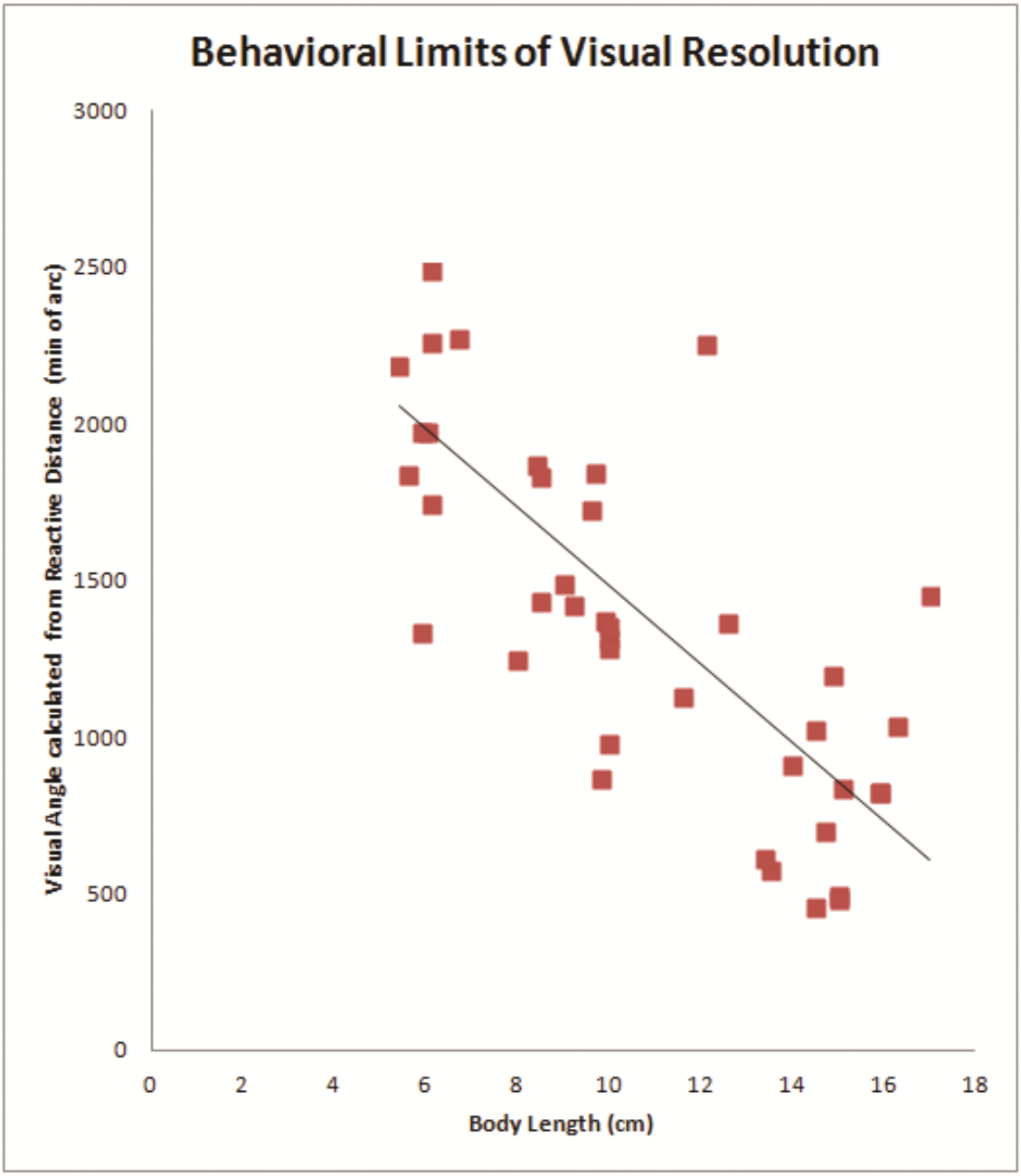

Figure 2.: Improved behaviourally measured visual resolution during development
Behaviourally measured visual resolution for individual fish from all age groups demonstrated a clear linear relationship with the body length (R^2 = 0.556). The behaviourally determined visual angles subtended in the retina decreased as seahorses grew in size which implied that larger fish have better visual resolution. The vertical axis indicates the visual resolution or the visual angles subtended in the eye in minutes of arc calculated from reactive distances, while the horizontal axis displays the body length in centimetres indicating the maturity of the animal.

Table 2: Behaviourally measured visual resolution

Size Group	Behaviourally measured Visual Resolution (min of arc)
1	2108.31 ± 452.19
2	1575.25 ± 269.35
3	1352.38 ± 310.76
4	1584.41 ± 593.58
5	817.31 ± 292.07

smaller fish (bottom panels in Figure 3-7 (green), white arrows). All of the labeled cells in the INL were located at the scleral margin of the layer. As fish grew, there were fewer BrdU positive cells present. No cells were labeled at the retinal margin in the ONL at all age groups.

The foveal region of all five age groups lacked BrdU positive cells in the ONL (bottom panels in Figure 3-7). BrdU positive cells were detected in the middle of the INL and GCL at the vitreal margin. The number of these cells did not decrease as the fish grew. Another distinguishing characteristic of the labeled cells in the INL was their location within the layer.

Cell Death was not prevalent in the ONL

TUNEL positive cells in the INL, GCL and nerve fibre layer (NFL) were observed within the rod-free zone across the retinas of all size groups although the number of cells labeled varied (data not shown). In group 1, only 3 TUNEL positive apoptotic cells were observed in the ONL at the margins of the rod-free zone. The nuclear double labeling (blue) confirmed that the TUNEL positive cells (red) were rod nuclei (Figure 8). In the retinas of larger fish (group 2 to 5), no TUNEL positive cells were detected in the ONL at the margin of RFZ or throughout the RFZ. However, TUNEL positive cells were observed in GCL and NFL at all retinal eccentricities.

Figure 3-7.: Proliferating cells in wholemount retina

Each figure represents each age group; Figure 3 = group 1, Figure 4 = group 2, Figure 5 = group 3, Figure 6 = group 4, and Figure 7 = group 5. BrdU labeled proliferating cells were found at the retinal margin known as CGZ (black arrows in the top panel). There were more cells labeled at the nasal margin of the *H. taeniopterus* retina. The bottom left panel demonstrated the absence of proliferating cells in the ONL of the foveal region. The bottom right panel displayed proliferating cells present in the INL of the nasal retina. Scale bars=100 μm.

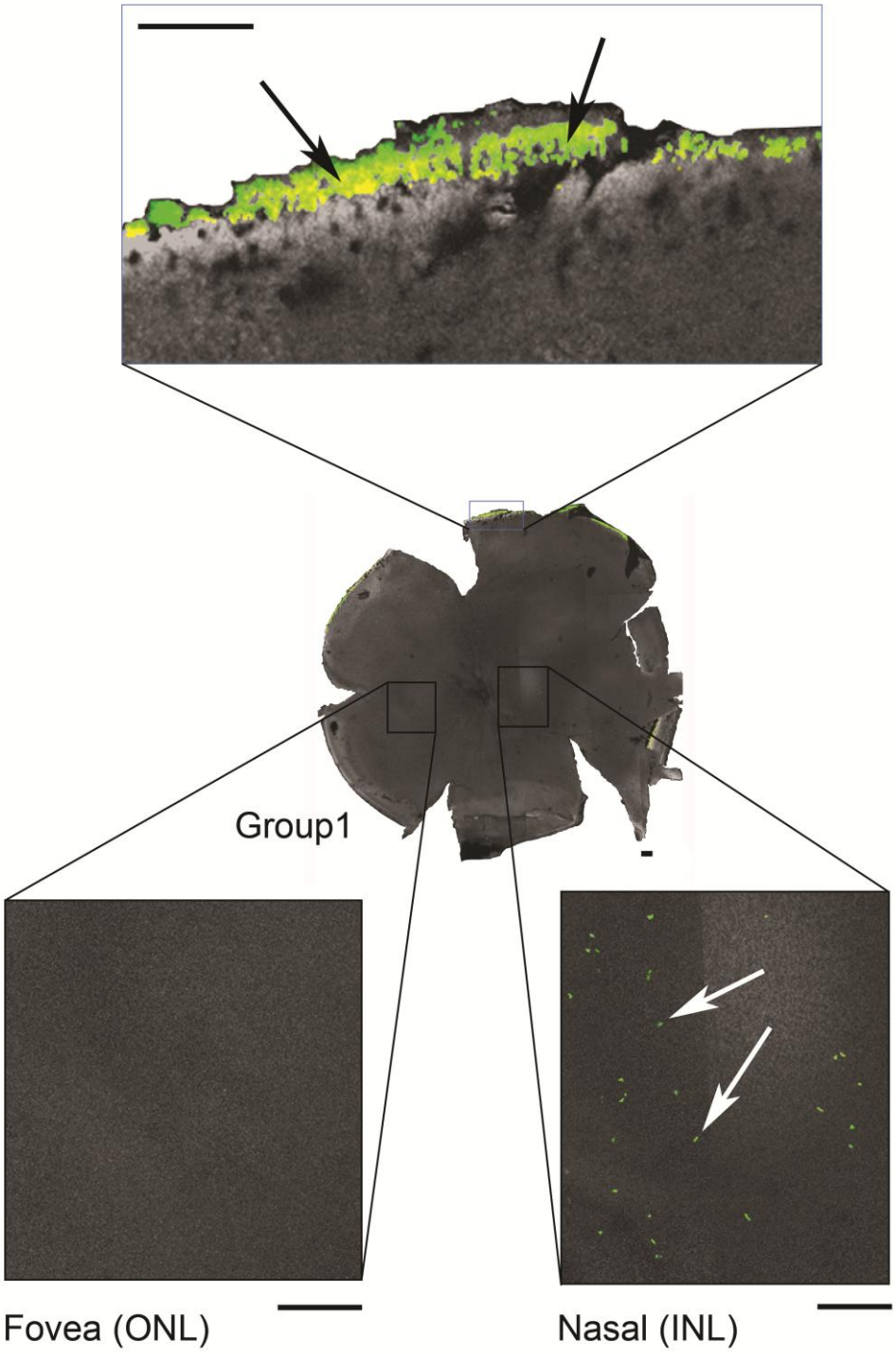

Figure 3.: Proliferating cells in wholemount retina (Group 1)

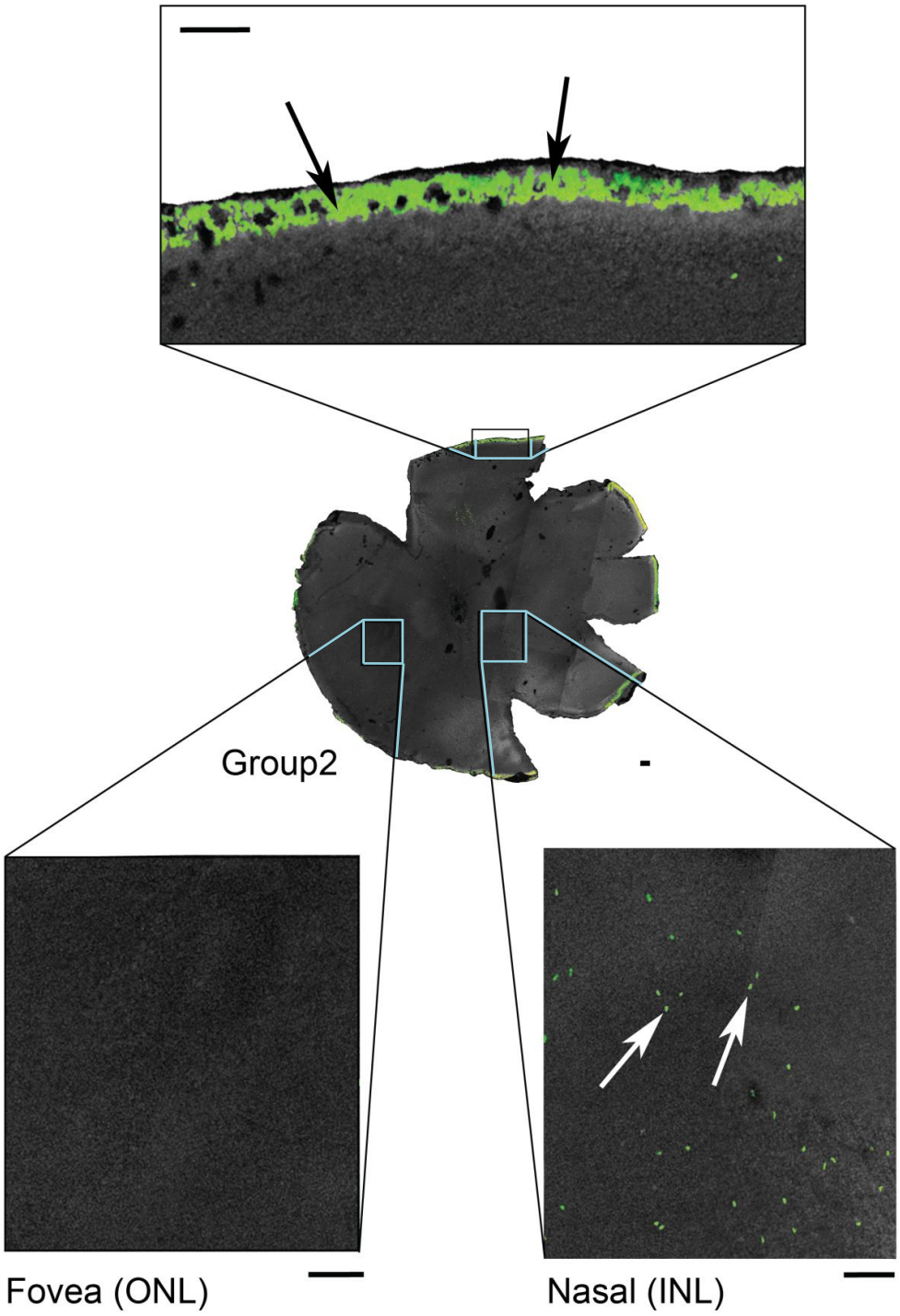

Figure 4.: Proliferating cells in wholemount retina (Group 2)

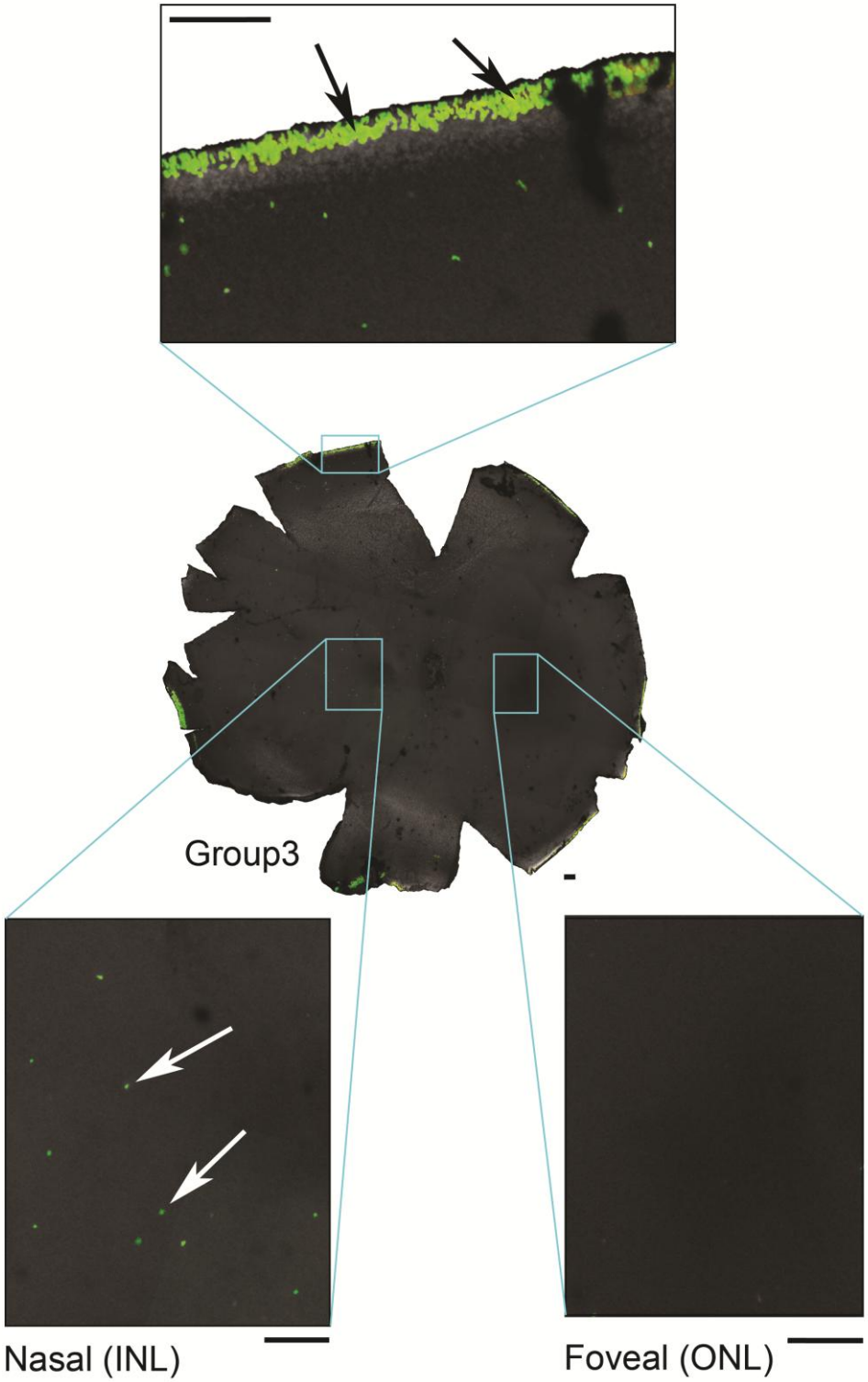

Figure 5.: Proliferating cells in wholemount retina (Group 3)

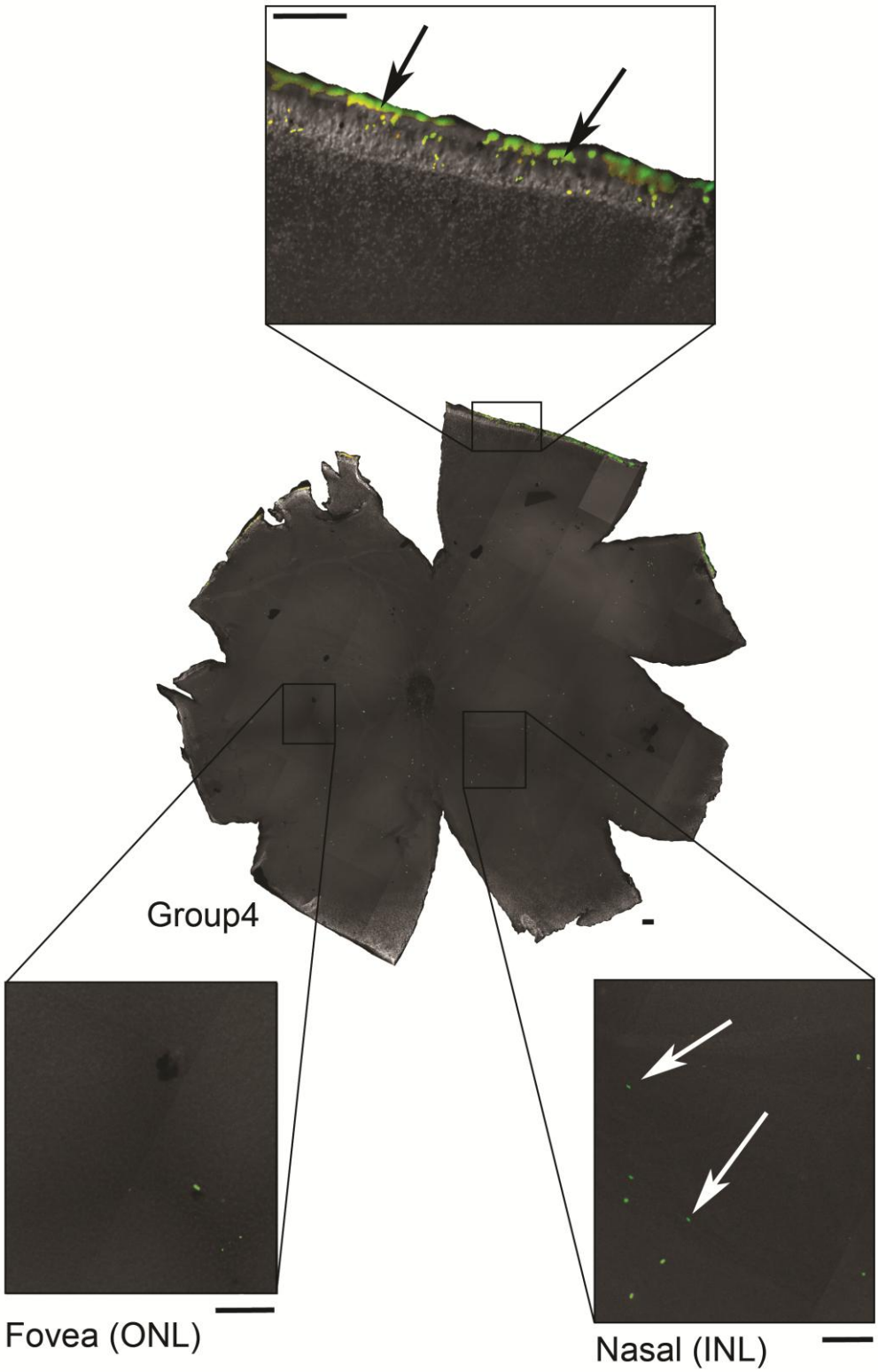

Figure 6.: Proliferating cells in wholemount retina (Group 4)

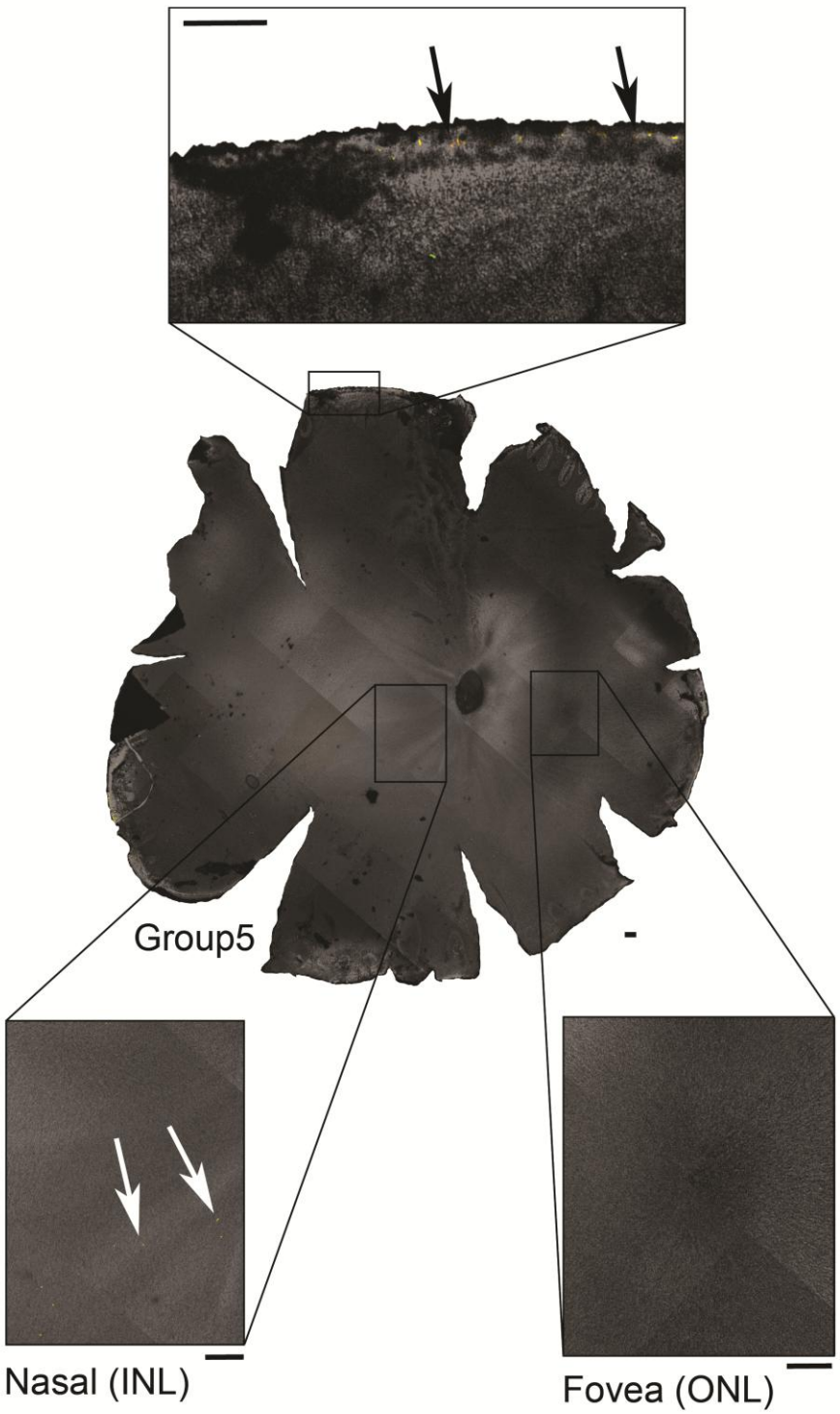

Figure 7.: Proliferating cells in wholemount retina (Group 5)

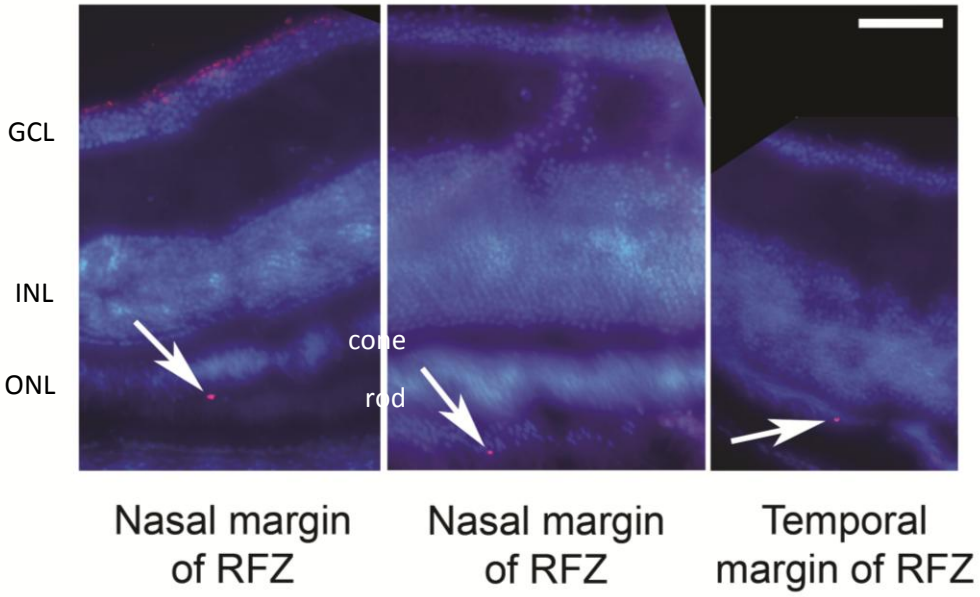

Figure 8.: Apoptotic cells in group 1 *H.taeniopterus* retina
In and around the margin of RFZ, the TUNEL positive cells in the ONL were only found in the smallest age group (group 1). In seahorse retina, rods and cones are segregated within the ONL where cone nuclei are located vitreal to rods. The double labeled TUNEL positive cells were rod photoreceptors (white arrows). Scale = 100 μm.

DISCUSSION

As the *H. taeniopterus* grows in size, the eye size and the lens diameter increases. The ocular enlargement during development is correlated with the improvement of behavioural visual resolution. For all the size groups of seahorses investigated in this chapter, BrdU labeling demonstrated the presence of proliferation cells at the CGZ and the absence of dividing cells in the ONL in and around the RFZ. However, it is notable that proliferating cells were present at the INL in more central retina. TUNEL positive cells were not detected, indicating that massive apoptotic activity in and around the RFZ was absent. Behaviourally estimated visual resolution improved as fish grew in size.

The Developmental Changes of Behavioural Visual Resolution

The behavioural visual resolution of *H. taeniopterus* improved with increasing fish size. The changes in behavioural visual resolution were discussed in depth in the previous result chapter (2nd Result Chapter). The spatial visual resolution in teleosts has been shown to improve during development (Otten, 1980, Hairston et al., 1982, Breck and Gitter, 1983, Li et al., 1985, Fernald, 1990, Miller et al., 1993). This improvement is attributed to various factors occurring during development including the increased angular density of photoreceptor cells (Guma'a, 1982, Fernald, 1988, Pankhurst et al., 1993) and the enlargement of the eye (Easter et al., 1977, Hairston et al., 1982, Collin and Pettigrew, 1989). An enlarged eye and increased lens size generate a longer focal length allowing a larger retinal area to be stimulated (Pankhurst et al., 1993). The stimulation of a larger number of cones results in a magnified retinal image (Easter et al., 1977) and better visual resolution (Guma'a, 1982, Neave, 1984, Browman et al., 1990). Retinal circuitry, visual pathways to the brain, and a well-developed accommodative system (Pankhurst, 1994, Shand et al., 1999) also contribute to improved behavioural visual resolution.

The Retinal Growth

In the developing *H.taeniopterus* retinas, abundant proliferating cells were observed at the retinal margin. This indicated that the seahorse retina also possesses a CGZ where new neurons are added during ocular enlargement. The number of BrdU labeled cells increased

between groups 1-3, and then gradually reduced as the fish grew in size (groups 3-5). Rod photoreceptors have been reported to be generated and added into the already differentiated retina (Johns, 1977, Fernald and Johns, 1980, Johns and Fernald, 1981, Raymond, 1985b, Fernald, 1988, Collin and Shand, 2003, Otteson and Hitchcock, 2003, Hitchcock and Raymond, 2004). BrdU labelled cells were not detected in the ONL. This may indicate that this region lacks newly generated rod photoreceptors as well as rod precursors (Otteson and Hitchcock, 2003). The observed lack of BrdU positive cells may also have been due to the short pulse time of the BrdU. After the injection of BrdU, the eyes were harvested the following day. This may have been insufficient time for newly generated cells to become incorportated in the ONL (Otteson et al., 2001, Wu et al., 2001). BrdU positive cells were detected in the INL and GCL. Within the INL, the BrdU positive cells were located at the scleral margin, and theses cells given time may have migrated into the ONL.

Conflicting hypotheses have been proposed regarding the asymmetrical retinal cell addition and growth in teleosts. Following the BrdU injection, asymmetrical retinal cell addition was observed in *H. taeniopterus* retina. There were thicker bands of labeled proliferating cells in the nasal retina compared to the temporal retina, similar to that observed by Cameron (1995). In addition to the generation of new neuroretinal cells, retinal stretching plays a part in ocular enlargement in teleosts (Easter, 1992, Fadool, 2003, Otteson and Hitchcock, 2003, Morris et al., 2008). Zygar et al (1999) hypothesised that the nasal retina expands more in order to preserve the temporal retinal specialisation (Zygar et al., 1999). In teleosts with a temporal retinal specialisation, asymmetrical growth pattern was observed which displayed the uneven spaces between adjacent annuli, the largest nasoventrally and the smallest temporodorsally (Easter, 1992, Cameron, 1995, 1996, Zygar et al., 1999). From the actual length measurements of the flattened wholemount seahorse retina, the ratio of retinal growth increase was greater in the nasal compared to the temporal retina. This implies that retinal expansion occurs at a faster rate in the nasal retina in *H. taeniopterus*, which lends support to the hypothesis proposed by Zygar et al. (1999). Easter suggested that the smaller retinas stretch less compared with larger retinas (Easter, 1992). This differential expansion based on retinal size may preserve the relative

location of the fovea resulting in the thickening of the retinal layers in the temporal region compared to the nasal. For the seahorse, *H. taeniopterus*, I hypothesise that the asymmetrical retinal growth may occur with two different mechanisms, the greater number of cell generation as well as the larger expansion of existing retinal tissues in the nasal retina.

Developmental Changes in the Fovea

One of the null hypotheses of this study stated that increasing cone photoreceptor cell density within the RFZ was due to new cone photoreceptor cells being added within the RFZ. Despite the increase in cone photoreceptor cell density, the foveal region of developing *H. taeniopterus* lacked BrdU positive cells in the ONL. As discussed earlier, it is possible that this may have been due to experimental constraints rather than the lack of cells in the ONL; however, the number of BrdU positive cells in the INL would also have been able to account for the observed increase in cone denstiy in the fovea.

Despite the absence of BrdU positive neuroretinal cells within the ONL in the foveal region, BrdU injections revealed the presence of proliferating cells within the INL and the GCL. These proliferating cells in the foveal region, in contrast to those of the nasal mid-pheripheral retina, were located either at the vitreal margin or in the middle of the layer. These are normally where retinal stem cells (Otteson and Hitchcock, 2003) and INL progenitor cells (Julian et al., 1998)/Müller cells (Wagner and Raymond, 1991) would be located. As the rod photoreceptors are absent within the foveal region, those possible retinal stem cells and INL progenitor cells could develop into cone photoreceptors (Wu et al., 2001). Previous authors have demonstrated that the selective regeneration of cone photoreceptors occurred in the lesioned goldfish retina (Braisted et al., 1994). In the present study, we are unable to rule out that there is a selective generation of cone photoreceptors from the INL stem cells which can occur in *H. taeniopterus* retina; however, in order to demonstrate that cones are generated in the foveal region, a longer survival time is necessary for the fish after BrdU injection. With the protocol used in this study, the BrdU injected seahorses were not able to survive more than a day. This may be due to the nature of the fish being more sensitive to any manipulations in its ecological niche.

Modification to the protocol involving increasing the time of exposure to BrdU is necessary to resolve whether cone progenitors exist in the foveal region of the seahorse.

No TUNEL positive rod photoreceptor cells were observed at the RFZ margin except at the smallest eyes studied. This is similar to the findings in the human retina (Provis, 1987, Georges et al., 1999). The RFZ in the human retina was initially believed to be formed from the programmed cell death of inappropriately generated excessive rod photoreceptors. However, little evidence supported apoptosis in photoreceptor cells within the particular retinal region during development. In teleosts, apoptosis generally occurs during embryonic development. With age, cell death plays less of a role in regulating the quantity and types of cell population (Glucksmann, 1940, Hoke and Fernald, 1998). During the embryonic development of *H. burtoni*, peak apoptosis in the central retina occurs in advance of rod photoreceptor neurogenesis and after that the cell death is significantly reduced. In and around the RFZ in *H. taeniopterus* retina apoptotic rod photoreceptors were absent during development. Although all of the data collected in this study were from the post-hatch period, the absence of apoptotic cells during the enlargement of RFZ suggested that the programmed cell death of rod photoreceptors did not play a critical role in the post-hatch development of RFZ. How rods are excluded from the RFZ remains to be determined. It is possible that the seahorse, like the primate never generates rods or expresses rod associated proteins in this region (Bumsted O'Brien et al., 2004).

The improvement of behavioural visual resolution in *H. taeniopterus* correlates with the increased cone photoreceptor cell density in the foveal region. This increase in cell densities in and around the fovea attributes to various possible factors including the centripetal migration of cone photoreceptor cells and the selective generation of cone photoreceptors from INL retinal stem cells within the RFZ. Rod photoreceptors are absent and excluded in and around the RFZ throughout the post-hatch development (Bumsted O'Brien et al., 2004).

References

Braisted JE, Essman TF, Raymond PA (1994) Selective regeneration of photoreceptors in goldfish retina. Development 120:2409-2419.

Breck JE, Gitter MJ (1983) Effect of fish size on the reactive distance of bluegill (Lepomis macrochirus) sunfish. Can J Fish Aquat Sci 40:162-167.

Browman HI, Gordon WC, Evans BI, O'Brien WJ (1990) Correlation between histological and behavioral measures of visual acuity in a zooplanktivorous fish, the white crappie (Pomoxis annularis). Brain Behav Evol 35:85-97.

Bumsted O'Brien KM, Cheng H, Jiang Y, Schulte D, Swaroop A, Hendrickson AE (2004) Expression of photoreceptor-specific nuclear receptor NR2E3 in rod photoreceptors of fetal human retina. Invest Ophthalmol Vis Sci 45:2807-2812.

Cameron DA (1995) Asymmetric retinal growth in the adult teleost green sunfish (Lepomis cyanellus). Vis Neurosci 12:95-102.

Cameron DA (1996) Asymmetric retinal growth: evidence for regulation by a retinotopic mechanism. Vis Neurosci 13:493-500.

Cameron DA (2000) Cellular proliferation and neurogenesis in the injured retina of adult zebrafish. Visual Neuroscience 17:789-797.

Chiu JF, Mack AF, Fernald RD (1995) Daily rhythm of cell proliferation in the teleost retina. Brain Res 673:119-125.

Collin SP, Pettigrew JD (1989) Quantitative Comparison of the Limits on Visual Spatial Resolution Set by the Ganglion Cell Layer in Twelve Species of Reef Teleosts. Brain Behav Evol 34:184-192.

Collin SP, Shand J (2003) Retinal Sampling and the Visual Field in Fishes. In: Sensory Processing in Aquatic Environments (Collin, S. P. and Marshall, N. J., eds), pp 139-169 New York: Springer Verlag.

Diaz Araya C, Provis JM (1992) Evidence of photoreceptor migration during early foveal development: A quantitative analysis of human fetal retinae. Visual Neuroscience 8:505-514.

Easter SS, Jr. (1992) Retinal growth in foveated teleosts: nasotemporal asymmetry keeps the fovea in temporal retina. J Neurosci 12:2381-2392.

Easter SS, Jr., Johns PR, Baumann LR (1977) Growth of the adult goldfish eye--I: Optics. Vision Res 17:469-477.

Fadool JM (2003) Development of a rod photoreceptor mosaic revealed in transgenic zebrafish. Developmental Biology 258:277-290.

Fernald RD (1985) Growth of the teleost eye: novel solutions to complex constraints. Environmental Biology of Fishes 13:113-123.

Fernald RD (1988) Aquatic adaptations in fish eyes. In: Sensory Biology of Aquatic Animals (Atema, J. et al., eds), pp 435-466 Berlin: Springer.

Fernald RD (1990) Teleost vision: seeing while growing. J Exp Zool Suppl 5:167-180.

Fernald RD, Johns PR (1980) Retinal structure and growth in the cichlid fish, *Haplochromis burtoni*. Invest Ophthalmol Vis Sci supp.:69.

Gavrieli Y, Sherman Y, Ben-Sasson SA (1992) Identification of programmed cell death in situ via specific labeling of nuclear DNA fragmentation. J Cell Biol 119:493-501.

Georges P, Madigan MC, Provis JM (1999) Apoptosis during development of the human retina: Relationship to foveal development and retinal synaptogenesis. The Journal of Comparative Neurology 413:198-208.

Glucksmann A (1940) Development and differentiation of the tadpole eye. The British journal of ophthalmology 24:153-178.

Guma'a SA (1982) Retinal development and retinomotor responses in perch, Perca fluviatilis L. Journal of Fish Biology 20:611-618.

Hairston NG, Jr., Li KT, Easter SS, Jr. (1982) Fish vision and the detection of planktonic prey. Science 218:1240-1242.

Hitchcock PF, Raymond PA (2004) The teleost retina as a model for developmental and regeneration biology. Zebrafish 1:257-271.

Hoke KL, Fernald RD (1997) Rod photoreceptor neurogenesis. Progress in Retinal and Eye Research 16:31-49.

Hoke KL, Fernald RD (1998) Cell death precedes rod neurogenesis in embryonic teleost retinal development. Developmental Brain Research 111:143-146.
Job SD, Bellwood DR (1996) Visual acuity and feeding in larval *Premnas biaculeatus*. Journal of Fish Biology 48:952-963.
Johns PR (1977) Growth of the adult goldfish eye. III. Source of the new retinal cells. The Journal of Comparative Neurology 176:343-357.
Johns PR (1982) Formation of photoreceptors in larval and adult goldfish. J Neurosci 2:178-198.
Johns PR, Easter SS, Jr. (1977) Growth of the adult goldfish eye. II. Increase in retinal cell number. J Comp Neurol 176:331-341.
Johns PR, Fernald RD (1981) Genesis of rods in teleost fish retina. Nature 293:141-142.
Julian D, Ennis K, Korenbrot JI (1998) Birth and fate of proliferative cells in the inner nuclear layer of the mature fish retina. J Comp Neurol 394:271-282.
Lee HR, Bumsted O'Brien KYM (2011) Morphological and behavioral limit of visual resolution in temperate (Hippocampus abdominalis) and tropical (Hippocampus taeniopterus) seahorses. Visual Neuroscience 28:351-360.
Li KT, Wetterer JK, Nelson G. Hairston, Jr. (1985) Fish Size, Visula Resolution, and Prey Selectivity. Ecology 66:1729-1735.
Lyall AH (1957a) Cone Arrangements in Teleost Retinae. Quarterly Journal of Microscopical Science s3-98:189-201.
Maslim J, Valter K, Egensperger R, Holländer H, Stone J (1997) Tissue oxygen during a critical developmental period controls the death and survival of photoreceptors. Investigative Ophthalmology & Visual Science 38:1667-1677.
Miller T, Crowder L, Rice J (1993) Ontogenetic changes in behavioural and histological measures of visual acuity in three species of fish. Environmental Biology of Fishes 37:1-8.
Morris AC, Scholz T, Fadool JM (2008) Rod Progenitor Cells in the Mature Zebrafish Retina Recent Advances in Retinal Degeneration. vol. 613 (Anderson, R. E. et al., eds), pp 361-368: Springer New York.
Mueller KP, Neuhauss SCF (2010) Quantitative measurements of the optokinetic response in adult fish. Journal of Neuroscience Methods 186:29-34.
Müller H (1952) Bau und Wachstum der Netzhaut des Guppy (Lebistes reticulatus). Zool Jb, Abt f allg Zool u Physiol 275–324.
Neave DA (1984) The development of visual acuity in larval plaice (Pleuronectes platessa L.) and turbot (Scophthalmusmaximus L.). Journal of Experimental Marine Biology and Ecology 78:167-175.
Otten E (1980) Vision During Growth of a Generalized Haplochromis Species: H. Elegans Trewavas 1933 (Pisces, Cichlidae). Netherlands Journal of Zoology 31:650-700.
Otteson DC, D'Costa AR, Hitchcock PF (2001) Putative Stem Cells and the Lineage of Rod Photoreceptors in the Mature Retina of the Goldfish. Developmental Biology 232:62-76.
Otteson DC, Hitchcock PF (2003) Stem cells in the teleost retina: persistent neurogenesis and injury-induced regeneration. Vision Res 43:927-936.
Pankhurst PM (1994) Age-related changes in the visual acuity of larvae of New Zealand snapper, Pagrus auratus. Journal of the Marine Biological Association of the United Kingdom 74:337-349.
Pankhurst PM, Pankhurst NW, Montgomery JC (1993) Comparison of behavioural and morphological measures of visual acuity during ontogeny in a teleost fish, Forsterygion varium, tripterygiidae (Forster, 1801). Brain Behav Evol 42:178-188.
Provis JM (1987) Patterns of cell death in the ganglion cell layer of the human fetal retina. J Comp Neurol 259:237-246.
Provis JM, Diaz CM, Dreher B (1998) Ontogeny of the primate fovea: a central issue in retinal development. Prog Neurobiol 54:549-580..
Raymond PA (1985b) The unique origin of rod photoreceptors in the teleost retina. Trends in Neurosciences 8:12-17.
Raymond PA, Reifler MJ, Rivlin PK (1988) Regeneration of goldfish retina: rod precursors are a likely source of regenerated cells. J Neurobiol 19:431-463.
Raymond PA, Rivlin PK (1987) Germinal cells in the goldfish retina that produce rod photoreceptors. Dev Biol 122:120-138.

Stenkamp DL, Barthel LK, Raymond PA (1997) Spatiotemporal coordination of rod and cone photoreceptor differentiation in goldfish retina. The Journal of Comparative Neurology 382:272-284.
Wagner EC, Raymond PA (1991) Muller glial cells of the goldfish retina are phagocytic in vitro but not in vivo. Exp Eye Res 53:583-589.
Wanzenbock J, Schiemer F (1989) Prey Detection in Cyprinids during Early Development. Can J Fish Aquat Sci 46:995-1001.
Wu DM, Schneiderman T, Burgett J, Gokhale P, Barthel L, Raymond PA (2001) Cones regenerate from retinal stem cells sequestered in the inner nuclear layer of adult goldfish retina. Invest Ophthalmol Vis Sci 42:2115-2124.
Zygar CA, Lee MJ, Fernald RD (1999) Nasotemporal asymmetry during teleost retinal growth: preserving an area of specialization. J Neurobiol 41:435-442.

Chapter Five

SUMMARY AND CONCLUSIONS

The teleost eye is a good model for studies investigating morphological and behavioural changes during normal development. This owes to the advantages of teleost model systems including good availability and ease of access for manipulation. Furthermore, the presence of one or more retinal specialisations that are responsible for high visual resolution makes a number of teleost species valuable for studying teleost vision, which may play a crucial role in foraging and survival. The results reported in this thesis have provided insights into seahorse vision and retinal development. Collectively the results contribute valuable insights concerning how seahorse retinal architecture is related to their habitats. In addition, these data report new findings detailing how the seahorse retina develops morphologically and functionally, and focuses on how the fovea and RFZ develops.

The results of Chapter 2 compare two different seahorse species inhabiting disparate aquatic environments, *H. abdominalis* from temperate waters and *H. taeniopterus* from tropical waters. Both species share common retinal characteristics in that they possess a ventrotemporally located fovea characterised by the absence of rod photoreceptors, increased cell densities and a convexiclivate pit formation. When their behaviourally measured visual resolution was calculated, *H. taeniopterus* had higher cone and ganglion cell densities within the fovea region and had better visual resolution. These findings reflect the differences in their environments as well as their visual requirements for foraging behaviour. These results led us to focus on the development of morphological and functional vision in *H. taeniopterus*.

Chapter 3 characterises the developmental changes of the *H. taeniopterus* fovea. As the fish grew in size, the retinal dimensions enlarged. The size of the rod-free zone increased and the convexiclivate fovea became more mature in shape: the pit became deeper and wider. Retinal topographic patterns of the total photoreceptor and ganglion cell densities remained consistant for all age groups studied. The topographic patterns showed a ventrotemporal retinal specialisation with concentric isodensity lines around it. The cell densities increased towards the foveal slope. Then, slightly decreased at the foveal centre and towards the periphery. The cone photoreceptor cell density pattern followed the general pattern, which resulted in the improved theoretical visual resolution during development calculated at both the foveal centre and the

slope. The ganglion cell density decreased at the foveal rim; however, the visual resolution estimated from these ganglion cell density values did not change statistically during development. At the foveal centre, the ganglion cell density did not change amongst the size groups studied here, but the theoretically calculated visual resolution using ganglion cell density improved during development. The findings demonstrated that the developmental changes of theoretically calculated visual resolution are correlated to that estimated behaviourally. In addition, the changes in cell density at the foveal region deviate from the general rule for teleost retinal development, which states that both cone photoreceptor and ganglion cell densities decrease as the fish grows. This indicates that the presence of a temporal retinal specialisation induces a unique mechanism for the development of this region including the asymmetrical retinal growth.

In the Chapter 4, the issue of how the retina enlarges during development while conserving the rod-free zone was studied. The results were in agreement with previous literature (Easter, 1992, Zygar et al., 1999). *H. taeniopterus* showed asymmetrical retinal growth where more cells were added in the nasal retina, which also expands more in order to preserve the relative location of the temporal retinal specialisation. As shown in Chapter 3, the size of the rod-free zone and the cone photoreceptor density within the rod-free zone increased with age. The BrdU injection, followed by the immunolabeling using anti-BrdU antibody, revealed that there were no proliferating cells in the ONL within the rod-free zone during development. However, it is noteworthy that proliferating cells were present in the INL of the rod-free zone. These cells may be INL stem cells producing cones, rather than rods specifically in that retinal region during ocular enlargement. TUNEL confirmed no major apoptotic activity around the margin of the rod-free zone, either. Therefore, the apoptosis of rod photoreceptors did not cause the enlargement of the rod-free zone during development of *H. taeniopturous* from the size groups studied here. This also suggested an exclusive mechanism for the development of retinal specialisation in *H. taeniopterus* retina. Again, the behavioural tests revealed that the larger seahorses had better spatial visual resolution.

In conclusion, the seahorse is a good model system for studying high resolution vision. Seahorses with their convexiclivate fovea are certainly visually guided feeders and in particular their feeding behaviour requires acute vision with an accurate judgement of depth. Being born as a live baby seahorse, instead of from an egg, provides advantages in terms of easy access to the eyes as well. The most common teleosts that have been used for vision studies include zebrafish and goldfish. Both species have their own peculiarities leading onto specific investigations, for instance, for zebrafish having regenerative properties to recover from retinal damage. Other non-teleost foveate creatures involved in developmental studies include pigeons and chameleons. Pigoens have a concaviclivate fovea with a shallow pit while chameleon possesses a convexiclivate fovea. Again, the fovea of each species possesses unique peculiarities reflecting their unique ecological niche and visual needs. The primate fovea is concaviclivate in shape similar to that in pigeon. However, the pigeon fovea contains all three nuclear layers as in the seahorse fovea. This could be a result of lacking inner retinal vasculatures which may possibly be one of the factors determining the shape of fovea. This requires further investigations. Furthermore, investigations using even smaller seahorses would reveal early developmental changes in the region of retinal specialisation. In addition to that, further manipulating studies could uncover the intrinsic factors deriving the formation and maturation of the retinal specialisation and provide insights into the teleost retinal development.

Appendix

Appendix 1: Complete list of references

Ammermuller J, Itzhaki A, Weiler R, Perlman I (1998) UV-sensitive input to horizontal cells in the turtle retina. Eur J Neurosci 10:1544-1552.

Anstis S, Harris J (1987) Magnification factor for adaptation of a visual transient mechanism. J Opt Soc Am A 4:1688-1698.

Arshavsky V (2002) Like night and day: rods and cones have different pigment regeneration pathways. Neuron 36:1-3.

Arshavsky VY, Lamb TD, Pugh EN, Jr. (2002) G proteins and phototransduction. Annu Rev Physiol 64:153-187.

Ban Y, Rizzolo LJ (2000) Differential regulation of tight junction permeability during development of the retinal pigment epithelium. Am J Physiol Cell Physiol 279:C744-750.

Barnstable CJ (1980) Monoclonal antibodies which recognize different cell types in the rat retina. Nature 286:231-235.

Barrow Heaton M (1982) A technique for improved resolution of [3H]thymidine autoradiography in the avian embryo: a preliminary report. Journal of Neuroscience Methods 5:61-72.

Beck JC, Gilland E, Tank DW, Baker R (2004) Quantifying the ontogeny of optokinetic and vestibuloocular behaviors in zebrafish, medaka, and goldfish. J Neurophysiol 92:3546-3561.

Bergert BA, Wainwright PC (1997) Morphology and kinematics of prey capture in the syngnathid fishes Hippocampus erectus and Syngnathus floridae. Marine Biology 127:563-570.

Bernardos RL, Barthel LK, Meyers JR, Raymond PA (2007) Late-Stage Neuronal Progenitors in the Retina Are Radial Müller Glia That Function as Retinal Stem Cells. The Journal of Neuroscience 27:7028-7040.

Biehlmaier O, Neuhauss S, Kohler K (2001) Onset and time course of apoptosis in the developing zebrafish retina. Cell Tissue Res 306:199-207.

Bilotta J, Powers MK (1991) Spatial contrast sensitivity of goldfish: Mean luminance, temporal frequency and a new psychophysical technique. Vision Research 31:577-585.

Blaxter JHS, Jones MP (1967) The Development of the Retina and Retinomotor Responses in the Herring. Journal of the Marine Biological Association of the United Kingdom 47:677-697.

Blaxter JHS, Staines M (1970) Pure-Cone Retinae and Retinomotor Responses in Larval Teleosts. Journal of the Marine Biological Association of the United Kingdom 50:449-464.

Blumer LS (1979) Male Parental Care in the Bony Fishes. The Quarterly Review of Biology 54:149-161.

Boire D, Dufour JS, Theoret H, Ptito M (2001) Quantitative analysis of the retinal ganglion cell layer in the ostrich, Struthio camelus. Brain Behav Evol 58:343-355.

Boothe RG, Dobson V, Teller DY (1985) Postnatal development of vision in human and nonhuman primates. Annu Rev Neurosci 8:495-545.

Bowmaker JK, Govardovskii VI, Shukolyukov SA, Zueva LV, Hunt DM, Sideleva VG, Smirnova OG (1994) Visual pigments and the photic environment: the cottoid fish of Lake Baikal. Vision Res 34:591-605.

Boycott B, Wassle H (1999) Parallel processing in the mammalian retina: the Proctor Lecture. Invest Ophthalmol Vis Sci 40:1313-1327.

Bozzano A, Catalán IA (2002) Ontogenetic changes in the retinal topography of the European hake, Merluccius merluccius : implications for feeding and depth distribution.

Braisted JE, Essman TF, Raymond PA (1994) Selective regeneration of photoreceptors in goldfish retina. Development 120:2409-2419.

Breck JE, Gitter MJ (1983) Effect of fish size on the reactive distance of bluegill (Lepomis macrochirus) sunfish. Can J Fish Aquat Sci 40:162-167.

Bringmann A, Pannicke T, Grosche J, Francke M, Wiedemann P, Skatchkov SN, Osborne NN, Reichenbach A (2006) Muller cells in the healthy and diseased retina. Prog Retin Eye Res 25:397-424.
Browman HI, Gordon WC, Evans BI, O'Brien WJ (1990) Correlation between histological and behavioral measures of visual acuity in a zooplanktivorous fish, the white crappie (Pomoxis annularis). Brain Behav Evol 35:85-97.
Bumsted O'Brien KM, Cheng H, Jiang Y, Schulte D, Swaroop A, Hendrickson AE (2004) Expression of photoreceptor-specific nuclear receptor NR2E3 in rod photoreceptors of fetal human retina. Invest Ophthalmol Vis Sci 45:2807-2812.
Burns ME, Baylor DA (2001) Activation, deactivation, and adaptation in vertebrate photoreceptor cells. Annu Rev Neurosci 24:779-805.
Butcher EO (1938) The structure of the retina of fundulus heteroclitus and the regions of the retina associated with the different chromatophoric responses. Journal of Experimental Zoology 79:275-297.
Cajal SR (1909) Histologie du système nerveux de l'homme & des vertébrés. Paris: A. Maloine.
Cajal SR (1982) La retina de los teleosteos y algunas observaciones sobre la de los vertebrados superiores. Anales Sociedad Esppanola de Historia Natural Madrid 21:281-305.
Cameron DA (1995) Asymmetric retinal growth in the adult teleost green sunfish (Lepomis cyanellus). Vis Neurosci 12:95-102.
Cameron DA (1996) Asymmetric retinal growth: evidence for regulation by a retinotopic mechanism. Vis Neurosci 13:493-500.
Cameron DA (2000) Cellular proliferation and neurogenesis in the injured retina of adult zebrafish. Visual Neuroscience 17:789-797.
Cameron DA, Easter SS (1993) The cone photoreceptor mosaic of the green sunfish, Lepomis cyanellus. Visual Neuroscience 10:375-384.
Cameron DA, Pugh EN (1991) Double cones as a basis for a new type of polarization vision in vertebrates. Nature 353:161-164.
Campbell FW, Green DG (1965) Optical and retinal factors affecting visual resolution. J Physiol 181:576-593.
Campenhausen MV, Kirschfeld K (1998) Spectral sensitivity of the accessory optic system of the pigeon. J Comp Physiol A 183:1-6.
Chiu JF, Mack AF, Fernald RD (1995) Daily rhythm of cell proliferation in the teleost retina. Brain Res 673:119-125.
Choo CK, Liew HC (2006) Morphological development and allometric growth patterns in the juvenile seahorse Hippocampus kuda Bleeker. Journal of Fish Biology 69:426-445.
Collin HB, Collin SP (1995) Ultrastructure and organisation of the cornea, lens and iris in the pipefish, Corythoichthyes paxtoni (Syngnathidae, Teleostei). Histol Histopathol 10:313-323.
Collin HB, Collin SP (1996) The fine structure of the cornea of the salamanderfish, Lepidogalaxias salamandroides (Lepidogalaxiidae, Teleostei). Cornea 15:414-426.
Collin SP (1988) The retina of the shovel-nosed ray, Rhinobatos batillum (Rhinobatidae): morphology and quantitative analysis of the ganglion, amacrine and bipolar cell populations. Experimental biology 47:195-207.
Collin SP (1997) Specialisations of the teleost visual system: adaptive diversity from shallow-water to deep-sea. Acta Physiol Scand Suppl 161:5-24.
Collin SP (1999) Behavioural ecology and retinal cell topography. In: Adaptive Mechanisms in The Ecology of Vision (Archer, S. N. et al., eds), pp 509-535 Dordrecht: Kluwer Academic Publishers.
Collin SP, Ali MA (1994) Multiple areas of acute vision in two freshwater teleosts, the creek chub, Semotilus atromaculatus (Mitchill) and the cutlips minnow, Exoglossum maxillingua (Lesuer). Can J Zool 72:721-730.
Collin SP, Collin HB (1988a) The morphology of the retina and lens of the sandlance, Limnichthyes fasciatus (Creeiidae). Experimental biology 47:209-218.
Collin SP, Collin HB (1988b) Topographic analysis of the retinal ganglion cell layer and optic nerve in the sandlance Limnichthyes fasciatus (Creeiidae, Perciformes). J Comp Neurol 278:226-241.

Collin SP, Collin HB (1999) The foveal photoreceptor mosaic in the pipefish, Corythoichthyes paxtoni (Syngnathidae, Teleostei). Histol Histopathol 14:369-382.
Collin SP, Pettigrew JD (1988a) Retinal ganglion cell topography in teleosts: a comparison between Nissl-stained material and retrograde labelling from the optic nerve. J Comp Neurol 276:412-422.
Collin SP, Pettigrew JD (1988b) Retinal Topography in Reef Teleosts, I. Some Species with Well-Developed Areae but Poorly-Developed Streaks. Brain Behav Evol 31:269-282.
Collin SP, Pettigrew JD (1988c) Retinal Topography in Reef Teleosts, II. Some Species with Prominent Horizontal Streaks and High-Density Areae. Brain Behav Evol 31:283-295.
Collin SP, Pettigrew JD (1989) Quantitative Comparison of the Limits on Visual Spatial Resolution Set by the Ganglion Cell Layer in Twelve Species of Reef Teleosts. Brain Behav Evol 34:184-192.
Collin SP, Shand J (2003) Retinal Sampling and the Visual Field in Fishes. In: Sensory Processing in Aquatic Environments (Collin, S. P. and Marshall, N. J., eds), pp 139-169 New York: Springer Verlag.
Costen NP, Parker DM, Craw I (1994) Spatial content and spatial quantisation effects in face recognition. Perception 23:129-146.
Cummings ME, Partridge JC (2001) Visual pigments and optical habitats of surfperch (Embiotocidae) in the California kelp forest. J Comp Physiol A Neuroethol Sens Neural Behav Physiol 187:875-889.
Curcio CA, Allen KA (1990) Topography of ganglion cells in human retina. J Comp Neurol 300:5-25.
Curcio CA, Sloan KR, Kalina RE, Hendrickson AE (1990) Human photoreceptor topography. J Comp Neurol 292:497-523.
Diaz Araya C, Provis JM (1992) Evidence of photoreceptor migration during early foveal development: A quantitative analysis of human fetal retinae. Visual Neuroscience 8:505-514.
Dobson V, Teller DY (1978) Visual acuity in human infants: A review and comparison of behavioral and electrophysiological studies. Vision Research 18:1469-1483.
Dowling JE, Ehinger B (1975) Synaptic organization of the amine-containing interplexiform cells of the goldfish and Cebus monkey retinas. Science 188:270-273.
Easter Jr SS, Johns PR, Baumann LR (1977) Growth of the adult goldfish eye—I: Optics. Vision Research 17:469-477.
Easter SS, Jr. (1972) Pursuit eye movements in goldfish (Carassius auratus). Vision Res 12:673-688.
Easter SS, Jr. (1992) Retinal growth in foveated teleosts: nasotemporal asymmetry keeps the fovea in temporal retina. J Neurosci 12:2381-2392.
Easter SS, Jr., Johns PR, Baumann LR (1977) Growth of the adult goldfish eye--I: Optics. Vision Res 17:469-477.
Easter SS, Jr., Nicola GN (1996) The development of vision in the zebrafish (Danio rerio). Dev Biol 180:646-663.
Fadool JM (2003) Development of a rod photoreceptor mosaic revealed in transgenic zebrafish. Developmental Biology 258:277-290.
Fekete DM, Barnstable CJ (1983) The subcellular localization of rat photoreceptor-specific antigens. J Neurocytol 12:785-803.
Fernald RD (1981) Chromatic organization of a cichlid fish retina. Vision Res 21:1749-1753.
Fernald RD (1985) Growth of the teleost eye: novel solutions to complex constraints. Environmental Biology of Fishes 13:113-123.
Fernald RD (1988) Aquatic adaptations in fish eyes. In: Sensory Biology of Aquatic Animals (Atema, J. et al., eds), pp 435-466 Berlin: Springer.
Fernald RD (1990) Teleost vision: seeing while growing. J Exp Zool Suppl 5:167-180.
Fernald RD, Johns PR (1980) Retinal structure and growth in the cichlid fish, *Haplochromis burtoni*. Invest Ophthalmol Vis Sci supp.:69.
Fernald RD, Wright SE (1985) Growth of the visual system in the African cichlid fish, Haplochromis burtoni. Optics. Vision Res 25:155-161.
Fite KV, Lister BC (1981) Bifoveal vision in anolis lizards. Brain Behav Evol 19:144-154.

Fite KV, Rosenfield-Wessels S (1975) A Comparative Study of Deep Avian Foveas. Brain, Behavior and Evolution 12:97-115.
Fleisch VC, Neuhauss SC (2006) Visual behavior in zebrafish. Zebrafish 3:191-201.
Foster SJ, Vincent ACJ (2004) Life history and ecology of seahorses: implications for conservation and management. Journal of Fish Biology 65:1-61.
Fritsches KA, Marshall NJ (2002) Independent and conjugate eye movements during optokinesis in teleost fish. J Exp Biol 205:1241-1252.
Galifret Y (1968) Les diverses aires fonctionnelles de la retine du pigeon. Z Zellforsch Mikrosk Anat 86:535–545.
Garciá M, Ruiz-Ederra J, Hernández-Barbáchano H, Vecino E (2005) Topography of pig retinal ganglion cells. J Comp Neurol 486:361-372.
Garoutte B (1981) Survey of functional neuroanatomy: Jones Medical Publications.
Gavrieli Y, Sherman Y, Ben-Sasson SA (1992) Identification of programmed cell death in situ via specific labeling of nuclear DNA fragmentation. J Cell Biol 119:493-501.
Gehres M, Neumeyer C (2007) Small field motion detection in goldfish is red-green color blind and mediated by the M-cone type. Vis Neurosci 24:399-407.
Georges P, Madigan MC, Provis JM (1999) Apoptosis during development of the human retina: Relationship to foveal development and retinal synaptogenesis. The Journal of Comparative Neurology 413:198-208.
Glucksmann A (1940) Development and differentiation of the tadpole eye. The British journal of ophthalmology 24:153-178.
Gratzner HG (1982) Monoclonal antibody to 5-bromo- and 5-iododeoxyuridine: A new reagent for detection of DNA replication. Science 218:474-475.
Gratzner HG, Leif RC, Ingram DJ, Castro A (1975) The use of antibody specific for bromodeoxyuridine for the immunofluorescent determination of DNA replication in single cells and chromosomes. Experimental Cell Research 95:88-94.
Guma'a SA (1982) Retinal development and retinomotor responses in perch, Perca fluviatilis L. Journal of Fish Biology 20:611-618.
Hairston NG, Jr., Li KT, Easter SS, Jr. (1982) Fish vision and the detection of planktonic prey. Science 218:1240-1242.
Hamann S (2002) Molecular mechanisms of water transport in the eye. In: International Review of Cytology, vol. Volume 215 (Thomas Zeuthen, W. D. S., ed), pp 395-431: Academic Press.
Harkness L, Bennet-Clark HC (1978) The deep fovea as a focus indicator. Nature 272:814-816.
Harosi FI, MacNichol EF, Jr. (1974) Visual pigments of goldfish cones. Spectral properties and dichroism. J Gen Physiol 63:279-304.
Haug MF, Biehlmaier O, Mueller KP, Neuhauss SC (2010) Visual acuity in larval zebrafish: behavior and histology. Front Zool 7:8.
Hawryshyn CW, Arnold MG, Chaisson DJ, Martin PC (1989) The ontogeny of ultraviolet photosensitivity in rainbow trout (Salmo gairdneri). Vis Neurosci 2:247-254.
Hawryshyn CW, Moyer HD, Allison WT, Haimberger TJ, McFarland WN (2003) Multidimensional polarization sensitivity in damselfishes. J Comp Physiol A Neuroethol Sens Neural Behav Physiol 189:213-220.
Hemmi JM, Grünert U (1999) Distribution of photoreceptor types in the retina of a marsupial, the tammar wallaby (Macropus eugenii). Visual Neuroscience 16:291-302.
Hendrickson A (1992) A morphological comparison of foveal development in man and monkey. Eye 6 (Pt 2):136-144.
Hendrickson AE, Yuodelis C (1984) The morphological development of the human fovea. Ophthalmology 91:603-612.
Hitchcock PF, Macdonald RE, VanDeRyt JT, Wilson SW (1996) Antibodies against Pax6 immunostain amacrine and ganglion cells and neuronal progenitors, but not rod precursors, in the normal and regenerating retina of the goldfish. J Neurobiol 29:399-413.
Hitchcock PF, Raymond PA (2004) The teleost retina as a model for developmental and regeneration biology. Zebrafish 1:257-271.
Hodel C, Neuhauss SCF (2008) Computer-Based Analysis of the Optokinetic Response in Zebrafish Larvae. Cold Spring Harbor Protocols 2008:pdb.prot4961.

Hodos W, Ghim MM, Potocki A, Fields JN, Storm T (2002) Contrast sensitivity in pigeons: a comparison of behavioral and pattern ERG methods. Doc Ophthalmol 104:107-118.
Hodson S, Miller F, Riley M (1977) The electrogenic pump of rabbit corneal endothelium. Experimental Eye Research 24:249-253.
Hoke KL, Fernald RD (1997) Rod photoreceptor neurogenesis. Progress in Retinal and Eye Research 16:31-49.
Hoke KL, Fernald RD (1998) Cell death precedes rod neurogenesis in embryonic teleost retinal development. Developmental Brain Research 111:143-146.
Hollyfield JG (1972) Histogenesis of the retina in the killifish, Fundulus heteroclitus. J Comp Neurol 144:373-380.
Hughes A (1971) Topographical relationships between the anatomy and physiology of the rabbit visual system. Documenta Ophthalmologica 30:33-159.
Hughes A (1977) The topography of vision oin mammals. Berlin: Springer-Verlag.
Ito H, Murakami T (1984) Retinal ganglion cells in two teleost species, Sebastiscus marmoratus and Navodon modestus. J Comp Neurol 229:80-96.
James P, Heck Jr K (1994) The effects of habitat complexity and light intensity on ambush predation within a simulated seagrass habitat. Journal of Experimental Marine Biology and Ecology 176:187-200.
Jerlov NG (1976) Marine Optics: Elsevier Science.
Job SD, Bellwood DR (1996) Visual acuity and feeding in larval *Premnas biaculeatus*. Journal of Fish Biology 48:952-963.
Johns PR (1977) Growth of the adult goldfish eye. III. Source of the new retinal cells. The Journal of Comparative Neurology 176:343-357.
Johns PR (1981) Growth of Fish Retinas. American Zoologist 21:447-458.
Johns PR (1982) Formation of photoreceptors in larval and adult goldfish. J Neurosci 2:178-198.
Johns PR, Easter SS, Jr. (1977) Growth of the adult goldfish eye. II. Increase in retinal cell number. J Comp Neurol 176:331-341.
Johns PR, Fernald RD (1981) Genesis of rods in teleost fish retina. Nature 293:141-142.
Julian D, Ennis K, Korenbrot JI (1998) Birth and fate of proliferative cells in the inner nuclear layer of the mature fish retina. J Comp Neurol 394:271-282.
Juliusson B, Bergström A, Röhlich P, Ehinger B, van Veen T, Szél A (1994) Complementary cone fields of the rabbit retina. Investigative Ophthalmology & Visual Science 35:811-818.
Kahmann H (1934) ijber die Vorkommen einer Fovea centralis im Knochenfischauge. Zool Anz 106:49-55.
Kamermans M, Hawryshyn C (2011) Teleost polarization vision: how it might work and what it might be good for. Philosophical Transactions of the Royal Society B: Biological Sciences 366:742-756.
Kaneko A (1970) Physiological and morphological identification of horizontal, bipolar and amacrine cells in goldfish retina. J Physiol 207:623-633.
Kaneko A (1973) Receptive field organization of bipolar and amacrine cells in the goldfish retina. J Physiol 235:133-153.
Kaneko A, Hashimoto H (1969) Electrophysiological study of single neurons in the inner nuclear layer of the carp retina. Vision Research 9:37-55.
Kock JH (1982) Neuronal addition and retinal expansion during growth of the crucian carp eye. J Comp Neurol 209:264-274.
Krauss A, Neumeyer C (2003) Wavelength dependence of the optomotor response in zebrafish (Danio rerio). Vision Res 43:1273-1282.
Kroger RH, Knoblauch B, Wagner HJ (2003) Rearing in different photic and spectral environments changes the optomotor response to chromatic stimuli in the cichlid fish Aequidens pulcher. J Exp Biol 206:1643-1648.
Kuiter RH (2000) The Marine Fish Families Series, Seahorses Pipefishes and their relatives, A comprehensive Guide to Syngnathiformes. Chorleywood, UK: TMC Publishing.
Land MF (1995) Fast-focus telephoto eye. Nature 373:658-659.
Land MF (1999) Visual optics: The sandlance eye breaks all the rules. Current biology : CB 9:R286-R288.

Lazzaro X (1987) A review of planktivorous fishes: Their evolution, feeding behaviours, selectivities, and impacts. Hydrobiologia 146:97-167.
Lee HR, Bumsted O'Brien KYM (2011) Morphological and behavioral limit of visual resolution in temperate (Hippocampus abdominalis) and tropical (Hippocampus taeniopterus) seahorses. Visual Neuroscience 28:351-360.
Li KT, Wetterer JK, Nelson G. Hairston, Jr. (1985) Fish Size, Visula Resolution, and Prey Selectivity. Ecology 66:1729-1735.
Li L, Dowling JE (1997) A dominant form of inherited retinal degeneration caused by a non-photoreceptor cell-specific mutation. Proceedings of the National Academy of Sciences 94:11645-11650.
Locket NA (1992) Problems of deep foveas. Aust New Zeal J Ophthalmol 20:281-295.
Loew ER, Lythgoe JN (1978) The ecology of cone pigments in teleost fishes. Vision Research 18:715-722.
Loew ER, McFarland WN, Mills EL, Hunter D (1993) A chromatic action spectrum for planktonic predation by juvenile yellow perch, Perca flavescens. Canadian Journal of Zoology 71:384-386.
Losey GS, Cronin TW, Goldsmith TH, Hydes D, Marshall NJ, McFarland WN (1999) The UV vusyal world of fishes: A review. Journal of Fish Biology 54:921-943.
Losey GS, McFarland WN, Loew ER, Zamzow JP, Nelson PA, Marshall NJ, Montgomery WL (2003) Visual Biology of Hawaiian Coral Reef Fishes. I. Ocular Transmission and Visual Pigments. Copeia 2003:433-454.
Lyall AH (1957a) Cone Arrangements in Teleost Retinae. Quarterly Journal of Microscopical Science s3-98:189-201.
Lyall AH (1957b) The growth of the trout retina. Quarterly Journal of Microscopical Science 98:101-110.
Lythgoe JN (1975) The Structure and Function of Iridescent Corneas in Teleost Fishes. Proceedings of the Royal Society of London Series B Biological Sciences 188:437-457.
Lythgoe JN (1979) The ecology of vision: Clarendon Press.
Lythgoe JN (ed.) (1980) Vision in fishes: ecological adaptations. New York: Premium Press.
Lythgoe JN (1984) Visual pigments and environmental light. Vision Research 24:1539-1550.
Lythgoe JN, Muntz WRA, Partridge JC, Shand J, Williams DM (1994) The ecology of the visual pigments of snappers (Lutjanidae) on the Great Barrier Reef. Journal of Comparative Physiology A: Neuroethology, Sensory, Neural, and Behavioral Physiology 174:461-467.
Lythgoe JN, Partridge JC (1989) Visual pigments and the acquisition of visual information. J Exp Biol 146:1-20.
Maaswinkel H, Li L (2003) Spatio-temporal frequency characteristics of the optomotor response in zebrafish. Vision Res 43:21-30.
Mack AF, Sussmann C, Hirt B, Wagner HJ (2004) Displaced amacrine cells disappear from the ganglion cell layer in the central retina of adult fish during growth. Invest Ophthalmol Vis Sci 45:3749-3755.
Mangrum WI, Dowling JE, Cohen ED (2002) A morphological classification of ganglion cells in the zebrafish retina. Visual Neuroscience 19:767-779.
Marchiafava PL (1976) Centrifugal actions on amacrine and ganglion cells in the retina of the turtle. J Physiol 255:137-155.
Marchiafava PL (1985) Cell Coupling in Double Cones of the Fish Retina. Proceedings of the Royal Society of London Series B Biological Sciences 226:211-215.
Marshak DW, Dowling JE (1987) Synapses of cone horizontal cell axons in goldfish retina. The Journal of Comparative Neurology 256:430-443.
Marshall J, Vorobyev M (2003) The Design of Color Signals and Color Vision in Fishes. In: Sensory processing in aquatic environments (Collin, S. P. and Marshall, N. J., eds), pp 194-222 New York: Springer.
Marshall J, Vorobyev M, Siebeck U (2006) What does a reef fish see when sees a reef fish? In: Communication in fishes (Kapoor, B. G. et al., eds) Enfield U.S.A.: Science Publisher Inc.

Marshall NJ, Jennings K, McFarland WN, Loew ER, Losey GS, Montgomery WL (2003) Visual Biology of Hawaiian Coral Reef Fishes. III. Environmental Light and an Integrated Approach to the Ecology of Reef Fish Vision. Copeia 2003:467-480.
Maslim J, Valter K, Egensperger R, Holländer H, Stone J (1997) Tissue oxygen during a critical developmental period controls the death and survival of photoreceptors. Investigative Ophthalmology & Visual Science 38:1667-1677.
Matthiessen L (1880) Untersuchungen über den Aplanatismus und die Periscopie der Krystalllinsen in den Augen der Fische. Pflügers Archiv European Journal of Physiology 21:287-307.
McFarland WN, Loew ER (1994) Ultraviolet visual pigments in marine fishes of the family pomacentridae. Vision Research 34:1393-1396.
Merigan WH, Maunsell JHR (1993) How Parallel are the Primate Visual Pathways? Annual Review of Neuroscience 16:369-402.
Meyer RL (1978) Evidence from thymidine labeling for continuing growth of retina and tectum in juvenile goldfish. Experimental Neurology 59:99-111.
Miller T, Crowder L, Rice J (1993) Ontogenetic changes in behavioural and histological measures of visual acuity in three species of fish. Environmental Biology of Fishes 37:1-8.
Mitarai G, Goto T, Takagi S (1978) Receptive field arrangement of color-opponent bipolar and amacrine cells in the carp retina. Sens Processes 2:375-382.
Mö11er A (1950) Die Struktur des Auges bei Urodelen verschiedener K6rpergr6sse. Zool Jahrb Abt Allg Zool Physiol 62:138-182.
Moreland JD, Lythgoe JN (1968) Yellow corneas in fishes. Vision Research 8:1377-1380.
Morris AC, Scholz T, Fadool JM (2008) Rod Progenitor Cells in the Mature Zebrafish Retina Recent Advances in Retinal Degeneration. vol. 613 (Anderson, R. E. et al., eds), pp 361-368: Springer New York.
Moshiri A, Close J, Reh TA (2004) Retinal stem cells and regeneration. Int J Dev Biol 48:1003-1014.
Mosk V, Thomas N, Hart NS, Partridge JC, Beazley LD, Shand J (2007) Spectral sensitivities of the seahorses Hippocampus subelongatus and Hippocampus barbouri and the pipefish Stigmatopora argus. Vis Neurosci 24:345-354.
Mueller KP, Neuhauss SC (2012) Automated visual choice discrimination learning in zebrafish (Danio rerio). J Integr Neurosci 11:73-85.
Mueller KP, Neuhauss SCF (2010) Quantitative measurements of the optokinetic response in adult fish. Journal of Neuroscience Methods 186:29-34.
Müller H (1952) Bau und Wachstum der Netzhaut des Guppy (Lebistes reticulatus). Zool Jb, Abt f allg Zool u Physiol 275–324.
Munk O (1975) On the eyes of 2 foveate notosudid teleosts scopelosaurus hoedti and ahliesaurus berryi. Videnskabelige Meddelelser fra Dansk Naturhistorisk Forening 138:87-125.
Murakami M, Shimoda Y (1977) Identification of amacrine and ganglion cells in the carp retina. J Physiol 264:801-818.
Neave DA (1984) The development of visual acuity in larval plaice (Pleuronectes platessa L.) and turbot (Scophthalmusmaximus L.). Journal of Experimental Marine Biology and Ecology 78:167-175.
Nelson R, Connaughton V (2013) Bipolar cell pathways in the vertebrate retina.
Neumeyer C (1986) Wavelength discrimination in the goldfish. J Comp Physiol A 158:203-213.
Neumeyer C (1992) Tetrachromatic color vision in goldfish: evidence from color mixture experiments. J Comp Physiol A 171:639-649.
Nguyen-Legros J, Hicks D (2000) Renewal of photoreceptor outer segments and their phagocytosis by the retinal pigment epithelium. Int Rev Cytol 196:245-313.
Niemeye G, Gouras P (1973) Rod and cone signals inS-potentials of the isolated perfused cat eye. Vision Research 13:1603-1612.
Northmore DP, Dvorak CA (1979) Contrast sensitivity and acuity of the goldfish. Vision Res 19:255-261.

Novales-Flamarique H, Hawryshyn C (1994) Ultraviolet photoreception contributes to prey search behaviour in two species of zooplanktivorous fishes. Journal of Experimental Biology 186:187-198.
O'Brien WJ (1979) The Predator-Prey Interaction of Planktivorous Fish and Zooplankton: Recent research with planktivorous fish and their zooplankton prey shows the evolutionary thrust and parry of the predator-prey relationship. American Scientist 67:572-581.
O'Brien WJ, Browman HI, Evans BI (1990) Search strategies of foraging animals. Amer Sci 78:152-160.
Ollivier FJ, Samuelson DA, Brooks DE, Lewis PA, Kallberg ME, Komáromy AM (2004) Comparative morphology of the tapetum lucidum (among selected species). Veterinary Ophthalmology 7:11-22.
Orger MB, Baier H (2005) Channeling of red and green cone inputs to the zebrafish optomotor response. Vis Neurosci 22:275-281.
Orger MB, Gahtan E, Muto A, Page-McCaw P, Smear MC, Baier H (2004) Behavioral screening assays in zebrafish. Methods Cell Biol 77:53-68.
Otten E (1980) Vision During Growth of a Generalized Haplochromis Species: H. Elegans Trewavas 1933 (Pisces, Cichlidae). Netherlands Journal of Zoology 31:650-700.
Otteson DC, D'Costa AR, Hitchcock PF (2001) Putative Stem Cells and the Lineage of Rod Photoreceptors in the Mature Retina of the Goldfish. Developmental Biology 232:62-76.
Otteson DC, Hitchcock PF (2003) Stem cells in the teleost retina: persistent neurogenesis and injury-induced regeneration. Vision Res 43:927-936.
Packer O, Hendrickson AE, Curcio CA (1989) Photoreceptor topography of the retina in the adult pigtail macaque (Macaca nemestrina). J Comp Neurol 288:165-183.
Packer O, Hendrickson AE, Curcio CA (1990) Development redistribution of photoreceptors across the Macaca nemestrina (pigtail macaque) retina. J Comp Neurol 298:472-493.
Pankhurst NW, Montgomery JC (1990) Ontogeny of vision in the Antarctic fish Pagothenia borchgrevinki (Nototheniidae). Polar Biology 10:419-422.
Pankhurst PM (1994) Age-related changes in the visual acuity of larvae of New Zealand snapper, Pagrus auratus. Journal of the Marine Biological Association of the United Kingdom 74:337-349.
Pankhurst PM, Pankhurst NW, Montgomery JC (1993) Comparison of behavioural and morphological measures of visual acuity during ontogeny in a teleost fish, Forsterygion varium, tripterygiidae (Forster, 1801). Brain Behav Evol 42:178-188.
Partridge JC (1990) The colour sensitivity and vision of fishes. In: Light and life in the sea (Herring, P. J. et al., eds), pp 167-184 Cambridge, England: Cambridge University Press.
Perlman I, Kolb H, Nelson R (2012) S-Potentials and Horizontal Cells. In: Webvision: The Organization of the Retina and Visual System.
Perry VH, Walker M (1980) Amacrine cells, displaced amacrine cells and interplexiform cells in the retina of the rat. Proc R Soc Lond B Biol Sci 208:415-431.
Peterson RE, Fadool JM, McClintock J, Linser PJ (2001) Müller cell differentiation in the zebrafish neural retina: Evidence of distinct early and late stages in cell maturation. The Journal of Comparative Neurology 429:530-540.
Pettigrew JD, Collin SP (1995) Terrestrial optics in an aquatic eye: The sandlance, *Limnichthytes fasciatus* (Creediidae, Teleostei). Journal of Comparative Physiology A: Neuroethology, Sensory, Neural, and Behavioral Physiology 177:397-408.
Pettigrew JD, Collin SP, Fritsches K (2000) Prey capture and accommodation in the sandlance, Limnichthyes fasciatus (Creediidae; Teleostei). J Comp Physiol [A] 186:247-260.
Pettigrew JD, Collin SP, Ott M (1999) Convergence of specialised behaviour, eye movements and visual optics in the sandlance (Teleostei) and the chameleon (Reptilia). Curr Biol 9:421-424.
Pignatelli V, Champ C, Marshall J, Vorobyev M (2010) Double cones are used for colour discrimination in the reef fish, Rhinecanthus aculeatus. Biol Lett 6:537-539.
Powers MK, Easter Jr SS (1978) Absolute visual sensitivity of the goldfish. Vision Research 18:1137-1147.

Powers MK, Easter Jr SS (1983) Behavioural significance of retinal structure and function in fishes In: Fish Neurobiology, vol. 1 (Northcutt, R. G. and Davis, R. E., eds), pp 377-404 Ann Arbor: University of Michigan Press.
ProjectSeahorse (1996-2013) Project Seahorse: Advancing marine conservation. The University of British Columbia.
Provis JM (1979) The distribution and size of ganglion cells in the regina of the pigmented rabbit: a quantitative analysis. J Comp Neurol 185:121-137.
Provis JM (1987) Patterns of cell death in the ganglion cell layer of the human fetal retina. J Comp Neurol 259:237-246.
Provis JM, Diaz CM, Dreher B (1998) Ontogeny of the primate fovea: a central issue in retinal development. Prog Neurobiol 54:549-580.
Pumphrey RJ (1948) The Theory of the Fovea. J Exp Biol 25:299-312.
Pushchin II, Podugolnikova TA, Kondrashev SL (2007) Morphology and spatial arrangement of large retinal ganglion cells projecting to the optic tectum in the perciform fish Pholidapus dybowskii. Vision Res 47:3212-3227.
Querubin A, Lee HR, Provis JM, Bumsted O'Brien KM (2009) Photoreceptor and ganglion cell topographies correlate with information convergence and high acuity regions in the adult pigeon (<I>Columba livia)</I> retina. The Journal of Comparative Neurology 517:711-722.
Rahmann H, Jeserich G, Zeutzius I (1979) Ontogeny of Visual Acuity of Rainbow Trout under Normal Conditions and Light Deprivation. Behaviour 68:315-322.
Ransom-Hogg A, Spillmann L (1980) Perceptive field size in fovea and periphery of the light- and dark-adapted retina. Vision Research 20:221-228.
Rapaport DH, Stone J (1984) The area centralis of the retina in the cat and other mammals: Focal point for function and development of the visual system. Neuroscience 11:289-301.
Raymond P, Barthel L, Bernardos R, Perkowski J (2006) Molecular characterization of retinal stem cells and their niches in adult zebrafish. BMC Developmental Biology 6:36.
Raymond PA (1985a) Cytodifferentiation of photoreceptors in larval goldfish: Delayed maturation of rods. The Journal of Comparative Neurology 236:90-105.
Raymond PA (1985b) The unique origin of rod photoreceptors in the teleost retina. Trends in Neurosciences 8:12-17.
Raymond PA, Reifler MJ, Rivlin PK (1988) Regeneration of goldfish retina: rod precursors are a likely source of regenerated cells. J Neurobiol 19:431-463.
Raymond PA, Rivlin PK (1987) Germinal cells in the goldfish retina that produce rod photoreceptors. Dev Biol 122:120-138.
Risner ML, Lemerise E, Vukmanic EV, Moore A (2006) Behavioral spectral sensitivity of the zebrafish (Danio rerio). Vision Research 46:2625-2635.
Salinas-Navarro M, Mayor-Torroglosa S, Jimenez-Lopez M, Aviles-Trigueros M, Holmes TM, Lund RD, Villegas-Perez MP, Vidal-Sanz M (2009) A computerized analysis of the entire retinal ganglion cell population and its spatial distribution in adult rats. Vision Res 49:115-126.
Schaerer S, Neumeyer C (1996) Motion detection in goldfish investigated with the optomotor response is "color blind". Vision Res 36:4025-4034.
Schmitt E, Kunz YW (1989) Retinal morphogenesis in the rainbow trout, Salmo gairdneri. Brain Behav Evol 34:48-64.
Scholes JH (1976) Neuronal Connections and Cellular Arrangement in the Fish Retina. In: Neural Principles in Vision (Zettler, F. and Weiler, R., eds), pp 63-93: Springer Berlin Heidelberg.
Schuster S, Amtsfeld S (2002) Template-matching describes visual pattern-recognition tasks in the weakly electric fish Gnathonemus petersii. J Exp Biol 205:549-557.
Schwassmann HO (1968) Visual projection upon the optic tectum in foveate marine teleosts. Vision Research 8:1337-IN1332.
Shand J (1997) Ontogenetic changes in retinal structure and visual acuity: a comparative study of coral-reef teleosts with differing post-settlement lifestyles. Environmental Biology of Fishes 49:307-322.

Shand J, Chin SM, Harman AM, Moore S, Collin SP (2000) Variability in the Location of the Retinal Ganglion Cell Area Centralis Is Correlated with Ontogenetic Changes in Feeding Behavior in the Black Bream, Acanthopagrus butcheri (Sparidae, Teleostei). Brain, Behavior and Evolution 55:176-190.
Shand J, Doving KB, Collin SP (1999) Optics of the developing fish eye: comparisons of Matthiessen's ratio and the focal length of the lens in the black bream Acanthopagrus butcheri (Sparidae, Teleostei). Vision Res 39:1071-1078.
Sharma SC, Ungar F (1980) Histogenesis of the goldfish retina. J Comp Neurol 191:373-382.
Siebeck UE, Marshall NJ (2001) Ocular media transmission of coral reef fish--can coral reef fish see ultraviolet light? Vision Res 41:133-149.
Siebeck UE, Wallis GM, Litherland L (2008) Colour vision in coral reef fish. J Exp Biol 211:354-360.
Sivak JG (1974) The refractive error of the fish eye. Vision Research 14:209-213.
Slonaker JR (1897) A comparative study of the area of acute vision in vertebrates. Journal of Morphology 13:445-502.
Steinberg RH (1985) Interactions between the retinal pigment epithelium and the neural retina. Documenta Ophthalmologica 60:327-346.
Stell WK (1967) The structure and relationships of horizontal cells and photoreceptor-bipolar synaptic complexes in goldfish retina. American Journal of Anatomy 121:401-423.
Stenkamp DL (2011) The rod photoreceptor lineage of teleost fish. Progress in Retinal and Eye Research 30:395-404.
Stenkamp DL, Barthel LK, Raymond PA (1997) Spatiotemporal coordination of rod and cone photoreceptor differentiation in goldfish retina. The Journal of Comparative Neurology 382:272-284.
Stone J (1965) A quantitative analysis of the distribution of ganglion cells in the cat's retina. J Comp Neurol 124:337-352.
Stone J, Johnston E (1981) The topography of primate retina: a study of the human, bushbaby, and new- and old-world monkeys. J Comp Neurol 196:205-223.
Strauss O (2005) The retinal pigment epithelium in visual function. Physiol Rev 85:845-881.
Tappeiner C, Gerber S, Enzmann V, Balmer J, Jazwinska A, Tschopp M (2012) Visual acuity and contrast sensitivity of adult zebrafish. Front Zool 9:10.
Teller DY (1979) The forced-choice preferential looking procedure: A psychophysical technique for use with human infants. Infant Behavior and Development 2:135-153.
Tucker VA (2000) The deep fovea, sideways vision and spiral flight paths in raptors. J Exp Biol 203:3745-3754.
Utne-Palm AC, Bowmaker JK (2006) Spectral sensitivity of the two-spotted goby Gobiusculus flavescens (Fabricius): a physiological and behavioural study. J Exp Biol 209:2034-2041.
van der Meer HJ (1994) Ontogenetic change of visual thresholds in the cichlid fish Haplochromis sauvagei. Brain Behav Evol 44:40-49.
van der Meer HJ (1995) Visual resolution during growth in a cichlid fish: a morphological and behavioural case study. Brain Behav Evol 45:25-33.
Van Wassenbergh S, Roos G, Genbrugge A, Leysen H, Aerts P, Adriaens D, Herrel A (2009) Suction is kid's play: extremely fast suction in newborn seahorses. Biology Letters 5:200-203.
Vilter V (1954) Differenciation foveale dans l'appareil visuel d'un poisson abyssal, le Bathylagus benedicti. Compte Rendu des Seances de la Societe de Biologie Paris 148.
Wagner EC, Raymond PA (1991) Muller glial cells of the goldfish retina are phagocytic in vitro but not in vivo. Exp Eye Res 53:583-589.
Wagner HJ, Frohlich E, Negishi K, Collin SP (1998) The eyes of deep-sea fish. II. Functional morphology of the retina. Prog Retin Eye Res 17:637-685.
Wagner HJ, Wagner E (1988) Amacrine cells in the retina of a teleost fish, the roach (Rutilus rutilus): a Golgi study on differentiation and layering. Philos Trans R Soc Lond B Biol Sci 321:263-324.
Walls GL (1942) The vertebrate eye and its adaptive radiation. . Bloomfield Hills, Michigan: Cranbrook Institute of Science.

Wanzenbock J, Schiemer F (1989) Prey Detection in Cyprinids during Early Development. Can J Fish Aquat Sci 46:995-1001.
Wanzenböck J, Zaunreiter M, Wahl CM, Noakes DL (1996) Comparison of behavioural and morphological measures of visual resolution during ontogeny of roach (Rutilus rutilus) and yellow perch (Perca flavescens). Can J Fish Aquat Sci 53:1506–1512
Wassle H, Chun MH, Muller F (1987) Amacrine cells in the ganglion cell layer of the cat retina. J Comp Neurol 265:391-408.
Werblin FS (1970) Response of retinal cells to moving spots: intracellular recording in Necturus maculosus. J Neurophysiol 33:342-350.
Werblin FS, Dowling JE (1969) Organization of the retina of the mudpuppy, Necturus maculosus. II. Intracellular recording. J Neurophysiol 32:339-355.
West RW, Dowling JE (1972) Synapses onto different morphological types of retinal ganglion cells. Science 178:510-512.
Wikler KC, Szel A, Jacobsen AL (1996) Positional information and opsin identity in retinal cones. J Comp Neurol 374:96-107.
Witkovsky P, Dowling JE (1969) Synaptic relationships in the plexiform layers of carp retina. Z Zellforsch Mikrosk Anat 100:60-82.
Wu DM, Schneiderman T, Burgett J, Gokhale P, Barthel L, Raymond PA (2001) Cones regenerate from retinal stem cells sequestered in the inner nuclear layer of adult goldfish retina. Invest Ophthalmol Vis Sci 42:2115-2124.
Wunder W (1926) Ober den Bau der Netzhaut von Sfisswasser fischen, die in grosser Tiefe leben. Z Vergl Physiol 4:22-36.
Yazulla S, Studholme K, Wu JY (1986) Comparative distribution of 3H-GABA uptake and GAD immunoreactivity in goldfish retinal amacrine cells: a double-label analysis. J Comp Neurol 244:149-162.
Yuodelis C, Hendrickson A (1986) A qualitative and quantitative analysis of the human fovea during development. Vision Res 26:847-855.
Yurco P, Cameron DA (2005) Responses of Muller glia to retinal injury in adult zebrafish. Vision Res 45:991-1002.
Zaunreiter M, Junger H, Kotrschal K (1991) Retinal morphology of cyprinid fishes: A quantitative histological study of ontogenetic changes and interspecific variation. Vision Research 31:383-394.
Zhao XC, Yee RW, Norcom E, Burgess H, Avanesov AS, Barrish JP, Malicki J (2006) The Zebrafish Cornea: Structure and Development. Investigative Ophthalmology & Visual Science 47:4341-4348.
Zou SQ, Yin W, Zhang MJ, Hu CR, Huang YB, Hu B (2010) Using the optokinetic response to study visual function of zebrafish. J Vis Exp.
Zygar CA, Lee MJ, Fernald RD (1999) Nasotemporal asymmetry during teleost retinal growth: preserving an area of specialization. J Neurobiol 41:435-442.

Appendix 2: Published paper

Lee, H. R. and Bumsted O'Brien, K. M. (2011) "Morphological and behavioral limit of visual resolution in temperate (*Hippocampus abdominalis*) and tropical (*Hippocampus taeniopterus*) seahorses." Visual Neuroscience, 28(4):351-360.